

ISTANBUL TECHNICAL UNIVERSITY ★ GRADUATE SCHOOL OF SCIENCE
ENGINEERING AND TECHNOLOGY

**PRODUCTION OF ELECTROSPUN NANOFIBERS OF BIOCOMPATIBLE
POLYMERS AND A STUDY OF STREPTAVIDIN IMMOBILIZATION**

M.Sc. THESIS

Ece POLAT

Department of NanoScience & NanoEngineering

NanoScience & NanoEngineering Programme

JUNE 2012

ISTANBUL TECHNICAL UNIVERSITY ★ GRADUATE SCHOOL OF SCIENCE
ENGINEERING AND TECHNOLOGY

**PRODUCTION OF ELECTROSPUN NANOFIBERS OF BIOCOMPATIBLE
POLYMERS AND A STUDY OF STREPTAVIDIN IMMOBILIZATION**

M.Sc. THESIS

**Ece POLAT
(513101027)**

Department of NanoScience & NanoEngineering

NanoScience & NanoEngineering Programme

Thesis Advisor: Prof. Dr. A. Sezai SARAÇ

JUNE 2012

İSTANBUL TEKNİK ÜNİVERSİTESİ ★ FEN BİLİMLERİ ENSTİTÜSÜ

**ELEKTO ÇEKİM YÖNTEMİ İLE BİYOUYUMLU POLİMERLERDEN
NANOLİF ÜRETİMİ VE STREPTAVİDİN İMMOBİLİZASYONU**

YÜKSEK LİSANS TEZİ

**Ece POLAT
(513101027)**

NanoBilim & NanoMühendislik Anabilim Dalı

NanoBilim & NanoMühendislik Programı

Tez Danışmanı: Prof. Dr. A. Sezai SARAÇ

HAZİRAN 2012

Ece Polat, a **M.Sc.** student of **ITU Graduate School of Science, Engineering and Technology** student ID **513101027** successfully defended the **thesis** entitled **“PRODUCTION OF ELECTROSPUN NANOFIBERS OF BIOCOMPATIBLE POLYMERS AND A STUDY OF STREPTAVIDIN IMMOBILIZATION”**, which she prepared after fulfilling the requirements specified in the associated legislations, before the jury whose signatures are below.

Thesis Advisor : **Prof. Dr. A. Sezai SARAÇ**
İstanbul Technical University

Jury Members : **Prof. Dr. Zeynep Petek ÇAKAR**
İstanbul Technical University

Prof. Dr. Tülay TULUN
Cyprus International Universty

Date of Submission : 04 May 2012
Date of Defense : 08 June 2012

To my family,

FOREWORD

I would like to express my gratitude to my thesis supervisor, Prof. Dr. A. Sezai SARAÇ for his guidance and discussions in my studies.

I would like to give my special thanks to my laboratory friends Timucin BALKAN, Hacer DOLAŞ, Zeliha GÜLER, Yasemin YERLİKAYA, Diğdem GİRAY, Keziban HÜNER, Derya ÇETECİOĞLU, Başak DEMİRCİOĞLU, Selda ŞEN, Burcu ARMAN, Cem ÜNSAL, Giray ERSÖZOĞLU, Ezgi İŞMAR and Mehmet Tolga SATICI for their collaborative and friendly manner.

Finally, I would like to thank my parents Pervin POLAT and Zekai POLAT, my brothers Emre POLAT and Yahya POLAT and my grandmother, Şükriye YAMALI and also my aunt Ayhan BUSCH for her supporting during my undergraduate education and graduate education. Especially thanks to my mother due to her patience during my thesis and my father for supplying the materials that is needed. And also, I would like to thank everyone who supports me.

May 2012

Ece POLAT
(Environmental Engineer and Molecular Biolog)

TABLE OF CONTENTS

	<u>Page</u>
FOREWORD	ix
TABLE OF CONTENTS	xi
ABBREVIATIONS	xiii
LIST OF TABLES	xiii
LIST OF FIGURES	xiii
LIST OF SYMBOLS	xiii
SUMMARY	xiii
ÖZET	xxvii
1. INTRODUCTION	1
2. THEORETICAL PART	3
2.1 Conducting Polymers	3
2.1.1 Polyaniline	5
2.1.2 Poly (anthranilic acid)	6
2.2 Biocompatible Polymers	7
2.2.1 Poly (vinyl pyrrolidone)	7
2.2.2 Polycaprolactone	8
2.3 Electrospinning	9
2.3.1 Electrospinning process	9
2.3.2 Electrospinning parameters	10
2.3.2.1 Polymer solution parameters	11
2.3.2.2 Polymer processing parameters	13
2.3.2.3 Environmental conditions	14
2.3.3 Biomedical applications of nanofibers	15
2.4 Characterization Techniques	16
2.4.1 Principle of UV-Vis spectrophotometry	16
2.4.2 Principle of FTIR-ATR spectrophotometry	18
2.4.3 Principle of scanning electron microscopy	20
2.4.4 Principle of electrochemical impedance spectroscopy	21
2.5 Streptavidin	21
3. EXPERIMENTAL PART	23
3.1 Materials	23
3.2 Electrospinning	23
3.1.1 Electrospinning of PANA/PVP blends	23
3.1.2 Electrospinning of PANA/PCL blends	23
3.1.3 Electrospinning of PANA/PCL/PVP blends	24
3.3 Process Setup and Electrospinning	24
3.4 UV-Visible and FTIR-ATR Spectroscopy	24
3.5 Scanning Electron Microscopy	24
3.6 Electrochemical Measurement of Electrospinning Solutions	25

3.7 Conductivity	25
3.8 Electrochemical Impedance Spectroscopy (EIS) and Equivalent Circuit Modelling (ECM) for Electrospun Nanofibers	25
3.9 Streptavidin Immobilization	26
3.10 Microscopic Observation	26
4. RESULTS AND DISCUSSIONS.....	27
4.1 Characterization of PANA/PVP Blends	27
4.1.1 UV-Vis spectrophotometer results of PANA/PVP blends	27
4.1.2 FTIR-ATR spectrophotometric analysis of PANA/PVP blends	29
4.1.3 SEM results of PANA/PVP blends	32
4.1.4 Electrochemical impedance results of DMF solutions	37
4.2 Characterization of PANA/PCL Blends	43
4.2.1 UV-Vis spectrophotometer results of PANA/PCL blends	43
4.2.2 FTIR-ATR spectrophotometric analysis of PANA/PCL blends	43
4.2.3 SEM results of PANA/PCL blends	45
4.2.4 Electrochemical impedance results of THF solutions	48
4.3 Characterization of PANA/PCL/PVP Blends	51
4.3.1 UV-Vis spectrophotometer results of PANA/PCL/PVP blends.....	51
4.3.2 FTIR-ATR spectrophotometric analysis of PANA/PCL/PVP blends...	51
4.3.3 SEM results of PANA/PCL/PVP blends	52
4.3.4 Electrochemical impedance results of DMF/THF solutions	55
4.4 Electrochemical Impedance Spectroscopy (EIS) and Equivalent Circuit Modelling (ECM) for Electrospun Nanofibers	57
4.5 Streptavidin Immobilization	60
5. CONCLUSIONS AND RECOMMENDATIONS	65
REFERENCES	67
CURRICULUM VITAE	75

ABBREVIATIONS

AC	: Alternating current
Cdl	: Double layer capacitance
cm	: Centimetre
CPE	: Constant phase element
CV	: Cyclic voltammetry
DAS	: 4-diazostilbene-2,2-disulfonic acid disodium salt
DC	: Direct current
DMF	: Dimethylformamide
DMSO	: Dimethyl sulfoxide
dPBS	: Dulbecco's phosphate buffered saline
DTAB	: Dodecyltrimethylammonium bromide
EDC	: N-(3-Dimethylaminopropyl)-N'-ethylcarbodiimide hydrochloride
EIS	: Electrochemical impedance spectroscopy
EtOH	: Ethanol
FTIR-ATR	: Attenuated total reflection -fourier transform infrared spectroscopy
Ge	: Germanium
HCl	: Hydrochloric acid
H₂SO₄	: Sulphuric acid
HOMO	: Highest occupied molecular orbital
Hz	: Hertz
IR	: Infrared
kV	: Kilovolts
LUMO	: Lowest unoccupied molecular orbital
MES	: 2-(N-morpholino) ethane sulfonic acid
mF	: Millifarad
ml	: Milliliter
mm	: Millimeter
μm	: Micrometer
NHS	: N-Hydroxysulfosuccinimide sodium salt
nm	: Nanometre
PAc	: Poly (acetylene)
PANA	: Poly antranilic acid
PANI	: Polyaniline
PCL	: Polycaprolactone
PEDOT	: Poly (3,4-ethylenedioxythiophene)
PPy	: Poly (pyrrole)
PT	: Poly (thiophene)
PVP	: Poly (vinyl pyrrolidone)
SEM	: Scanning electron microscopy

STV	: Tetrabutylammonium chloride
TBAC	: Dulbecco's phosphate buffered saline
THF	: Tetrahydrofuran
UV	: Ultraviolet light
UV-Vis	: Ultraviolet-visible
ZnSe	: Zinc selenide

LIST OF TABLES

	<u>Page</u>
Table 2.1: The summary of parameters that effect fiber formation.	10
Table 2.2: Dielectric constants of solvents	12
Table 2.3: Colour and light absorption in UV-Vis spectroscopy	17
Table 2.4: Some vibrations in FTIR-ATR spectroscopy.....	19
Table 4.1: The summary of electrospun nanofibers with electrospinning conditions and diameters of nanofibers.....	37
Table 4.2: The impedance data of electrospinnig solutions prepared in EtOH/DMF.	38
Table 4.3: The double layer capacitance of electrospinning solutions prepared in EtOH/DMF	40
Table 4.4: The impedance data of electrospinnig solutions prepared in DMF	41
Table 4.5: The double layer capacitance of electrospinning solutions prepared in DMF	43
Table 4.6: The summary of electrospun nanofibers of PANA/PCLwith electrospinning conditions and diameters of nanofibers.	47
Table 4.7: The impedance data of electrospinning solutions prepared in THF	49
Table 4.8: The double layer capacitance of electrospinning solutions prepared in THF	50
Table 4.9: The summary of electrospun nanofibers of PANA/PCL/PVP with electrospinning conditions and diameters of nanofibers	54
Table 4.10: The impedance data of electrospinning solutions prepared in DMF/THF solutions	55
Table 4.11: The double layer capacitance of solutions prepared in DMF/THF solutions	56
Table 4.12: The double layer capacitance of the nanofibers	59
Table 4.13: Parameters calculated from the equivalent circuit model of R(Q(R(CR))).	60

LIST OF FIGURES

	<u>Page</u>
Figure 2.1 : Structures of conducting polymers.	3
Figure 2.2 : Conjugated backbone and ionic properties.	4
Figure 2.3 : Conduction mechanism ...	4
Figure 2.4 : Molecular orbitals.....	5
Figure 2.5 : Doping process of polyaniline.....	6
Figure 2.6 : Structures of aniline (left), anthranilic acid (right)	7
Figure 2.7 : Structure of poly anthranilic acid.....	7
Figure 2.8 : Photocrosslinking reaction of PVP.....	8
Figure 2.9 : Polycaprolactone chemical structure ...	9
Figure 2.10 : Experimental setup of electrospinning	10
Figure 2.11 : Drug loaded nanofibers	15
Figure 2.12 : Nanofiber scaffolds	16
Figure 2.13 : Ultraviolet spectrum	16
Figure 2.14 : Orbital and energy transfer.....	17
Figure 2.15 : Working principle of FTIR-ATR	18
Figure 2.16 : Asymmetric and symmetric stretching	18
Figure 2.17 : Bending between atoms.....	19
Figure 2.18 : Schematic diagram of scanning electron microscopy	20
Figure 2.19 : Schematic diagram of electrochemical impedance spectroscopy	21
Figure 2.20 : Subunits of streptavidin.....	22
Figure 4.1 : UV-Vis spectra of PANA/PVP blend nanofibers dissolved in EtOH/DMF.. ...	27
Figure 4.2 : UV-Vis results of PANA/PVP blend nanofibers dissolved in DMF. ...	28
Figure 4.3 : Absorbance peaks of PANA/PVP blend nanofibers dissolved in EtOH/DMF... ..	28
Figure 4.4 : Absorbance peaks of PANA/PVP blend nanofibers dissolved in DMF	29
Figure 4.5 : FTIR-ATR spectra of PANA/PVP nanofibers electrospun in EtOH/DMF.. ...	30
Figure 4.6 : FTIR-ATR spectra of PANA/PVP nanofibers electrospun in DMF.. ..	30
Figure 4.7 : The change in the specific peak of PANA in the nanofibers of PANA/PVP that was electrospun in EtOH/DMF solution.. ...	31
Figure 4.8 : The change in the specific peak of PANA in the nanofibers of PANA/PVP that was electrospun in DMF solution	31
Figure 4.9 : SEM micrograph of PVP in EtOH/DMF.	32
Figure 4.10 : SEM micrograph of PANA/PVP (1/30) in EtOH/DMF	32
Figure 4.11 : SEM micrograph of PANA/PVP (1/10) in EtOH/DMF.	33
Figure 4.12 : SEM micrograph of nanofibers of PVP prepared by using DMF.....	33
Figure 4.13 : SEM micrograph of PANA/PVP (1/10) DMF... ..	34
Figure 4.14 : SEM micrograph of PANA/PVP (1/20) in DMF. ...	34

Figure 4.15 : Distribution of the PANA/PVP nanofibers with their diameters..	35
Figure 4.16 : Distribution of the diameters of nanofibers of PVP...	36
Figure 4.17 : Distribution of the diameters of nanofibers of PANA/PVP prepared in EtOH/DMF solution..	36
Figure 4.18 : Distribution of the diameters of nanofibers of PANA/PVP prepared in DMF solution.	37
Figure 4.19 : Nyquist diagram of electrospinning solutions prepared in EtOH/DMF	38
Figure 4.20 : Bode phase of electrospinning solutions prepared in EtOH/DMF.	39
Figure 4.21 : Bode magnitude of electrospinning solutions of PANA/PVP dissolved in EtOH/DMF.	40
Figure 4.22 : Nyquist diagram of electrospun prepared in DMF..	41
Figure 4.23 : Bode phase of electrospinning solutions prepared in DMF..	42
Figure 4.24 : Bode magnitude of electrospinning solutions prepared in DMF..	42
Figure 4.25 : UV-Vis results of nanofibers of PANA/PCL blend dissolved in THF... ..	43
Figure 4.26 : FTIR-ATR spectrums of PANA/PCL nanofibers..	44
Figure 4.27 : Specific peaks of PANA in PANA/PCL blended nanofibers..	44
Figure 4.28 : SEM result of nanofibers of PCL prepared in THF...	45
Figure 4.29 : SEM result of nanofibers that contain 5% of PANA..	45
Figure 4.30 : SEM result of nanofibers that contain 15% of PANA..	46
Figure 4.31 : SEM result of nanofibers that contain 25% of PANA..	46
Figure 4.32 : Distribution of the PANA/PCL blend nanofibers diameters...	47
Figure 4.33 : Distribution of the diameters of nanofibers of PCL containing 25 % of PANA... ..	48
Figure 4.34 : Nyquist diagram of electrospinning solutions of PANA/PCL prepared in THF... ..	48
Figure 4.35 : Bode phase of electrospinning solutions prepared in THF..	49
Figure 4.36 : Bode magnitude of electrospinning solutions of PANA/PCL dissolved in THF.	50
Figure 4.37 : UV-Vis spectrum of PANA/PCL/PVP blend nanofibers dissolved in DMF/THF ...	51
Figure 4.38 : FTIR-ATR spectra of PANA/PCL/PVP blended nanofibers..	52
Figure 4.39 : SEM result of PCL/PVP blended nanofibers ...	52
Figure 4.40 : Diameter distribution of nanofibers of PCL/PVP..	53
Figure 4.41 : SEM results of PANA/PCL/PVP blended nanofibers..	53
Figure 4.42 : Diameter distribution of nanofibers of PANA/PCL/PVP blends....	54
Figure 4.43 : Distribution of nanofibers diameter of PANA/PCL/PVP blends.	54
Figure 4.44 : Nyquist diagram of electrospun solutions prepared in DMF/THF..	55
Figure 4.45 : Bode phase of electrospinning solutions prepared in DMF/THF... ..	56
Figure 4.46 : Bode magnitude of electrospinning solutions prepared in DMF/THF	57
Figure 4.47 : Nyquist plots of PANA/PCL blended nanofibers; correlated with the calculated data from the equivalent circuit model; $R(Q(R(CR)))$..	58
Figure 4.48 : Bode Phase plots of PANA/PCL blended nanofibers; correlated with the calculated data from the equivalent circuit model; $R(Q(R(CR)))$..	58
Figure 4.49 : Bode Magnitude plots of PANA/PCL blended nanofibers; correlated with the calculated data from the equivalent circuit model; $R(Q(R(CR)))$...	59

Figure 4.50 : The equivalent circuit model of PANA/PCL blended nanofibers. (Rs=solution and pore resistance; Rct= charge transfer resistance; CPE is used for modelling the double layer capacitance, Cdl; Rf and Cf are resistance and capacitance of nanofibers)..	60
Figure 4.51 : FTIR-ATR spectra of streptavidin. . .	61
Figure 4.52 : FTIR-ATR spectra of nanofibers with and without streptavidin	61
Figure 4.53 : FTIR-ATR spectra of nanofibers modified with EDC-NHS with and without streptavidin.	62
Figure 4.54 : Microscopic observation of nanofibers after streptavidin immobilization.	62
Figure 4.55 : Microscopic observation of nanofibers after streptavidin adhesion not immobilization without EDC and NHS.	63
Figure 4.56 : Microscopic observation of nanofibers after modification with dye..	63

LIST OF SYMBOLS

ε	: Dielectric constant
Ω	: Ohm
$M\Omega$: Megaohm
π	: Bonding orbital
σ	: Bonding orbital
π^*	: Antibonding orbital
σ^*	: Antibonding orbital
n	: Nonbonding orbital
Q	: Constant phase element
R	: Resistance
R_a	: Pore resistance
R_{ct}	: Charge transfer resistance
R_f	: Resistance of nanofibers
R_s	: Electrolyte resistance
C	: Capacitance
C_a	: Pore capacitance
C_f	: Capacitance of nanofibers
K	: Kelvin
$^{\circ}C$: Celsius degree
v	: Volume
w	: Weight
χ^2	: Chi Squared
$ Z $: Impedance modulus
Z_{im}	: Imaginary part
Z_{re}	: Real part

PRODUCTION OF ELECTROSPUN NANOFIBERS OF BIOCOMPATIBLE POLYMERS AND A STUDY OF STREPTAVIDIN IMMOBILIZATION

SUMMARY

In this study, fabrication of biocompatible polymers with the blend of poly (anthranilic acid) was investigated. Poly (anthranilic acid) was blended with biocompatible polymers because of having carboxylic acid group that may be important for protein immobilization on nanofibers surfaces. In this study, especially THF and DMF solutions were preferred due to the poly (anthranilic acid) limited solubility in many solvents. First of all, poly (vinyl pyrrolidone) and poly (anthranilic acid) blends were obtained. For those nanofibers, two different solvent systems were studied. In ethanol and dimethylformamide solvent mixture, the maximum value of poly (anthranilic acid) that was used as 10 per cent of the weight of the poly (vinyl pyrrolidone). However, in only dimethylformamide solvent the solubility of poly (anthranilic acid) was achieved with the 20 per cent of the weight of the poly (vinyl pyrrolidone).

The obtained nanofibers were investigated with UV-Vis spectrophotometer and FTIR-ATR spectrophotometry and also morphology of the nanofibers were investigated with the scanning electron microscopy. As it is known that poly (vinyl pyrrolidone) dissolves in water rapidly and it was realized that the nanofibers with the blend of poly (vinyl pyrrolidone) and poly (anthranilic acid) has also ability to dissolve in water. Due to that property, conductometer can be used to investigate the conductivity of the nanofibers and as it was found that the amount of poly (anthranilic acid) makes the increase in conductivity.

Secondly, another biocompatible polymer named polycaprolactone was blended with the poly (anthranilic acid) with the weight ratio of 5%, 15% and 25% of poly (anthranilic acid) containing. For those nanofibers, tetrahydrofuran was chosen as solvent due to the two reasons. First one is the polycaprolactone gelation property in dimethylformamide that prevents and limits the electrospinning of polycaprolactone. Both polycaprolactone and poly (anthranilic acid) can dissolved in tetrahydrofuran is the second reason. For homogenous mixture the mixture of the solvent systems was kept for 24 hours under magnetic stirring. After that, the polymer solution was taken to the syringe and 1 ml/hour and 20 cm between the needle and the collector was chosen and electrospinning was applied. Characterization techniques were used compare the result of the UV-Vis spectrophotometer and FTIR-ATR spectrophotometer and it was found that the specific peaks of PANA are increasing proportional to the poly (anthranilic acid) concentration.

Thirdly, the nanofibers of the blend of PANA/PVL/PVP were investigated. For those nanofibers, the three polymers were dissolved in DMF and THF solvent system and electrospinning was done. The poly (anthranilic acid) weight ratio in the solvent system was 10%. The aim to produce the three blends of the nanofibers was to stop

the hydrophilic property of the poly (vinyl pyrrolidone) and make more hydrophobic nanofibers and for that reason high temperature during the mixing was preferred to be obtain the crosslinking of the polymers. To verify the nanofibers molecular structure, UV-Vis spectrophotometer and FTIR-ATR spectrophotometer was used to investigate the specific peaks of the poly (anthranilic acid). Finally, morphology of the nanofibers and the diameter of the nanofibers were investigated with the scanning electron microscopy and for average diameter calculation of the nanofibers, the counting of the nanofibers from number varies from 75 to 250 were done.

For the conductivity of the electrospinning solution three electrode systems (two platinum as working and counter and one silver as reference) was used and electrochemical measurement was done. For that electrochemical measurement, the impedance under the diluted electrospinning solution with the ratio of 1/30 was measured. As a result of the impedance measurement, nyquist diagrams, bode diagrams were obtained. Also, in impedance measurement the solvent without any polymer was also measured and they were compared with the solvents that have polymers. From the results, it was found that the conductivity of the tetrahydrofuran has the highest.

From the diluted measurement in UV-Vis spectrophotometer, each poly (anthranilic acid) peak was realized in the same region and increasing with the increasing concentrations. The experiments were with adding little amount of poly (anthranilic acid), but the peaks of PANA were seen in FTIR-ATR results and in polycaprolactone blends the region for PANA was increasing with the concentration. However, the peak of the PANA was shifted in the blends of the poly (vinyl pyrrolidone) which was prepared with dissolving in ethanol and DMF with the amount of 10 % of PANA containing.

If the three polymer blends of poly (vinyl pyrrolidone), polycaprolactone and poly (anthranilic acid), it was realized that the nanofibers were homogenous and the average nanofibers diameter was decreased from 1026 nm to 652 nm with the addition of the poly (anthranilic acid). Furthermore, from the FTIR-ATR results it was found that the specific peaks of polycaprolactone have dominant character, by the time the specific peak of poly (vinyl pyrrolidone) was also seen. The specific peak of poly (anthranilic acid) was also seen in FTIR-ATR results and the result was verified with UV-Vis spectrophotometer.

It was found that the highest water stability of the nanofibers were the polycaprolactone and poly (anthranilic acid) blends. Those nanofibers have hydrophobic properties that may be an advantage to be used as an electrode. To be used as an electrode the equivalent circuit modelling should be needed. For that reason 0.1 M HCl solvent was used to investigate the impedance properties of the poly (anthranilic acid). The same measurement was done with phosphate buffer saline; however due to the little solubility of the poly (anthranilic acid) in neutral pH, the modelling was not applied. In modelling with the 10^{-4} error for all 5%, 15% and 15% PANA containing nanofibers, the modelling of $R(Q(R(CR)))$ was chosen. When each nanofiber was investigated the value of n which can be used for defining the capacitive behaviour was 0.8 for both of them.

To show an application of those produced and characterized biocompatible nanofibers, protein immobilization was done. Used For that application, streptavidin was chosen that is defined as model protein and is being used in many applications due to the high affinity to biotin. To immobilize streptavidin, the blends with

polycaprolactone were chosen due to their hydrophobic properties that may be important for their interaction with hydrophilic surfaces without swelling. For immobilization study, crosslinkers named EDC and NHS were used to covalently bond the -COOH group of blended nanofibers and -NH_2 group of streptavidin. FTIR-ATR spectroscopy was used to investigate as if streptavidin immobilized efficiently onto the surface of PCL/PANA blended nanofibers. It was expected to see streptavidin's COOH peak in FTIR-ATR spectroscopy. To visualize the bounded protein the food dye was used and light microscopy investigation was realized.

ELEKTO ÇEKİM YÖNTEMİ İLE BİYOUYUMLU POLİMERLERDEN NANOLİF ÜRETİMİ VE STREPTAVİDİN İMMOBİLİZASYONU

ÖZET

Bu çalışmada, biyouyumlu polimerlerin poli (antranilik asit) polimeri ile karıştırılarak nanolif üretimi araştırılmıştır. Poli (antranilik asit)'in kullanım amaçlarından biri yapısında sahip olduğu karboksil grubu nedeniyle protein immobilizasyon çalışmalarında kullanılabilir olmasıdır. Bu çalışmalarda özellikle tetrahidrofuran ve dimetilformamid çözeltileri seçilmiştir; çünkü poli (antranilik asit)'in diğer çözücülerde çözünürlüğü sınırlıdır. İlk olarak polivinilpirolidon ve poli antranilik asit nanolifleri elde edilmiştir. Bunun için iki farklı çözücü ile çalışılmıştır. Etanol ve dimetilformamid çözücülerini ile maksimum yüzde 10 oranında poli (antranilik asit) karışımı elde edilebilirken, sadece poli (antranilik asit)'in dimetilformamid içinde olan çözünürlüğü kullanılarak yapılan deneylerde yüzde 20 poli (antranilik asit) içeren polimer çözeltileri elde edilmiştir. Sırasıyla, etanol ve dimetilformamid çözeltisi karışımı ile elde edilen nanoliflerde ağırlıkça %3,3, %5, %6,7 ve %10 poli (antranilik asit) kullanılmıştır. Polivinilpirolidonun sadece dimetilformamid çözeltisinde hazırlanarak üretilen nanoliflerinde de ağırlıkça %5, %10, %15 ve %20 oranında poli (antranilik asit) kullanılmıştır.

Polivinilpirolidonlu nanolifler elde etmek için, elektro çekim sırasında besleme hızı 0,5 ml/saat ve elektrot ile alüminyum toplayıcı elektrot arasındaki mesafe 20 cm olarak ayarlanmıştır. Elde edilen nanolifler ultraviyole-görünür bölge absorpsiyon spektroskopisi ve FTIR-ATR spektrofotometresi ile incelenmiş ve taramalı elektron mikroskopu ile morfolojik olarak karakterize edilmiştir. Ayrıca, poli vinil pirolidon bilindiği gibi suda çok iyi çözünen bir polimerdir ve polivinilpirolidonun poli (antranilik asit) ile oluşturduğu nanoliflerinde suda çözündüğü anlaşılmıştır. Bunun sonucu olarak sulu ortamlarda gerçekleştirilen kondüktometre yöntemi ile iletkenlik değişimi araştırılmıştır ve yapıda poli (antranilik asit) bulunduğu durumda ölçülen iletkenlikte artış gözlenmiştir.

İkinci biyouyumlu polimer polikaprolakton ile ağırlıkça %5, %15 ve %25 poli (antranilik asit) içeren karışımlar elde edilmiştir. Bunun için çözücü olarak dimetilformamid değil, tetrahidrofuran çözücüsü seçilmiştir. Bunun birinci nedeni polikaprolaktonun dimetilformamid içerisinde jelleşme göstermesidir ve ikinci nedeni ise tetrahidrofuran çözücüsünün hem polikaprolaktonu hem de poli (antranilik asit)'i çözebiliyor olmasıdır. Homojen karışımın sağlanması için 24 saat süre ile manyetik karıştırıcı ile karışım yapılmıştır. Sonrasında, şırıngaya çekilen polimer çözeltisine 1ml/saat besleme hızı ve 20 cm elektrotlar arası mesafe olacak şekilde elektro çekim yöntemi uygulanmıştır. Tüm deneyler oda sıcaklığında gerçekleştirilmiştir. Yine karakterizasyon işlemleri uygulanarak polikaprolakton ve poli (antranilik asit) karışımı ile elde edilmiş nanoliflerin ultraviyole-görünür bölge absorpsiyon spektroskopisi, FTIR-ATR spektrofotometre sonuçları karşılaştırılmıştır.

Konsantrasyona bağılı olarak poli (antranilik asit) piklerinde artış olduğu gözlenmiştir.

Son olarak da, PANA/PCL/PVP karışımı ile elde edilen nanofiberler incelenmiştir. Bunun için tetrahidrofuran ve dimetilformamid karışımı ile hazırlanan çözeltide bu üçlü polimerler çözülüp elektro çekim yöntemi uygulanmıştır. Karışımında kullanılan poli (antranilik asit) ağırlıkça yüzde 10 olarak kullanılmıştır. Ayrıca bu üçlü karışımın bir amacı da polivinilpirolidonun hidrofilik yani suyu seven ve suda çözünabilen özelliğini ortadan kaldırmak olduğu için 24 saat süreli elektro çekim öncesi yapılan karışım sırasında yüksek ısı kullanılmıştır. Elektro çekim yönteminde 1 ml/saat besleme hızı ve 20 cm elektrotlar arasındaki mesafe olacak şekilde parametreler seçilmiştir. Poli antranilik asit içeren nanofiberlerin yapısını doğrulamak için ultraviyole-görünür bölge absorpsiyon spektroskopisi ve FTIR-ATR spektrofotometre kullanılarak poli (antranilik asit)e ait spesifik pikler araştırılmıştır. Son olarak, nanofiberlerin morfolojik özellikleri ve çapları taramalı elektron mikroskobu kullanılarak incelenmiştir ve ortalama nanolif sayısı için 75 ile 250 arasında değişen oranlarda nanoliflerin çapları sayılmıştır.

Elektro çekim yöntemi için kullanılan polimer çözeltisinin iletkenlik ölçümü, üçlü elektrot sistemi kullanılarak (çalışma ve karşıt elektrot olarak iki platin ve referans elektrot olarak bir gümüş elektrot) incelenmiş ve elektrokimyasal ölçümleri yapılmıştır. Bunun için çalışma elektrotu olarak kullanılan platin ile 1/30 oranında seyreltilmiş elektro çekim çözeltilerinin empedans ölçümü gerçekleştirilmiştir. Empedans ölçümünde elektrokimyasal hücre, potansiyostat ve bilgisayar kullanılmıştır. Bu empedans ölçümleri sonucunda Nyquist diyagramları ve Bode diyagramları elde edilmiştir. Empedans ölçümlerinde polimer ilave edilmeden çözeltilerin kendi dirençleri de ölçülmüştür. Sonrasında, polimer içeren çözeltilerin ölçülen empedans değerleri karşılaştırılmıştır. Bu sonuçlara göre, tetrahidrofuran çözeltisinin iletkenliğin en çok olduğu sonucuna varılmıştır. Polikaprolaktonlu THF çözeltisinin iletkenliğinin düştüğü, bu karışımında poli (antranilik asit) içeren çözeltinin ise kullanılan polikaprolaktona göre daha iletken olduğu sonucuna varılmıştır. Aynı çalışma polivinilpirolidon ve çözeltileri için yapıldığında, kullanılan çözeltinin iletkenliğinin çok düşük olduğu, buna karşın polivinilpirolidonlu çözeltinin iletkenliğinin daha fazla olduğu, en iletken özelliğin ise poli (antranilik asit) içeren çözeltilerde olduğu gözlenmiştir. Bu çözeltilerin ayrıca çift faz kapasitans değerleri de hesaplanmıştır. Sonrasında, her bir empedansı ölçülmüş çözeltinin faz açıları, sanal ve gerçek kısımlarda okunan ohm değerleri karşılaştırılmıştır.

UV-Vis spektrofotometre ile ölçülen seyreltme ile elde edilen nanoliflerden alınan ölçümlerde poli (antranilik asit)e ait spesifik pikler her üç polimer karışımı içinde aynı bölgelerde ve konsantrasyon artışına bağılı olarak artış şeklinde elde edilmiştir. FTIR-ATR sonuçlarında da çok az miktarda poli (antranilik asit) ile yapılan deneyler olmasına rağmen poli (antranilik asit)e ait spesifik pik gözlenmiştir ve bu gözlenen pikler polikaprolaktonlu örneklerde ağırlıkça yüzde oranındaki artışa bağılı olarak arttığı gözlenmiştir. Fakat polivinilpirolidon poli (antranilik asit) karışımları ile elde edilen nanoliflerden etanol ve dimetilformamid içerisinde hazırlanmış olanlardan maksimum yüzde 10 poli (antranilik asit) çözölmüş örnekte artış değil pik noktasında kayma olduğu gözlenmiştir.

Taramalı elektron mikroskobu görüntüleri incelendiğinde PCL nanoliflerinin THF çözeltisi içinde elde edilen nanoliflerin homojen olmadığı, boyutlarının nano ve mikro düzeyde değişkenlik gösterdiği, buna karşın PCL/PVP karışımı ile elde edilen liflerin daha homojen olduğu gözlenmiştir. İncelendiğinde PCL'nin THF çözeltisi

içinde hazırlanarak elde edilen liflerin 1160 ile 655 nanometre aralığında değiştiği gözlenmiştir. Ortalama fiber çapındaki düşüş poli (antranilik asit)in miktarının artırılması ile doğru orantılıdır. Fakat PCL nanoliflerinde homojen olmayan dağılım nedeniyle 8 µm'ye kadar kalınlıkta nanoliflere rastlanmıştır.

Aynı zamanda, polimer çözeltisinin DMF içinde hazırlandığı durumlarda da lif çapında önemli bir düşüş olduğu görülmektedir. Özellikle polivinilpirolidon poli (antranilik asit) nanoliflerinde konsantrasyon arttıkça çapın artması beklenirken, çözücünün değişmesi etanol yerine dimetilformamidin kullanılması nedeniyle sadece polivinilpirolidon içeren nanoliflerde ortalama fiber çapının 1110 nanometreden 777 nanometreye düştüğü gözlenmiştir.

Üçlü polimer karışımlarından polivinilpirolidon, polikaprolakton ve poli (antranilik asit) ile elde edilen nanolifler incelendiğinde liflerin homojen olduğu, ortalama lif çapının 1026 nanometreden poli (antranilik asit) ilavesi ile 652 nanometreye düştüğü gözlenmiştir. Ayrıca, FTIR-ATR sonuçları incelendiğinde polivinilpirolidon ve polikaprolaktondan elde edilen nanoliflerde polikaprolaktona ait piklerin baskın olduğu buna karşın polivinilpirolidonun kendi spesifik pikinin de bu polimer karışımı ile elde edilen nanoliflerde olduğu gözlenmiştir. Poli (antranilik asit)e ait pik de yine bu üçlü polimer karışımında da gözlenmiştir ve bu sonuç ultraviyole-görünür bölge absorpsiyon spektroskopisi ile doğrulanmıştır.

Üretilen nanolifler incelendiğinde suya dayanımı en yüksek ve hidrofobik olan nanoliflerin poli (antranilik asit) ve polikaprolakton karışımı olduğu anlaşılmıştır. Elde edilen bu nanolif, hidrofobik olduklarından dolayı elektrot olarak kullanabilmek mümkün olabilir. Bu nanolifler ileride elektrot olarak kullanılabilmesi için elektrokimyasal devre modellemesine ihtiyaç vardır. Bunun için 0,1 M HCl içinde poli (antranilik asit) içeren nanoliflerin empedans özellikleri incelenmiştir. Bu ölçüm sırasında nanolifler çalışma elektrotu olarak kullanılmıştır. Ayrıca, aynı ölçüm fosfat tampon çözeltisinde gerçekleştirilmiş ama poli (antranilik asit)in nötral pH'larda kısmen çözünmesinden dolayı devre modellemesi yapılmamıştır. Devre modellemesine göre 10^{-4} değerinde hata payı ile %5, %15 ve %25 PANA içeren polikaprolakton nanoliflerinin devre modellemesi sonucu R(Q(R(CR))) devresi seçilmiştir. Bu devre her üç nanolif için de incelendiğinde kapasitif özelliği gösteren n değerinin her üçünde de 0,8 olduğu gözlenmiştir.

Bu üretilen ve karakterize edilen fonksiyonel grup eklenmiş biyouyumlu nanoliflerin uygulamasını göstermek amacıyla protein immobilizasyonu çalışması yapılmıştır. Bunun için özellikle biyotin ile olan yüksek bağlanma afinitesi nedeniyle birçok çalışmada tercih edilen model protein streptavidin seçilmiştir. Streptavidin proteinini immobilize etmek için polikaprolakton ve poli (antranilik asit) karışımı nanofiberler tercih edilmiştir; çünkü hidrofobik özelliklerinden dolayı hidrofilik yüzeylerle yapısında herhangi bir deformasyon olmadan etkileşebilmektedir. Diğer fiberlerin yapısında bulunan polivinilpirolidon suda çok iyi çözündüğü için proteinle yapılan çalışmalarda tercih edilmemiştir. Immobilizasyon çalışmasında, EDC ve NHS çapraz bağlayıcıları nanoliflerin sahip olduğu -COOH grubu (karboksil) ile proteinin -NH₂ (amin) grubunun etkileşmesinde kullanılmıştır. Öncelikle, EDC çözeltisi MES tampon çözeltisinde çözülerek hazırlanmıştır. Sonrasında 15 dakika reaksiyon süresi sonucunda NHS kimyasalı kullanılmıştır. En son olarak da streptavidin proteini karbonat tampon çözeltisi kullanılarak çözülmüş ve 30 dakika boyunca immobilizasyon işlemi için beklenmiştir. Son aşamada da spesifik ve spesifik olmayan bağlanmaları ayırmak için nanolif yüzeyini saf su ile yıkama işlemi yapılmıştır. Yıkama ve kurutuma sonrasında proteinin bağlanıp bağlanmadığının

FTIR-ATR spektroskopisi kullanılarak incelenmiştir. Protein bağlanan bölgeler de proteine ait spesifik FTIR-ATR spektrofotometre ile tespit edilmiştir.

Bağlanan proteinleri ışık mikroskobu ile görmek amacıyla gıda boyası ile boyama işlemi denenmiştir. Bunun için üç farklı çalışma yapılmıştır. İlk önce, streptavidini immobilize etmeden önce streptavidin çözeltisi içine bir miktar gıda boyası katılmıştır. Sonrasında, saf su ile yıkama ve kurutma işlemi gerçekleştirilmiştir ve sonrasında boyalı bölgeler ışık mikroskopunda 40 kat büyütme ile incelenmiştir. İkinci olarak, protein ve boyanın nanolifli yüzeye tutunup tutunmadığı incelenmiştir. Bunun için EDC ve NHS bağlayıcıları kullanılmadan sadece streptavidin ve boya içeren çözelti ile nanolifli yüzeye 30 dakika boyunca inkübe edilmiştir. Bu süre sonunda, nanolifli yüzey yıkama işlemine tabi tutulmuş ve mikroskopik gözlem sonucunda bir boyaların yüzeye tutunduğu gözlenmiştir. Son olarak da, streptavidin içermeyen boyalı çözelti nanolifli yüzeye uygulanmış ve yıkama işlemi sonrasında ve mikroskopik gözlem ile yine bir miktar boyanın nanolif yüzeyinde tutunduğu gözlenmiştir. Bu tutunmanın nanolifli yüzeylerin yüksek yüzey alanına sahip olmasından dolayı gerçekleştiği söylenebilir.

1. INTRODUCTION

Nowadays, biocompatible polymers draw great attention due to their usage in many areas such as applications in biomedicine. They are important because of being non-toxic to environment and health. Fabrication of biocompatible polymers has great importance for biomedical purposes due to their easy processability nature. To produce nanofibers, generally electrospinning method is most widely used method for being lab-scale and easy applications. The degradability of the biocompatible polymers can be important in biomedical applications such as controlled release in drug delivery systems and tissue engineering applications. The mixture of biocompatible polymers with conducting polymers would be important for sensor investigations of biomolecules. As conducting polymers cannot be used alone to produce nanofibers, the biocompatible polymers can be the best ones to blend the conducting polymers.

The aim of this study was to fabricate biocompatible nanofibers and to show their use in biological applications. Within the scope of this thesis, it focused on four main subjects. These are firstly the fabrication of biocompatible nanofibers, secondly blending biocompatible polymers with poly (anthranilic acid) to have functional groups, thirdly the characterization of those electrospun nanofibers and finally the immobilization of streptavidin on nanofibers by choosing the best appropriate nanofibers blend for immobilization study.

2. THEORETICAL PART

2.1 Conducting Polymers

Conducting polymers differ from the other polymers due to their properties of having conjugated bonds and unstable backbone that can be defined as having both single and double bonds [1]. The first synthesized polymer with having π electrons was polyacetylene [2]. The 2000 Nobel Prize was awarded to Hideki Shirakawa, Alan J. Heeger and Alan G. MacDiarmid due to their discoveries of polyacetylene and doping mechanisms with the presence of iodine [2]. Poly (pyrrole) (PPy), polyaniline (PANI), poly (thiophene) (PT), poly (3,4-ethylenedioxythiophene) (PEDOT), poly (acetylene) (PAC) and poly (phenylene vinylene) are mainly known conducting polymers as shown in Figure 2.1.

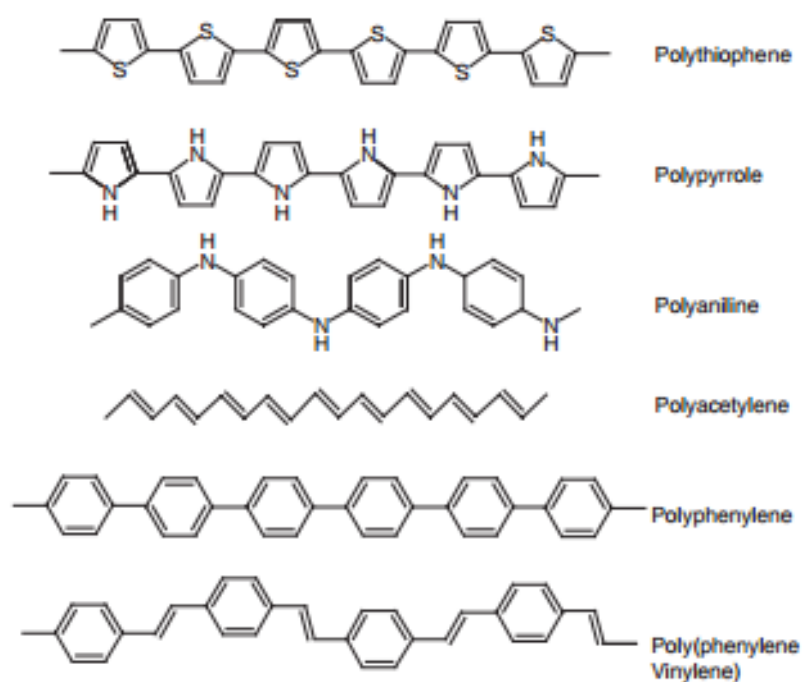


Figure 2.1 : Structures of conducting polymers [3].

Conducting polymers can be synthesized in both aqueous and non-aqueous media with chemical and electrochemical methods [4]. When conducting polymer is doped electrons is transferred in unstable backbone and an example of doping process is shown in Figure 2.2. Doping with ionic species by using HCl, H₂SO₄ makes the change in the conjugated structure, on electron is removed, and conjugated structure can be obtained.

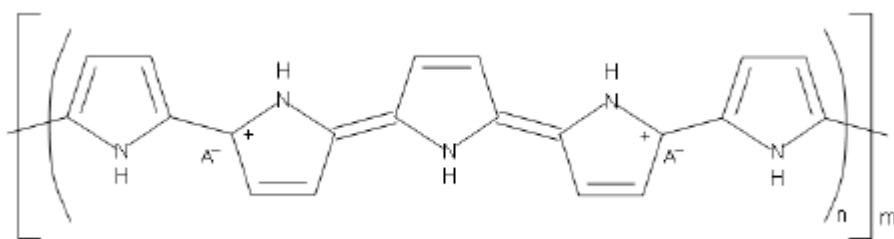


Figure 2.2 : Conjugated backbone and ionic properties [1].

In electrochemical synthesis of conducting polymers, three electrode systems in the solution of monomer can be used and conducting polymers can act as positive charged and electrodeposition on electrode surface can be obtained which can be controllable [1]. Electronic conduction in conjugated polymers can be explained by the difference between conductors, semiconductors and insulators as presented in Figure 2.3.

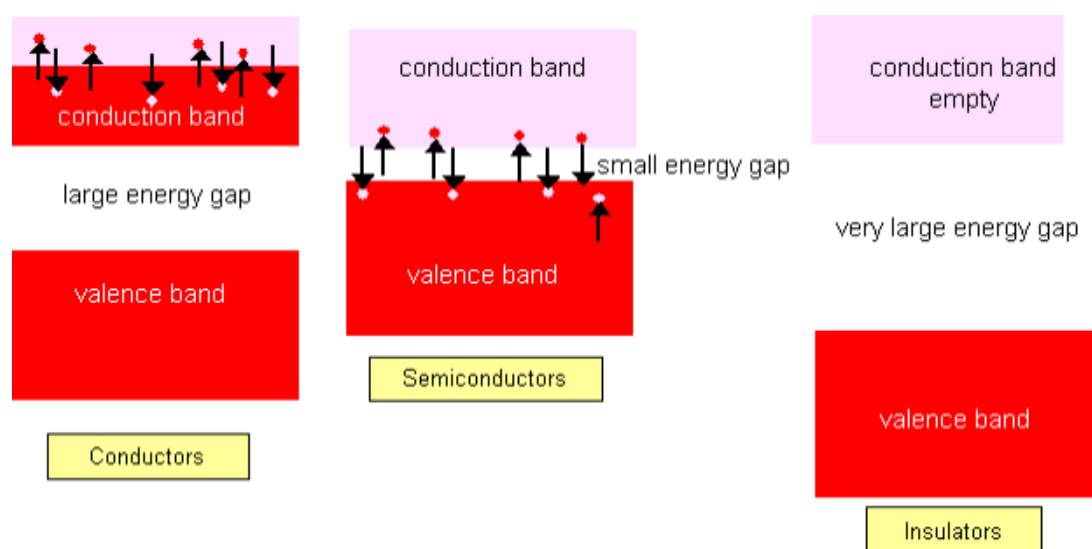


Figure 2.3 : Conduction mechanism [5].

While in conductors, valance band is fully filled and electron can jumped through valance band to conducting band, in insulators the gap between valance band and

conducting bands is too high that electrons cannot pass through the valance band. Furthermore, in semiconductors the external force like heating can make the electrons jump from valance band to the conducting band.

The π -conjugated polymers can be defined with the molecular orbitals. The highest molecular orbital (HOMO) and the lowest unoccupied molecular orbitals (LUMO) can defined the energy transform and electron donating of the orbitals that can be also refered to conducting band and valance band as shown in Figure 2.4 [6].

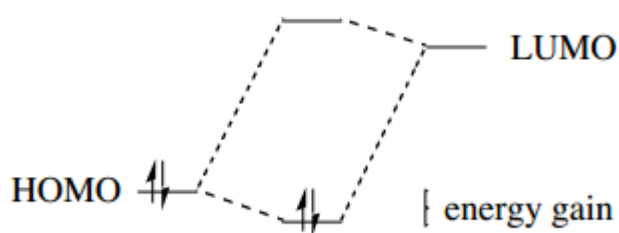


Figure 2.4 : Molecular orbitals [6].

Conducting polymers have wide applications in medicine, consumer products, capacitors, aerospace, drug delivery systems, battery separators, energy storage, electrochromic devices and fuel cells. They can be preferred to be use due to their improved impedance properties and being softer [1].

2.1.1 Polyaniline

Polyaniline can be produced from polymerization of aniline. It has stability to environment and thermal conditions and its electroactivity, conductivity and processability are its important main features to be used in many applications [4]. By the time acid doped form can be named as conducting, polyaniline can be named as non-conducting in basic and neutral forms [4]. Acid/base reactions are important for reversible doping and de-doping of polyaniline [7]. It has stiff backbone and its solubility and processability in most solvents are limited [7]. Polyaniline that has carboxylic group ($-\text{COOH}$) or sulfonyl hydroxide group ($-\text{SO}_3\text{H}$) are important due to their self-doping and faster doping mechanism [7]. Comonomers that involve $-\text{SO}_3\text{H}$, $-\text{COOH}$ groups can be used to prepare self-doped polyaniline, which has better conductivity and solubility in many organic solvents [7].

Generally as electrochemical methods, the monomer can be oxidized for synthesise polyaniline. Potassium dichromate, ammonium persulfate, hydrogen peroxide, cerium nitrate can be used as oxidizing agent to synthesise polyaniline in acidic media [8]. The form of polyaniline named leucoemeraldine, emeraldine and pernigraniline can be defined as reduced form, partially oxidized form and fully oxidized form respectively [8]. Moreover, emeraldine form is known with its electrical conductivity and doping mechanism of it, which can be achieved by protonation or de-protonation with acid bases as presented in Figure 2.5.

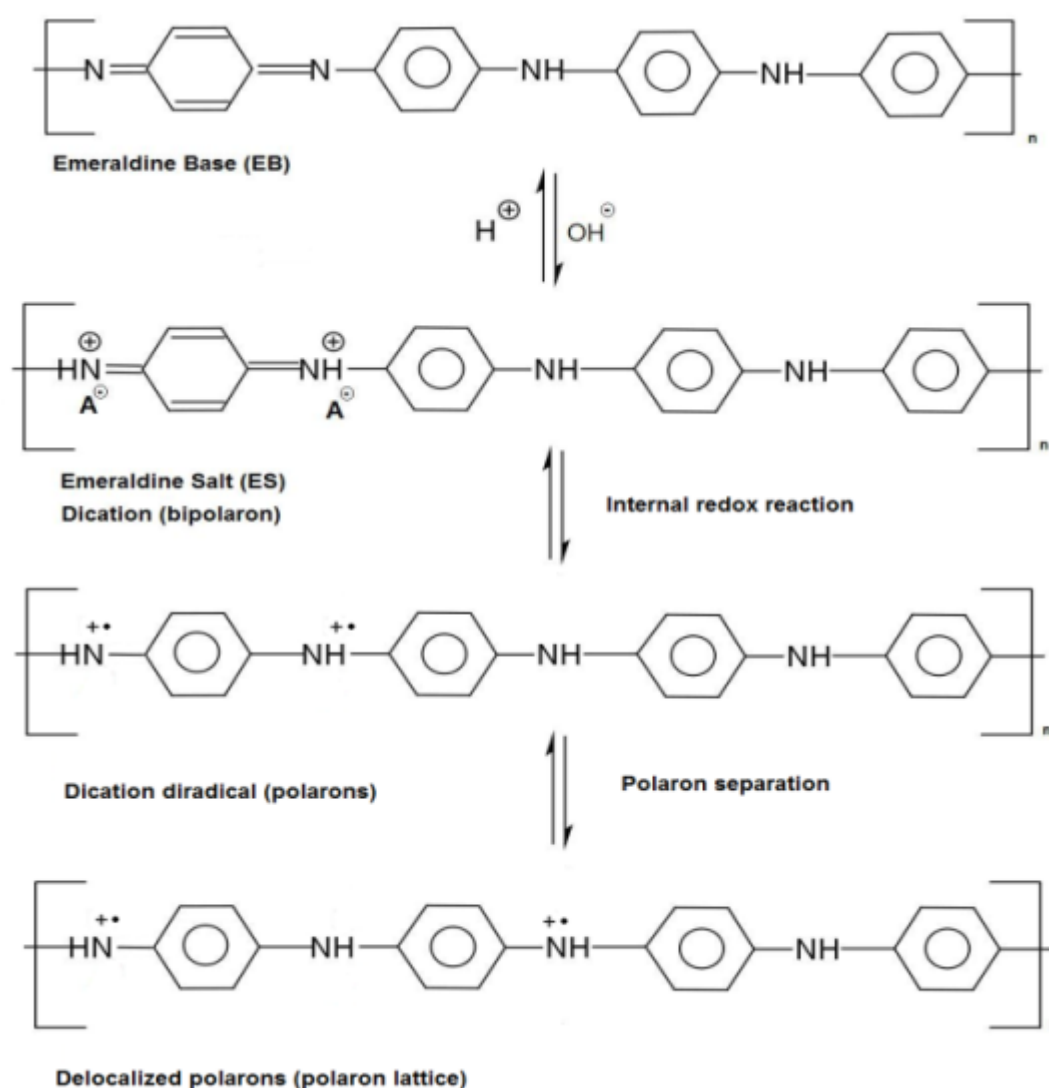


Figure 2.5 : Doping process of polyaniline [8].

2.1.2 Poly (anthranilic acid)

Poly (anthranilic acid) (PANA) is the carboxyl group containing of polyaniline and has property of self-doping. Anthranilic acid that can either named as 2-amino

benzoic acid is used for synthesizing the PANA [7]. Figure 2.6 shows the difference in anthranilic acid over aniline.



Figure 2.6 : Structures of aniline (left), anthranilic acid (right) [7].

To synthesize the carboxylic acid-doped aniline generally anthranilic acid (2-amino benzoic acid) is preferred as dopant. The structure of PANA is presented in Figure 2.7. PANA is not electro-active and generally preferred to be used in electrode materials, antistatic materials and microelectronics [9,10].

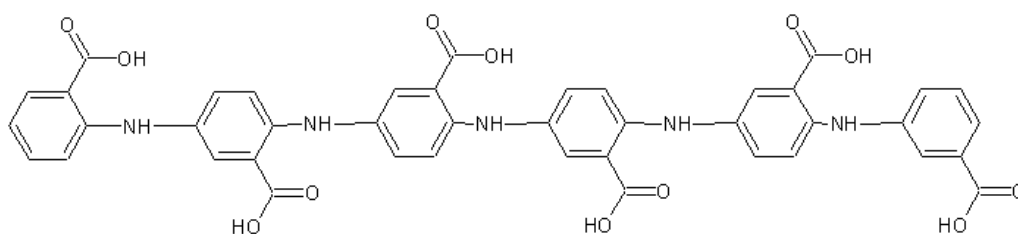


Figure 2.7 : Structure of poly anthranilic acid.

2.2 Biocompatible Polymers

Biocompatible polymers have wide application in the area of pharmaceutical to food industry. Biocompatible polymers are important for bacterial growth or other biomedical purposes [11]. Chitosan, collagens are named as natural biocompatible polymers and poly vinyl alcohol is example of synthetic biocompatible polymers [11]. Most of them are not stable in tissues and have permeability to water that may prevent their uses in biomedical applications like wound dressing.

2.2.1 Poly (vinyl pyrrolidone)

PVP is a synthetic polymer that can be dissolved in many solvents like water and other polar solvents with its flexible chain behaviour [12]. Due to its hydrophilic properties it is used in many areas like cosmetics, pharmaceutical and any other biological applications. PVP has properties like good adhesives that it is generally preferred to be used as food additives or binders in pharmaceutical [13]. Electrospinning of PVP with polypyrrole has increased conductivity that may further be used in sensor applications [14]. For medical applications like wound burn

dressings, PVP is preferred to be blended with polyethylene glycol (PEG) and agar to form hydrogels that may be important for controlling drug dosage and making barrier against bacteria [15]. Due to its hydrophilicity PVP with gold nanocomposites were used as humidity sensors [16]. PVP is used as capping agent in silver nanocrystals formation due to its stabilizing property [17].

Water solubility of PVP can be prevented by applying crosslinking reactions. Crosslinking of PVP can be achieved with 4-diazostilbene-2,2-disulfonic acid disodium salt (DAS) under ultraviolet light. DAS can substitute hydrogen and link with it under UV light with photocrosslinking reaction as presented in Figure 2.8 [18].

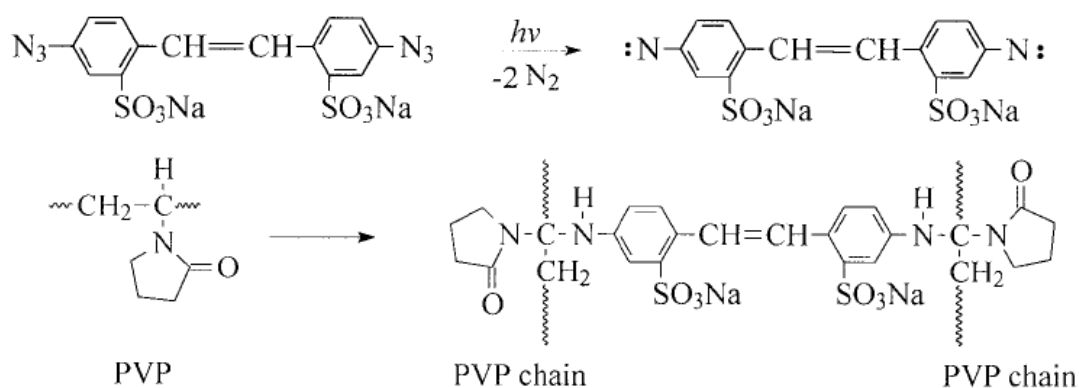


Figure 2.8 : Photocrosslinking reaction of PVP [18].

PVP has structure like protein so that it can be precipitated with many protein precipitators and has immunogenicity and antigenicity properties [19]. PVP is preferred in wound dressing applications with blend of chitosan and PVP as electrospun form [20]. PVP was blended with polyphenylene vinylene for production of nanofibers and there are some studies about crosslinking PVP without adding any chemical [21,22]. Gamma irradiation can be applied to PVP to increase the crosslinking of PVP for gel formation applications [23].

2.2.2 Polycaprolactone

Polycaprolactone is degradable aliphatic polyester that can be degraded in soil, sludge, sediments and biotic environments [24]. In degradation, first amorphous phase is degraded and crystallinity is increased, after that crystalline phase has been observed [24]. Polycaprolactone (PCL) chemical structure is presented in Figure 2.9. By the time PCL has low degradation rate, it has improved elasticity with improved

mechanical properties, non-toxic and easy processability [25,26]. However, PCL has lack of functional groups that may be disadvantages in cell adhesion studies in which generally protein-rich surface with hydrophilic properties gives the highest efficiency [26]. In some studies PCL can be blended with other polymers. In tissue engineering applications, PCL can be blended with starch due to low inflammatory response [27].

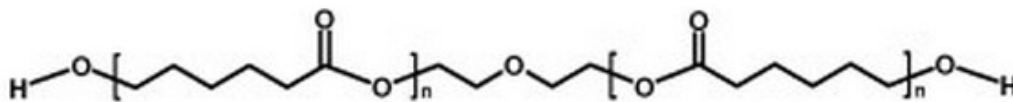


Figure 2.9 : Polycaprolactone chemical structure [28].

2.3 Electrospinning

Electrospinning is the technique that is used to form nanofibers. Under high voltage electrostatic field, nanofibers are formed from the polymer solution [29]. The formed fibers have generally high surface area and small pore size with higher porosity. Changing process parameters like voltage, distance and concentration of polymer would affect the result of the fiber formation [29].

2.3.1 Electrospinning process

The experimental setup of electrospinning is presented in Figure 2.10. Prepared polymer solution is pumped with an appropriate feed rate under high voltage supply and by the help of syringe pump or syringe driver. The polymer solution that is prepared with a volatile solvent forms nanofibers on the collector generally made of aluminium. The diameter of the nozzle that the polymer solution passes is general effect the fiber formation. The high voltage supply consists of negative and positive electrode. By the time negative electrode is attached to the aluminium collector, positive electrode is attached to the needle of the syringe. The collector can be placed with different shapes and orientation of nanofibers can be made [30]. As it was shown in Figure 2.10, Taylor Cone is created during the electrospinning process that can be made by the liquid jet from the spinneret [30]. The volatile solvent of the polymer solution is rapidly evaporated that nonwoven porous mat of nanofibers are obtained on the aluminium collector. Rotating drums or disc can be alternative to the flat aluminium collectors [31]. Hollow fiber nanofibers can also be produced.

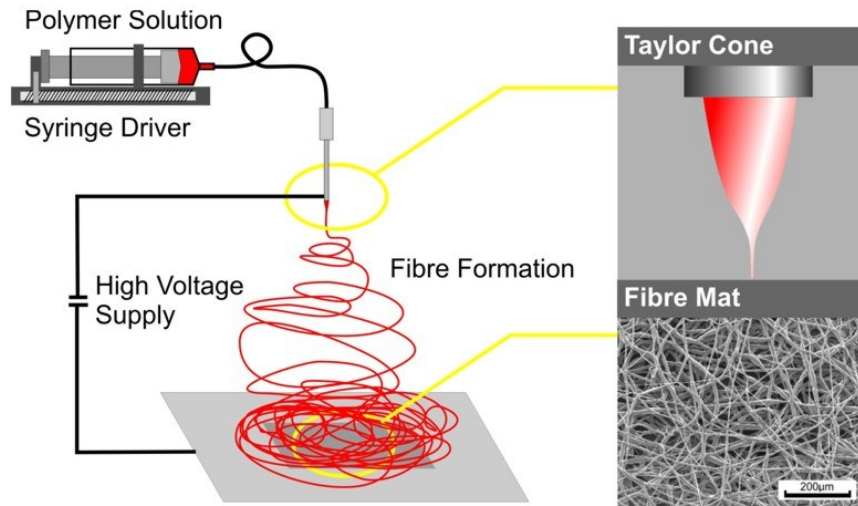


Figure 2.10 : Experimental setup of electrospinning [32].

2.3.2 Electrospinning parameters

In the electrospinning process, there are three parameter classes named solution parameters, process parameters, environmental conditions that are important for fiber formation process. In Table 2.1, it is determined the three main electrospinning parameters. Polymer solution concentration, viscosity, conductivity, surface tension, dielectric constant and solvent volatility are the main parameters that are defined as solution parameters. Electrical potential, feed rate of the polymer solution, diameter of the orifice and distance between the tip and the collector are the processing parameters that effect the nanofiber formation. Environmental conditions can be defined as temperature, humidity, pressure, and local atmosphere flow around the area [33].

Table 2.1 : The summary of parameters that effect the fiber formation [33].

Solution Parameters	Process Parameters	Environmental Conditions
Concentration	Electrostatic Potential	Temperature
Viscosity	Working Distance	Humidity
Surface Tension	Feed Rate	Local Atmosphere Flow
Conductivity	Orifice Diameter	Pressure
Dielectric Constant		
Solvent Volatility		

2.3.2.1 Polymer solution parameters

Polymer solution parameters are important for choosing the best appropriate polymer solvent mixture to obtain the desired homogeneity of nanofibers with the desired diameter. Same polymer can have different average diameter as the polymer solution properties become different.

By the time electrical conductivity of solvents are too low and they can be improved by adding salts, acids and bases, the result in the change in electrical conductivity can affect the nanofibers formation. Also, dielectric constant of the solvent can affect the result and make a difference in the produced nanofibers diameter. For instance, at the same polystyrene concentration with the different solvents like toluene, THF and DMF the produced nanofibers have different properties [34]. By the time THF has lower dielectric constant like 2.38 has the highest fiber diameter around 1.3 and 1.6 μm , DMF with the dielectric constant as 37.06 has nanofibers diameter about 0.43 μm [34]. As it is a result, solvent with higher dielectric constant makes the thinnest nanofibers. In Table 2.2, it is shown that some solvents dielectric constants are shown in Table 2.2.

Overcoming the surface tension of polymer solution can be achieved by the charges on the polymer solution [34]. Also, bead formation on nanofibers and surface tension is related to each other as surface tension is known the attractive forces from liquid to other liquid molecules [34]. In solvent mixtures, the surface tension can be related to the mole fraction of the solvents that are mixed [34]. Reducing the surface tension generally lowers the bead formation by the cause of small surface area per unit mass [36]. To lower the surface/interfacial tension, surfactants can be used as additives in production of electrospun nanofibers [34]. TritonX-405, dodecyltrimethylammonium bromide (DTAB) and tetrabutylammonium chloride (TBAC) are surfactants that can be used efficiently without forming any bead [37].

Solvent volatility is important parameter due to its effect in the electrospinning process. The solvent should be evaporated when electrospinning jet reaches to the collector to form nanofiber [34]. The volatility of solvent is also depending on boiling point, specific heat, enthalpy, vapour pressure, vaporization heat and interaction between solvent and solute molecules [34]. The rapid evaporation of solvents can cause the collected nanofibers with having some amount of solvent

which causes relaxation and need for post processes [38]. Evaporation of solvent and pore formation are related to each other [39].

Table 2.2 : Dielectric constants of solvents [35].

Solvent	Dielectric constant
Acetic acid	6.15
Acetone	20.7
Acetonitrile	37.5
Anisole	4.33
Benzene	2.27
Bromobenzene	5.17
Carbon disulfide	2.6
Carbon tetrachloride	2.24
Chlorobenzene	5.62
Chloroform	4.81
Cyclohexane	2.02
Dibutyl ether	3.1
Dichloromethane	8.93
Diethylamine	3.6
Diethyl ether	4.33
1,2-Dimethoxyethane	7.2
N,N	37.8
N,N	36.7
Dimethyl sulfoxide	46.7
1,4-Dioxane	2.25
Ethanol	24.5
Ethyl acetate	6.02
Ethyl benzoate	6.02
Formamide	111
Hexamethylphosphoramide	30
Isopropyl alcohol	17.9
Methanol	32.7
2-Methyl-2-propanol	10.9
Nitrobenzene	34.82
Nitromethane	35.87
Pyridine	12.4
Tetrahydrofuran	7.58
Toluene	2.38
Trichloroethylene	3.4
Triethylamine	2.42
Trifluoroacetic acid	8.55
2,2,2-Trifluoroethanol	8.55
Water	80.1

Viscosity can affect the fiber formation in electrospinning process. Viscosity measures the resistance of a material to flow and can be divided into four groups named relative viscosity, specific viscosity, reduced viscosity and intrinsic viscosity [34]. If the viscosity is too low no fiber can be formed, only polymer particles can be collected on the collector [34]. Also, in some studies fibers can be obtained but with many beads. For instance, PCL nanofibers with the concentrations of 4 (w/v) have many beads by the time PCL nanofibers with the concentrations of 15(w/v) have almost no beads [40]. By the time processing nanofibers with low viscosity has some problems, processing the nanofibers with high viscosity can also cause problems like pumping difficulties [33]. Viscosity and molecular weight of the polymer is related to each other. As compared to polymers with different molecular weights, it is known that polymer with higher molecular weight has the highest viscosity in the same solvent [33]. Polymer chain entanglement is also important as if it is related to molecular weight, concentration and viscosity.

2.3.2.2 Polymer processing parameters

The applied voltage supply, the feed rate, diameter of orifice and distance between the needle tip and collectors are the polymer processing parameters that affect the result of the change in fiber formation.

High electrical voltage is needed for the starting of nanofibers formation as the voltage helps to induce the charges in electrospinning solution. The change in the applied voltage can affect the result of the nanofibers. For instance, polyacrylonitrile nanofibers diameter is decreased with the increasing in the applied voltage [41]. And also, in some studies bead formation can be observed by the cause of the decrease in the initiation jet [41]. Moreover, the shape of bead can also be affected with the cause of high voltage [34]. To supply high voltage generally DC voltage is preferred, but in some studies AC voltage can also be used which can increase the diameter of nanofibers with less bending instability and less stretching [34].

Furthermore, the feed rate of the electrospinning solution can affect the result of the formed nanofibers. As it determines the volume of polymer solution that is used to form nanofibers in the time interval, it is generally determined as ml/hr, ml/min. If the feed rate is too high shots of polymer solution can be observed on the collector

and if it lowers, solution can be removed faster than the feed rate that may a result of bead formation [41].

Internal diameter of the orifice effects the fiber formation. The smaller diameter can cause the less exposure of the solution to atmosphere that may prevent the clogging the orifice and also, the fibers are formed with decreased average diameter [33].

Moreover, the distance between tip and collector can result in the change in the fiber diameter. The distance generally changes the travel time of the electrospinning solution. If the distance is too low, shorter travelling time is observed to form fibers. There may not enough time for polymer solution to evaporate the solvent so merging the fibers can be observed [34]. Also, fiber morphologies can be changed with the change in the distance between tip and collector. For instance, in shorter distance flat, wet and bundle of nanofibers can be observed by the time in the longer distance nanofibers with cylindrical, dry and straight morphology can be observed [41].

2.3.2.3 Environmental conditions

Another important parameter that affects the electrospinning process is the environmental conditions like temperature, humidity, pressure and local atmosphere flow. At high humidity like 60%, the electrospinning solution can absorb the ambient water and fibers are not well but have increased morphology like having porous structure [34,42]. Moreover, clogging in the office can be observed in the low humidity which may be the cause of drying the volatile solvent more rapidly [34]. Furthermore, temperature affects the result of fiber formation. In a study, there is no fiber formation is observed in the temperatures of 282 K and 303 K at the constant humidity of 60%. At low humidity with the low and high temperature, the fibers that are observed has decreased diameter [42]. At low temperatures the reduced fiber diameter can be explained by the decreased evaporation rate of the solvent with the decreased solvent and causing the longer time to solidification. However, at higher temperatures rigidity of the polymer changes and solution viscosity becomes lower and higher stretching rate with decreased diameter of nanofibers can be observed [42].

Furthermore, pressure is also effects the electrospinning process. At lower pressure under the atmospheric pressure electrospinning cannot be done with cause of direct discharge of electrical charges [34].

2.3.3 Biomedical applications of nanofibers

Beside the biomedical applications nanofibers have wide range applications. Supercapacitors, electrical conductive batteries, nanoelectronic devices, filtration membranes, photochromic devices and protective textile materials are the main applications of the nanofibers that are formed by electrospinning [43-48].

Electrospun nanofibers can be used in various biomedical applications like tissue engineering, drug delivery systems, sensor application and bone regeneration. Porous nature of nanofibers and allowing penetration of atmospheric oxygen to the wound makes the electrospun nanofibers to be used in wound dressings [49]. Controlled release of drug can be supplied with drug delivery systems with electrospun nanofibers as observed in Figure 2.11 [50,51].

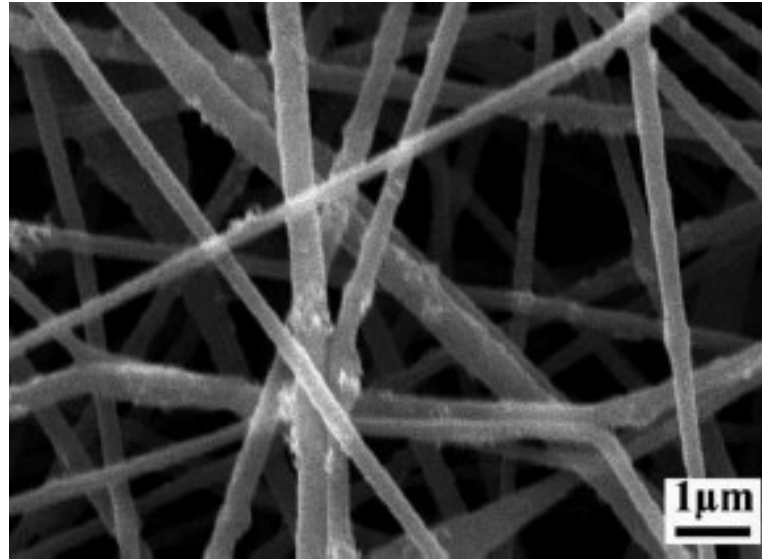


Figure 2.11: Drug loaded nanofibers [50].

Furthermore, electrospun nanofibers are used for cell adhesion and proliferation as it is shown in Figure 2.12 [52]. Moreover, electrospun nanofibers can be used in bone reconstruction studies by mimicking the natural bone [54]. Moreover, chemical modifications can be done to those nanofibers to immobilize proteins and enzymes [55]. Surface modification of electrospun nanofibers can be needed for biomedical applications. Bioactive molecules can interact with electrospun nanofibers with various ways such as plasma treatment, surface graft polymerization, wet chemical methods or co-axially electrospinning [56].

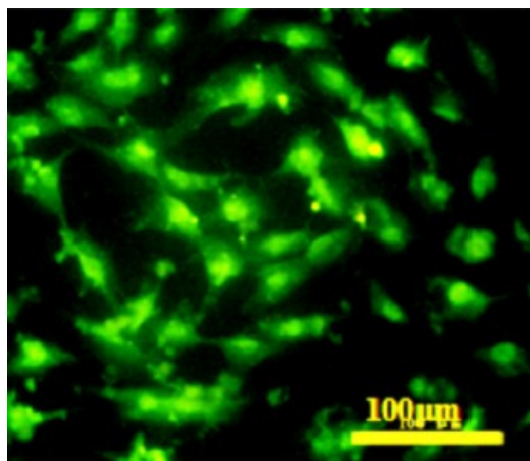


Figure 2.12: Nanofiber scaffolds [53].

2.4 Characterization Techniques

The electrospun nanofibers can generally be characterized with scanning electron microscopy and spectroscopic techniques like UV-Vis and FTIR-ATR and their impedance property can be measured with electrochemical impedance spectroscopy.

2.4.1. Principle of UV-Vis spectrophotometry

As it is presented in Figure 2.13, ultraviolet light has longer wavelength than X-rays and shorter wavelength than visible light. As it is known that there is an inverse proportion between the wavelength and energy. By the time microwave and radio waves have the highest wavelength, they have the lowest energy.

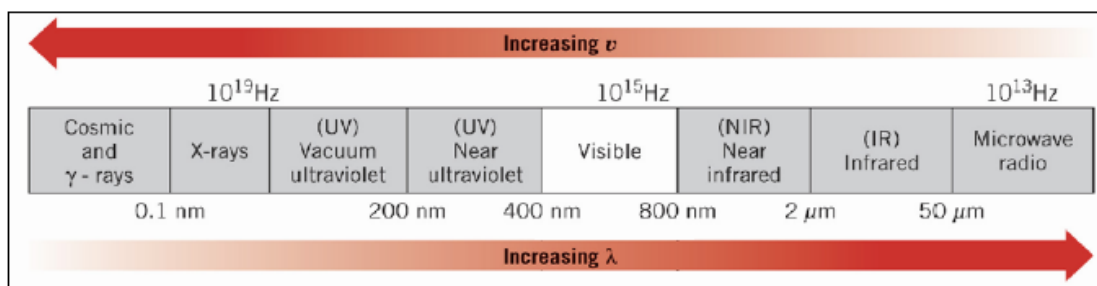


Figure 2.13: Ultraviolet spectrum [57].

In ultraviolet and visible spectroscopy, the absorption of light 190-400 nm as ultraviolet and 400-800 nm as visible light is measured by causing electronic transition in the molecules [58]. The common transitions in molecules are presented in Figure 2.14. π and σ are defined as bonding orbital, n is defined as non-bonding and π^* or σ^* are defined as anti-bonding orbitals. As energy is absorbed by molecule,

electron transport from non-bonding n or bonding π orbital to anti-bonding π^* or σ^* orbital can be observed.

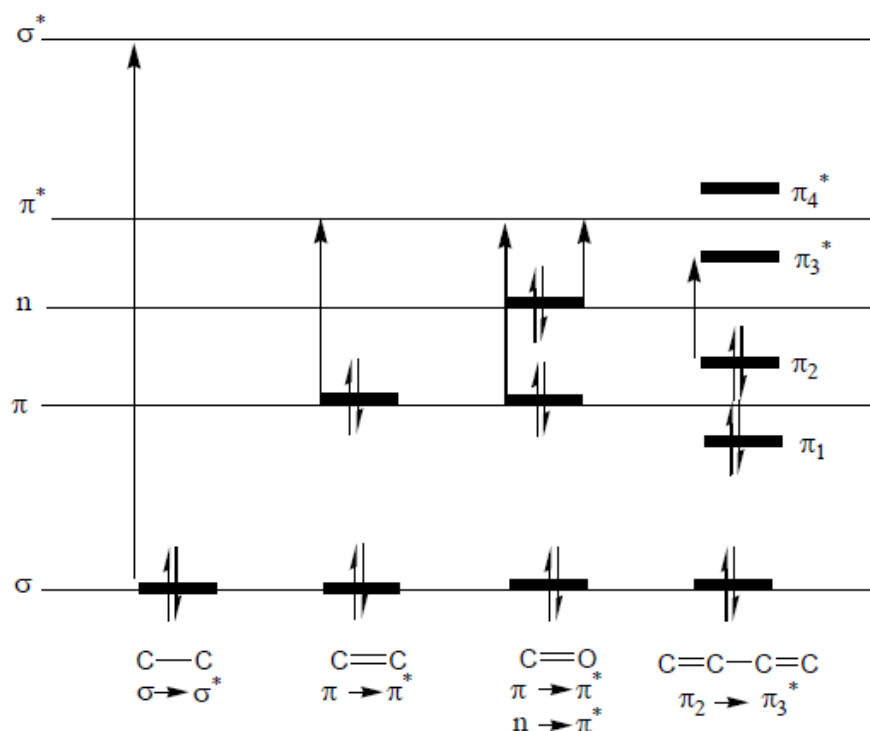


Figure 2.14: Orbitals and energy transfer [58].

As it is indicated in Table 2.3, the absorbed radiation and the colour are related to each other and these colours are specific to the absorbed energy and electron transition. The absorbance that is read in the UV-Vis spectroscopy is depended on the concentration of the solution, thickness of the measurement cell and cell absorption coefficient.

Table 2.3: Colour and light absorption in UV-Vis spectroscopy [59].

Color Absorbed	Color Observed	Absorbed Radiation (nm)
Violet	Yellow-green	400-435
Blue	Yellow	435-480
Green-blue	Orange	480-490
Blue-green	Red	490-500
Green	Purple	500-560
Yellow-green	Violet	560-580
Yellow	Blue	580-595
Orange	Green-blue	595-605
Red	Blue-green	605-750

2.4.2. Principle of FTIR-ATR spectrophotometry

FTIR-ATR spectrophotometry is a tool in which attenuated total reflectance is combined with infrared spectroscopy. Working principle is presented in Figure 2.15. The infrared radiation first comes to the transmitting crystal generally preferred ZnSe and Ge that have high refractive index and penetrated into the sample



Figure 2.15: Working principle of FTIR-ATR [60].

Each organic molecule has characteristics bending or stretching between the vibrations of bonds between atoms [61]. From the infrared radiation each atom has different vibrations like stretching and bending. Stretching vibrations can be divided into two that can be named as asymmetric stretching and symmetric stretching that are shown in Figure 2.16.

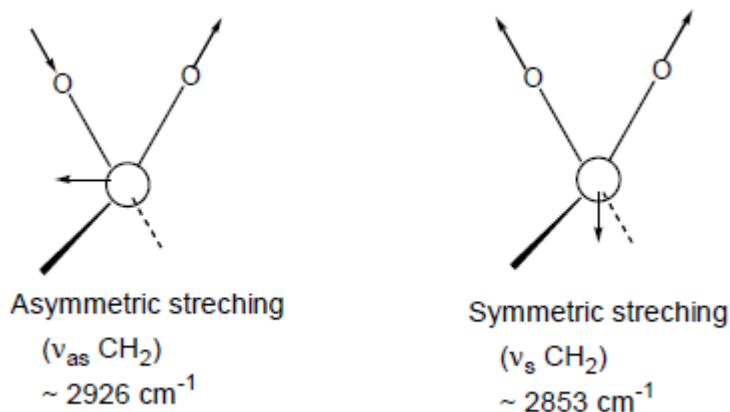


Figure 2.16: Asymmetric and symmetric stretching [58].

Moreover, bending between atoms can be in various shapes like in-plane bending and out-of-plane bending. That can be scissoring, rocking, twisting or either wagging as shown in Figure 2.17. Some examples of definition of vibrations are shown in Table 2.4.

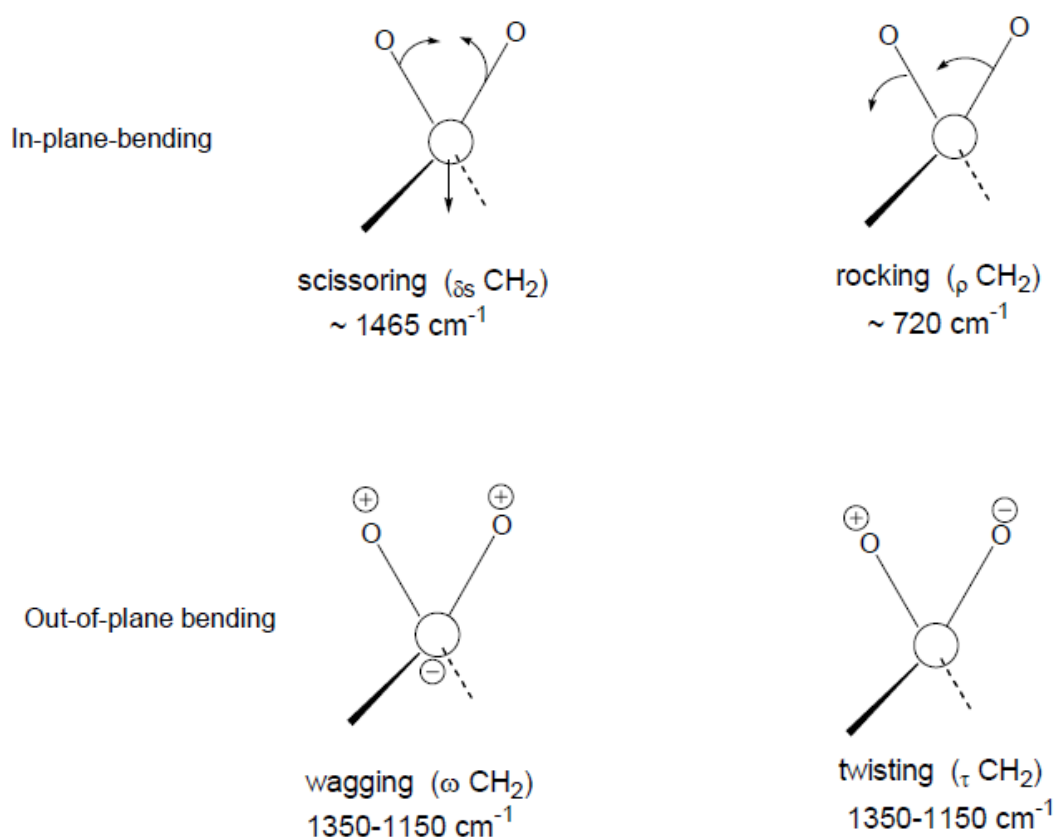


Figure 2.17: Bending between atoms [58].

Table 2.4: Some vibrations in FTIR-ATR spectroscopy [58].

Spectral Range, cm ⁻¹	Chemical Group	Group Vibration
3700-3200	-OH	O-H stretching
3400-3330	-NH ₂	Asymmetric stretching
3300-3250	-NH ₂	Aymmetric stretching
3065-3030	-C-H _{aromatic}	C-H stretching
3020-2950	-CH ₃	Asymmetric stretching
2960-2910	-CH ₂	Asymmetric stretching
2970-2860	-CH ₃	Aymmetric stretching
2860-2840	-CH ₂	Symmetric stretching
2590-2560	-SH	S-H stretching
2600-2350	-B-H	B-H stretching
2450-2275	-P-H	P-H stretching
2300-2230	-C≡C-	C≡C stretching
2260-2230	-C≡N-	C≡N stretching
2250-2100	-Si-H	Si-H stretching
2250-2100	-C-D	CD, CD ₂ , CD ₃ stretching
1760-1720	-C=O	In organic acids
1740-1700	-N-C=O	In ketones

2.4.3. Principle of scanning electron microscopy

Scanning electron microscopy (SEM) is the technique that is used to overcome the limitations of light microscopy that is based on the light. A schematic diagram of scanning electron microscopy is shown in Figure 2.18. In SEM, beams of electrons are used for illumination. SEM can easily be applied to conductive surfaces and generally suitable for particle size determination of nanoparticles, and investigation of surface morphology of many surfaces. The condenser lens is used to focus the electrons into beam and after beams passes through the objectives, the image can be taken.

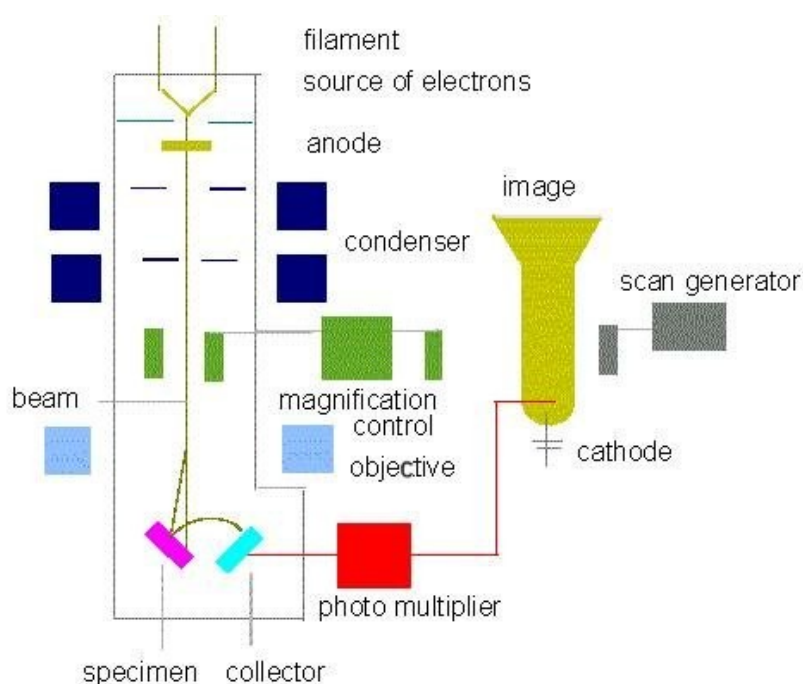


Figure 2.18: Schematic diagram of scanning electron microscopy [62].

The samples that are going to be investigated by SEM should be modified with gold sputtering. The gold sputtering of the samples that are prepared for SEM has higher resolution and improved result. For SEM visualization, the medium should be the vacuum medium. SEM has advantages over other microscopes like having 0.2 nm resolution with 100000X magnifying power. However, generally non-living objects can be investigated under SEM.

2.4.4 Principle of electrochemical impedance spectroscopy

In electrochemical impedance spectroscopy (EIS), AC frequency is used to determine the impedance properties of electrodes and complex interfaces [63]. Frequency of impedance measurement can vary from milli hertz to 100 kilohertz, and complex number of real and imaginary is obtained from the impedance measurement. In mid-frequency range like 1000 Hz to 1 Hz, high phase shift can be determined with the capacitive behaviour [64]. The Nyquist plots are important for determining the ohmic/solution resistance and total resistance in the electrochemical cell with the imaginary part of the impedance and real part of impedance [64]. Bode magnitude can be important for determining the circuit impedance [63]. A schematic diagram of EIS is shown in Figure 2.19.

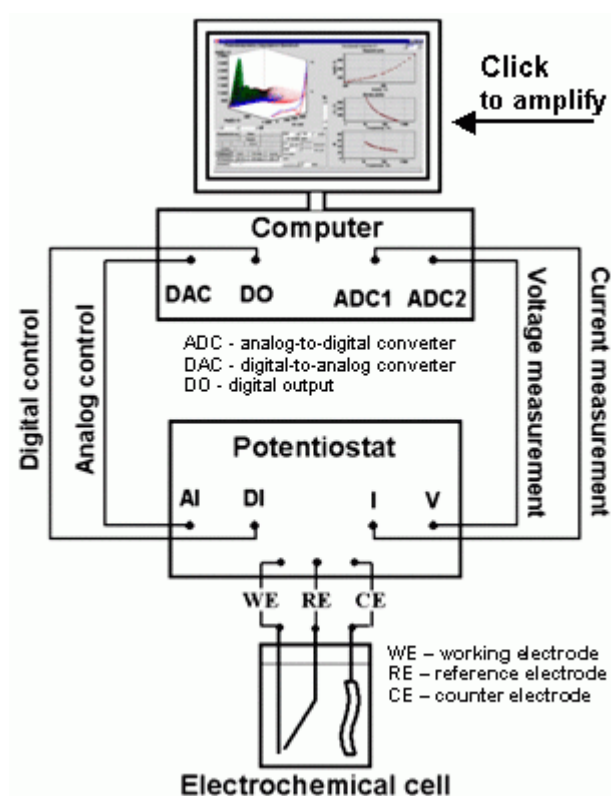


Figure 2.19: Schematic diagram of electrochemical impedance spectroscopy [65].

2.5 Streptavidin

Streptavidin is an important model protein and generally used in studied due to its high interaction with biotin. Biotinylation of proteins can be achieved by using biotin ligase and streptavidin was immobilized to surface due to the high binding capacity with biotin [66]. Streptavidin and biotin has tight and specific interaction that is

named as strong non-covalent interaction which is defined with femtomolar as dissociation constant [67].

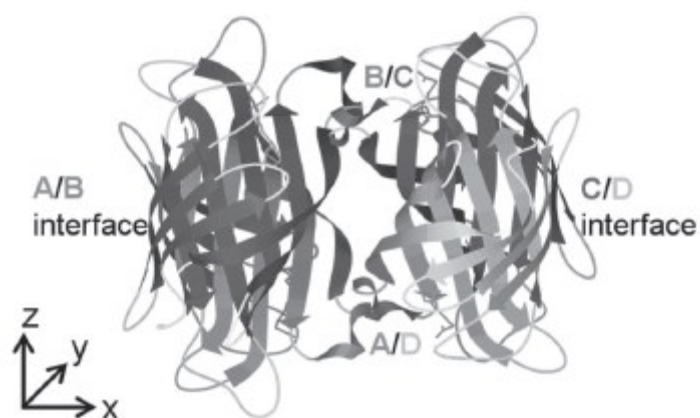


Figure 2.20: Subunits of streptavidin [68].

STV is important protein that has many binding molecules which can be divided into three subgroups named peptidic streptavidin binders, aptameric streptavidin binders and low-molecular weight streptavidin binders [69].

3. EXPERIMENTAL PART

3.1 Materials

Poly(vinyl pyrrolidone) (Aldrich, Mw=1 300 000) and poly(caprolactone) (Polyscience, Mw=43000-50000) were used in this study. Poly(anthranilic acid) was synthesized in Germany. Streptavidin from *Streptomyces avidinii*, N-(3-Dimethylaminopropyl)-N'-ethylcarbodiimide hydrochloride, N-Hydroxysuccinimide sodium salt were purchased from Sigma. Buffer solution pH 7.0 (20 °C) (Fluka), Dulbecco's Phosphate Buffered Saline (Sigma), Bicarbonate buffer solution (Fluka), MES Buffer pH 4.7 and borate buffer (Thermo Scientific) were used in this study. Dimethylformamide (DMF), tetrahydrofuran (THF) and ethanol (EtOH) obtained from Merck as analytical grade and were used without further purification. Hydrochloric acid (HCl) and sulphuric acid (H₂SO₄) were also purchased from Merck Chemicals.

3.2 Preparation of Electrospinning Solutions

3.2.1 Electrospinning of PANA/PVP blends

PVP and PANA were mixed in dimethylformamide (DMF) or a mixture of DMF and ethanol (EtOH) with a weight ratio of 50/50 (w/w). PVP was fixed to 2g in 10g DMF and PVP in mixture of EtOH and DMF was fixed to 1.5 g, the weight ratios between PVP and PANA in polymer solution were changed from 1/30 to 1/5 (%w/w) as blend. Prepared blend solutions were stirred for 3 hours before electrospinning.

3.2.2 Electrospinning of PANA/PCL blends

PCL was stirred in tetrahydrofuran (THF) for 24hours with 20% (w/v) ratio of PCL/THF. PANA was added with different weight ratios like 5, 15 and 25%.

3.2.3 Electrospinning of PANA/PCL/PVP blends

PCL and PVP of 1g were dissolved in THF/DMF solvent mixture for 20% (w/v) concentration at 45°C for 24 hours. PANA of 10% of weight ratio PCL/PVP was added to solvent mixture to obtain PANA/PCL/PVP blended nanofibers.

3.3 Process Setup and Electrospinning

All experiments were performed at room temperature. A syringe pump (NE-500 model, New Era Pump Systems, Inc., USA) and DC power supplier (ES50 model, Gamma High Voltage Inc., USA) were used as electrospinning equipment. Collector was covered with aluminium foil. The experiment was done in a plexiglass box. The electrospinning solutions were then loaded into a 2.5 ml syringe with a tip of 0.7 mm inner diameter. Distance between tip and collector was 20 cm. For, PANA/PVP blends 15 kV and 0.5 ml/hour was applied as voltage and feed rate. Moreover, this feed rate was increased to 1 ml/hour for PANA/PCL blends due to the high volatility of THF. For PANA/PCL/PVP blends the feed ratio was 0.5 ml/hour and voltage is 15 kV.

3.4 UV-Visible and FTIR-ATR Spectrophotometry

Nanofibers were analysed by FTIR-ATR spectrophotometry (Perkin Elmer, Spectrum One B, with an ATR attachment Universal ATR-with ZnSe crystal). Samples were scanned at the wavenumber range 4000–650 cm^{-1} . Perkin Elmer UV Spectrophotometer recorded UV–vis spectrophotometric results between 300–800 nm wavelengths. In FTIR-ATR spectroscopy measurement, the nanofibers were directly measured. For UV-Vis spectrophotometric measurement, nanofibers of 0.0015 g PANA/PVP was dissolved in 10g solution of EtOH/DMF and DMF. For PANA/PCL and PANA/PCL/PVP blends, 0.0024 g nanofibers were dissolved in 10 ml solution of THF and/or THF/DMF.

3.5 Scanning Electron Microscopy

The SEM images of the nanofibers were taken by using LEO SUPRA 35 VP SEM and Carl Zeiss EVO MA 10. SEM analysis was performed at an accelerating voltage

of 10 kV. Gold sputtering were applied to the samples. Diameters of nanofibers were measured by Image J analysis software.

3.6 Electrochemical Measurements of Electrospinning Solutions

Conductivity of electrospinning solutions was measured with Parstat 2263 Electrochemical Analyser via electrochemical impedance spectroscopy measurement. For measurement, electrospinning solutions were diluted as 1/30. Three-electrode system consist of two platinum as working and counter electrode and one silver as reference electrode was used. Electrochemical impedance software named PowerSine was used to carry out impedance measurements between 0.01 Hz and 100 kHz.

3.7 Conductivity

PANA has limited solubility on many solutions like water. It was realized that the nanofibers that were produced with the blend of PANA/PVP are soluble in water which makes possible to make measurement of nanofibers conductivity. Conductivity of dissolved electrospun nanofibers in aqueous solution was measured using a EC215 Conductometer HANNA Instruments. For this measurement 0.0025 g nanofibers were weighed and dissolved in 50 ml water.

3.8. Electrochemical Impedance Spectroscopy (EIS) and Equivalent Circuit Modelling (ECM) for Electrospun Nanofibers

EIS measurements were done using three electrode cell configuration in which counter electrode is platinum, reference electrode is silver and working electrode is nanofibers with the dimensions of 4cm to 0.5cm and electrode area was $2 \times 2 \text{ cm}^2$. The electrochemical cell was connected to a Potentiostat (PAR 2263) that was connected to a PC. An electrochemical impedance software, PowerSine, was used to carry out impedance measurements between 0.01 Hz and 100 kHz and 0.1M HCl, and PBS were used as EIS measurement solutions. The impedance spectra was analyzed using ZSimpWin V3.10, an AC-impedance data analysis software and modelling of nanofibers were done and investigated.

3.9 Streptavidin Immobilization

For streptavidin immobilization, the nanofibers of more hydrophobic with the functional groups of -COOH were chosen. So that, electrospun nanofibers of PCL in THF with the %25 PANA containing were used in streptavidin immobilization study. For 0.26M EDC preparation 0.1g EDC was dissolved in MES buffer with the pH 4.7 which was prepared with dissolving MES buffer packs in 500 ml distilled water. 15 minutes was waited for crosslinking reaction. After that, NHS of 0.23M was prepared with dissolving in phosphate buffer, PBS or borate buffer and was reacted with the nanofibers for 15 minutes. Investigation of borate buffer was preferred because being amine-free buffer that may be important for the immobilization result. After that, streptavidin was immobilised on that nanofibers by dissolving 0.2mg streptavidin in 1 ml bicarbonate buffer and waited for 30 minutes. Finally, to prevent the nonspecific bonding of streptavidin on nanofibers distilled water was used as washing step. As control reaction, EDC reaction without STV, EDC and NHS reaction without STV on those nanofibers was done. Their FTIR-ATR measurement was done to ensure that streptavidin was immobilized efficiently without any contamination.

3.10 Microscopic Observation

For observation of protein the food dye named Dye E133- Indigo Blue was used. In immobilization step, when protein was dissolved in bicarbonate buffer the dye is also added and after washing step the light microscope was used. As control reaction, the streptavidin was dissolved with dye but the EDC-NHS system was not used. Also, the fiber surface was only modified with dye solution to investigate the observation as it streptavidin or dye immobilization and adhesion of molecules or chemical reaction.

4. RESULTS AND DISCUSSION

4.1. Characterization of PANA/PVP Blends

4.1.1 UV-Vis spectrophotometer results of PANA/PVP blends

Nanofibers of PANA/PVP blends were dissolved in DMF for 20% (w/w) PVP containing and dissolved in EtOH/DMF (50% w/w) solution for 15% (w/w) PVP containing with the same weight ratio of nanofibers to measure their spectroscopic results. The UV-vis spectra of the PANA/PVP nanofibers in EtOH/DMF solutions are presented in Figure 4.1.

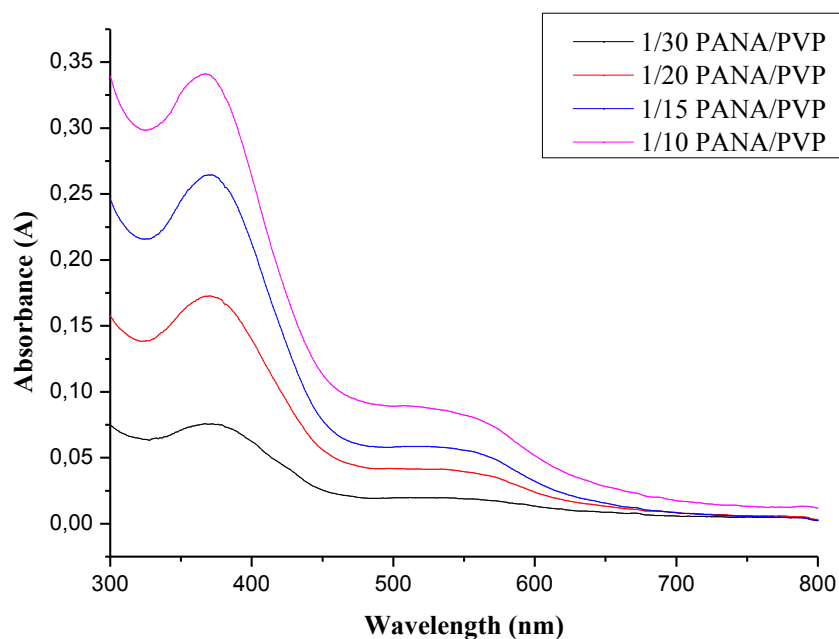


Figure 4.1 : UV-Vis spectra of PANA/PVP blend nanofibers dissolved in EtOH/DMF.

In Figure 4.2, the UV-vis spectra peaks of the PANA/PVP nanofibers in DMF are presented. The absorption peaks at 366-372 nm and 500-600 nm are presented in both Figure 4.1 and Figure 4.2. The absorption peak at about 370nm can be attributed to π - π^* transition in benzoid rings of PANA and the peak at 500-600 nm can be attributed to exciton like transition from benzoid to quionoid ring of PANA [70].

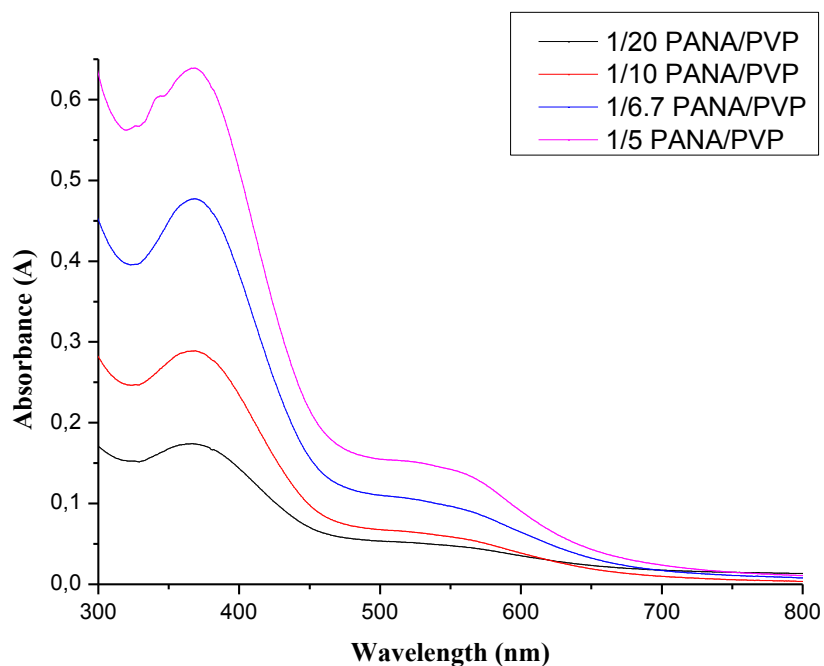


Figure 4.2: UV-Vis results of PANA/PVP blend nanofibers dissolved in DMF.

As it is shown in Figure 4.3, there is a proportional increase in absorption peaks due to the increase of PANA ratio in blended nanofibers. Also, it is presented in Figure 4.4 that absorbance at specific peak of PANA increases with the nanofibers that have increasing weight ratio of PANA in PANA/PVP blends.

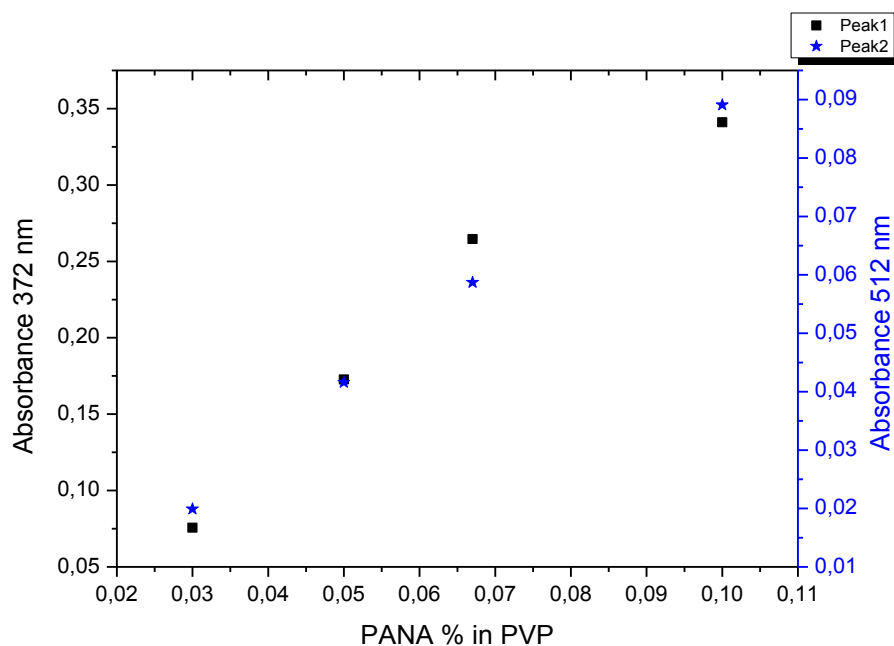


Figure 4.3 : Absorbance peaks of PANA/PVP blend nanofibers dissolved in EtOH/DMF.

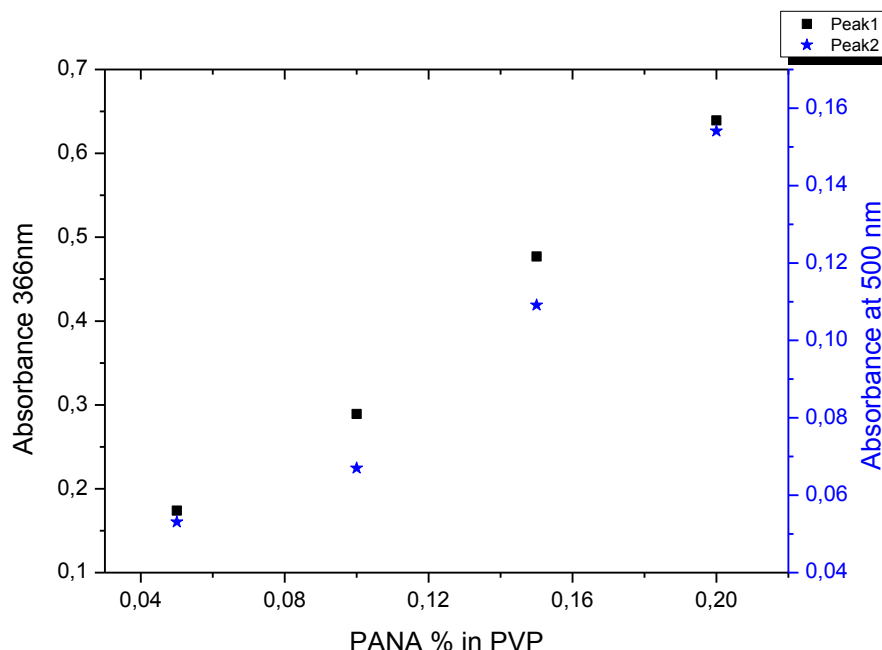


Figure 4.4: Absorbance peaks of PANA/PVP blend nanofibers dissolved in DMF.

4.1.2 FTIR-ATR spectrophotometric analysis of PANA/PVP blends

The FTIR-ATR spectra of PANA/PVP nanofibers are presented in Figure 4.5 and Figure 4.6. PVP has characteristic peaks at 3449, 2949, 1658, 1420, 1283, 1269, 1228 and 932 cm^{-1} . The peak at 3449 cm^{-1} is attributed to the O-H stretching, 2949 cm^{-1} is attributed to C-H out of plane stretching, 1658 cm^{-1} is attributed to C=O stretching, 1420 cm^{-1} is attributed to N bond stretching, the peaks at 1283 cm^{-1} , 1269 cm^{-1} , 1228 cm^{-1} are attributed to C-O stretching and 932 cm^{-1} is attributed to N-H stretching [71]. PANA have wide band between 3750-1800 cm^{-1} , and the peak 3200 cm^{-1} is attributed to O-H stretching and the peak at 3034 cm^{-1} can be attributed to C-H stretching. The peak at 1688 cm^{-1} is attributed C=O stretching, 1567 cm^{-1} is attributed C=C stretching, 1507 cm^{-1} is attributed -N-H stretching, 1251 cm^{-1} and 1103 cm^{-1} are attributed C-N stretching, the peaks at 821 cm^{-1} , 753 cm^{-1} , and 679 cm^{-1} are attributed C-N out of plane stretching of PANA. In blend nanofibers of PANA and PVP, a peak around 1570 cm^{-1} is observed which can be attributed to C=O stretching and is characteristics for PANA.

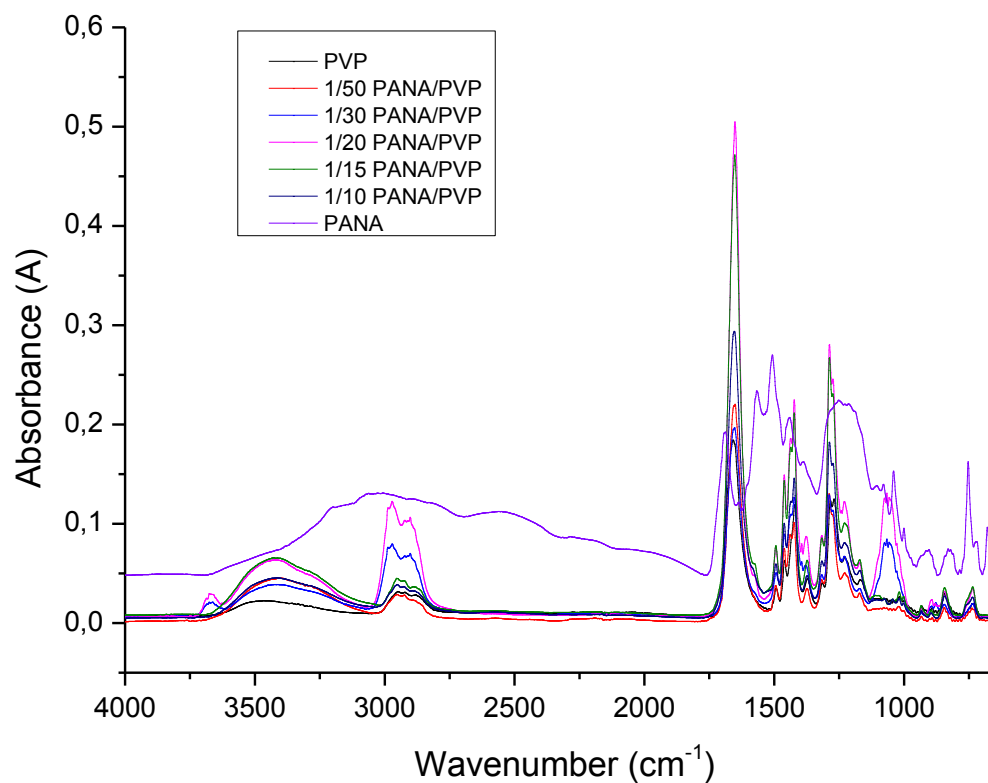


Figure 4.5 : FTIR-ATR spectra of PANA/PVP nanofibers electrospun in EtOH/DMF.

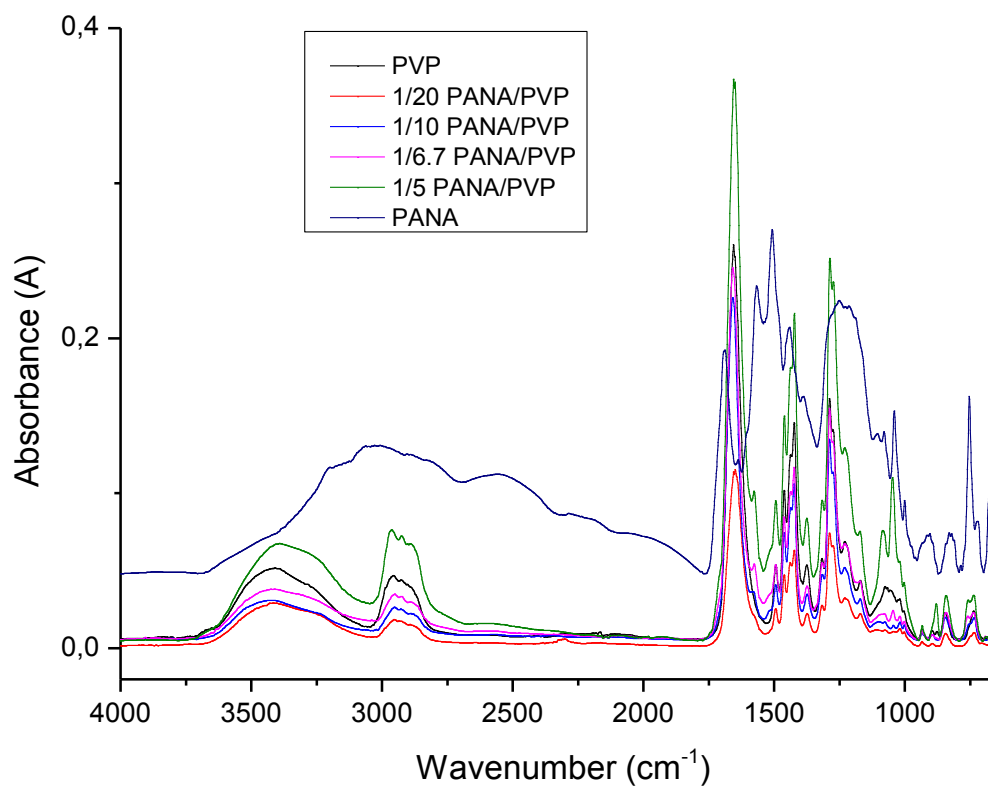


Figure 4.6 : FTIR-ATR spectra of PANA/PVP nanofibers electrospun in DMF.

Poly (anthranilic acid) has specific peaks at 3431 cm^{-1} (N-H stretching), 2615 cm^{-1} (O-H stretching), 1691 cm^{-1} (C=O), 1558 cm^{-1} (quinoid C=C stretching), 1506 cm^{-1} (benzenoid C=C stretching), 1450 cm^{-1} (stretching of aromatic ring), 1373 cm^{-1} (C-N stretching for secondary aromatic amine), 1247 cm^{-1} (C-H stretching), 1166 cm^{-1} (N=Q=N stretching), 1081 cm^{-1} and 1045 cm^{-1} (aromatic C-H in plane bending), 821 cm^{-1} and 756 cm^{-1} C-H out of plane bending [72]. In Figure 4.7 and Figure 4.8, there is an increase in absorbance of characteristic peak of PANA with the increase of PANA/PVP weight ratio. In blended nanofibers, the peak that is characteristic to PANA is increasing with the increase of PANA. However, the peak of 1/10 PANA/PVP containing nanofibers that were electrospun in EtOH/DMF was shifted to 1580 cm^{-1} .

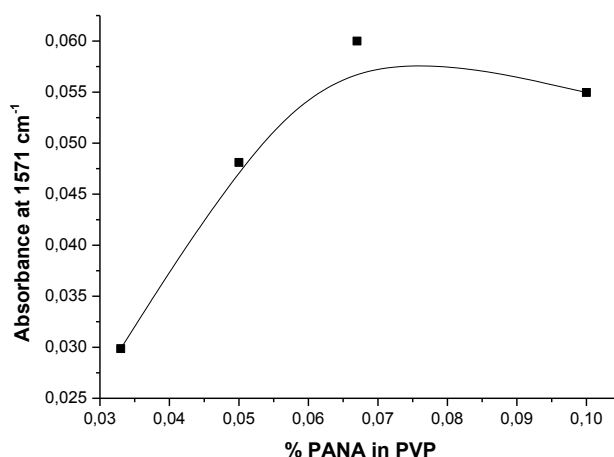


Figure 4.7 : The change in the specific peak of PANA in the nanofibers of PANA/PVP that was electrospun in EtOH/DMF solution.

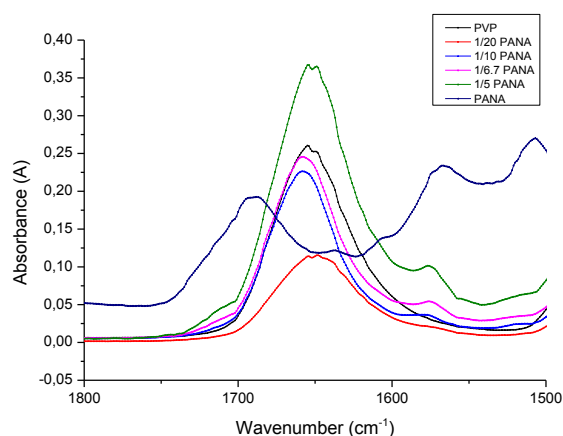


Figure 4.8: The change in the specific peak of PANA in the nanofibers of PANA/PVP that was electrospun in DMF solution.

4.1.3 SEM results of PANA/PVP blends

SEM micrograph of PVP that was electrospun in EtOH/DMF solution is presented in Figure 4.9. Electrospun nanofibers of PANA/PVP with the weight ratio of 1/30 and 1/10 are shown in Figure 4.10 and Figure 4.11.

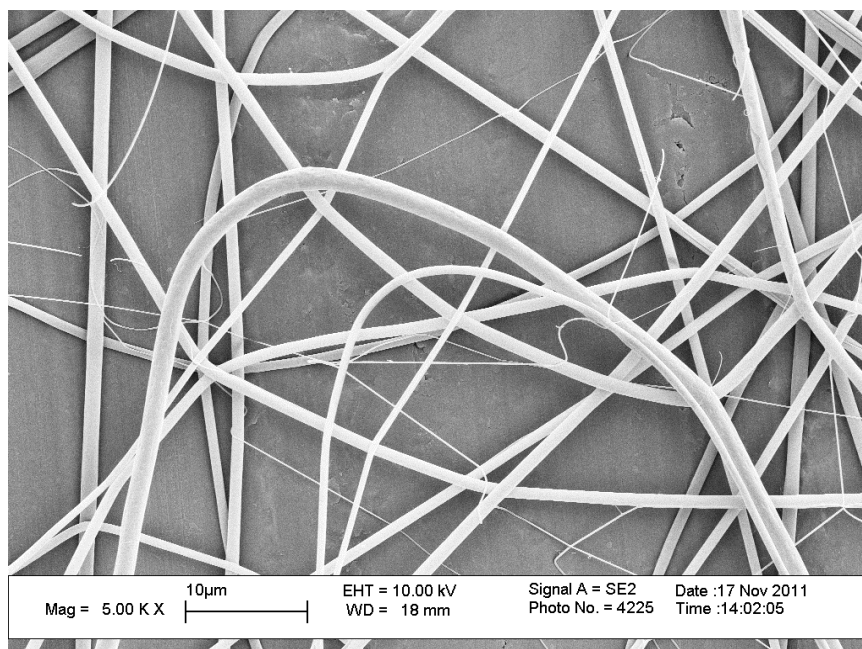


Figure 4.9 : SEM micrograph of PVP in EtOH/DMF.

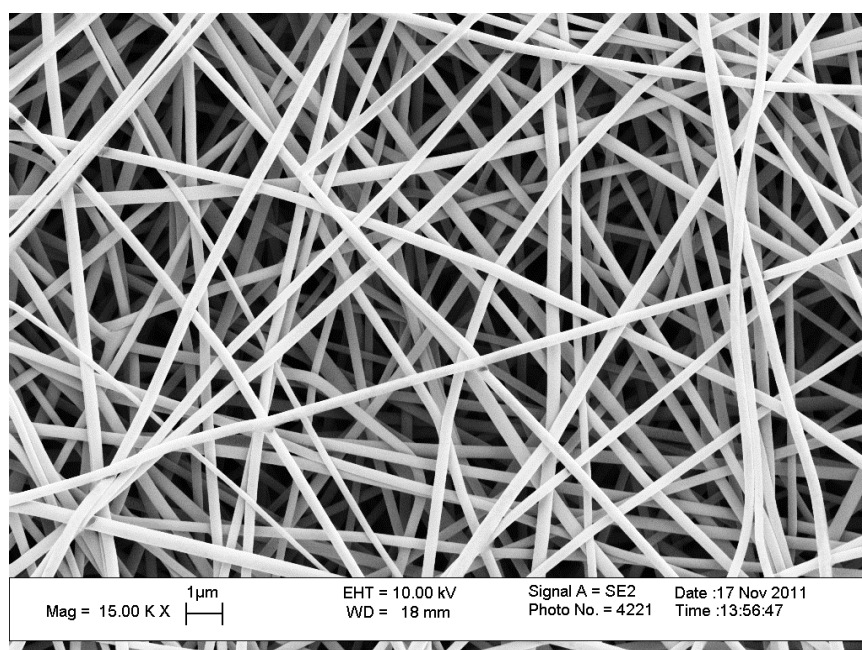


Figure 4.10 : SEM micrograph of PANA/PVP (1/30) in EtOH/DMF.

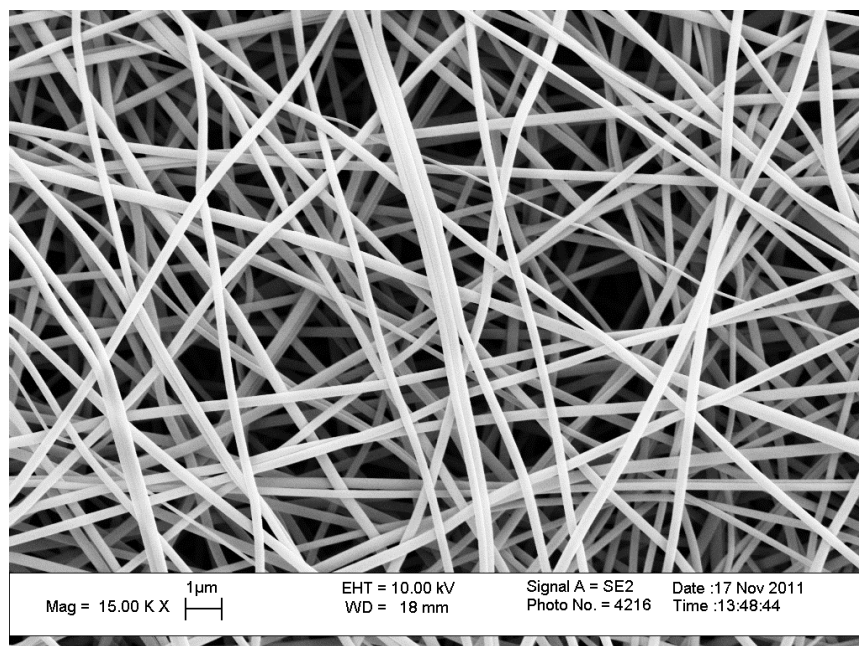


Figure 4.11 : SEM micrograph of PANA/PVP (1/10) in EtOH/DMF.

Nanofibers of PVP prepared in DMF solution is given in Figure 4.12 and PANA/PVP nanofiber blends with weight ratio of 1/10 and 1/20 are presented in Figure 4.13 and in Figure 4.14. Moreover, in DMF solution average fiber diameter changes from 187.6 nm to 110 nm with the increase weight ratio of PANA/PVP. As it is also observed, the fibers in DMF solutions have smaller fiber diameter.

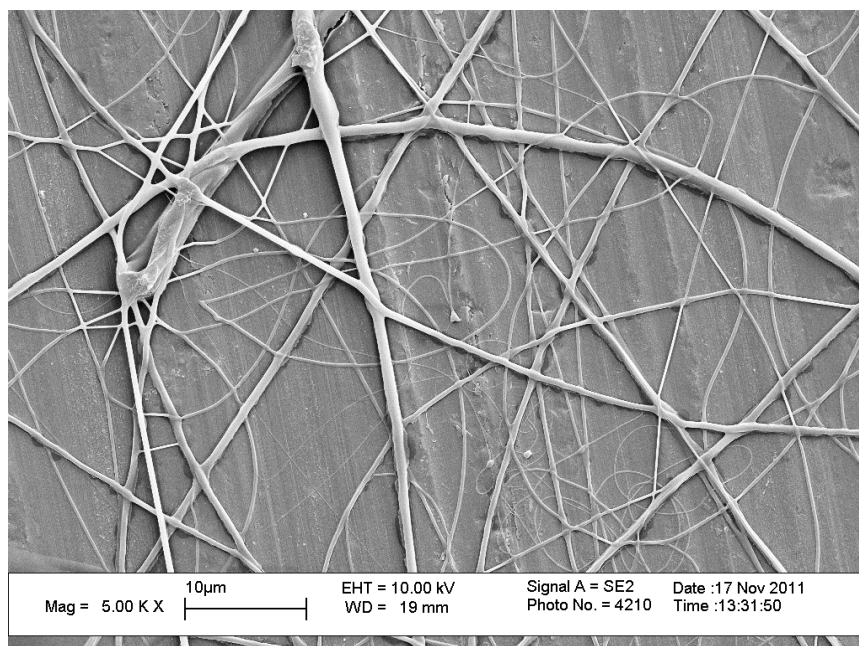


Figure 4.12 : SEM micrograph of nanofibers of PVP prepared by using DMF.

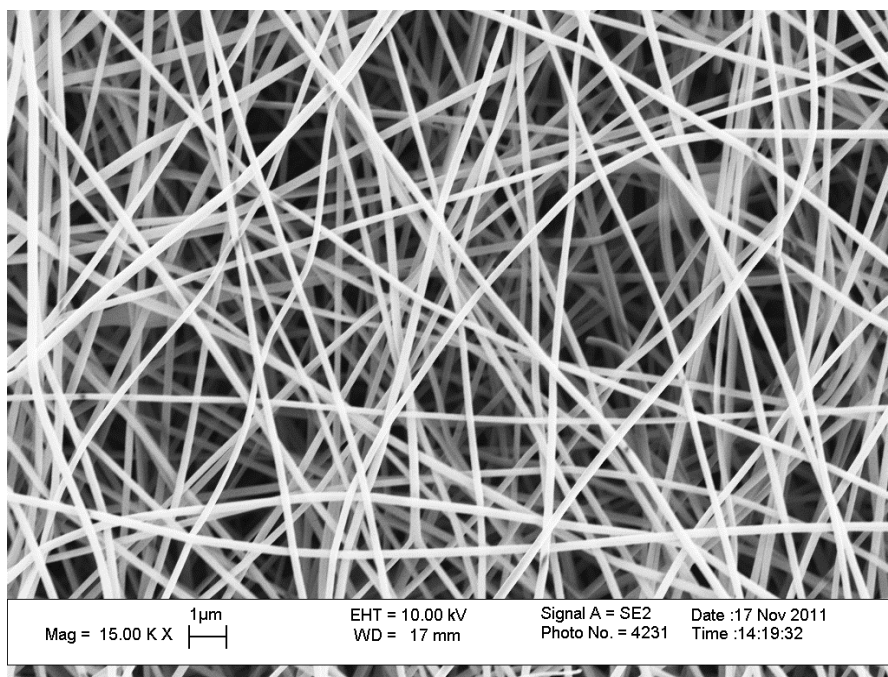


Figure 4.13 : SEM micrograph of PANA/PVP (1/10) DMF.

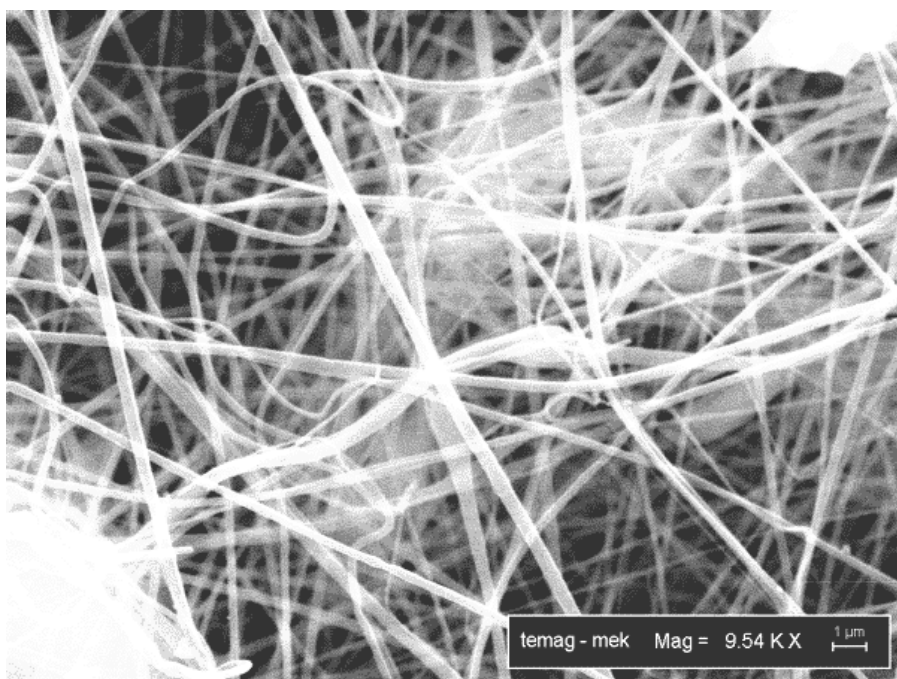


Figure 4.14 : SEM micrograph of PANA/PVP (1/20) in DMF.

For calculation of average nanofibers diameter, approximately 75 nanofibers were counted using the software named Image J. After that, OriginPro 8.5.1 programme was used to plot their distribution. If the Figure 4.15 was investigated with more detail, it is seen that although the concentration of PVP was increased, the nanofibers average diameter was decreased that may be explained by the DMF dielectric

properties as it is known that ethanol has dielectric constant of 22.4 while DMF has dielectric constant of 36.7 [35].

As we blend the electrospinning solutions, the dielectric constant can be calculated with the following equation (4.1).

$$\epsilon_m = \epsilon_1 x_1 + \epsilon_2 x_2 \quad (4.1)$$

where ϵ_1 and ϵ_2 is the dielectric constant of the solvent and x_1 and x_2 is the corresponding volume fraction of the solvent [73].

According to that equation the nanofibers that are electrospun in EtOH/DMF solution has solvent dielectric constant of 29.55 while the nanofibers that are electrospun in DMF solution has solvent dielectric constant of 36.7. This may explain the decreasing average diameter of nanofibers in electrospinning with DMF solution as it is presented in Figure 4.15. The average diameter of electrospun nanofibers prepared in EtOH/DMF with the dielectric constant of 29.55 was 1110 ± 770 nm, while the average diameter of electrospun nanofibers prepared in DMF with the dielectric constant of 36.7 was 777 ± 700 nm.

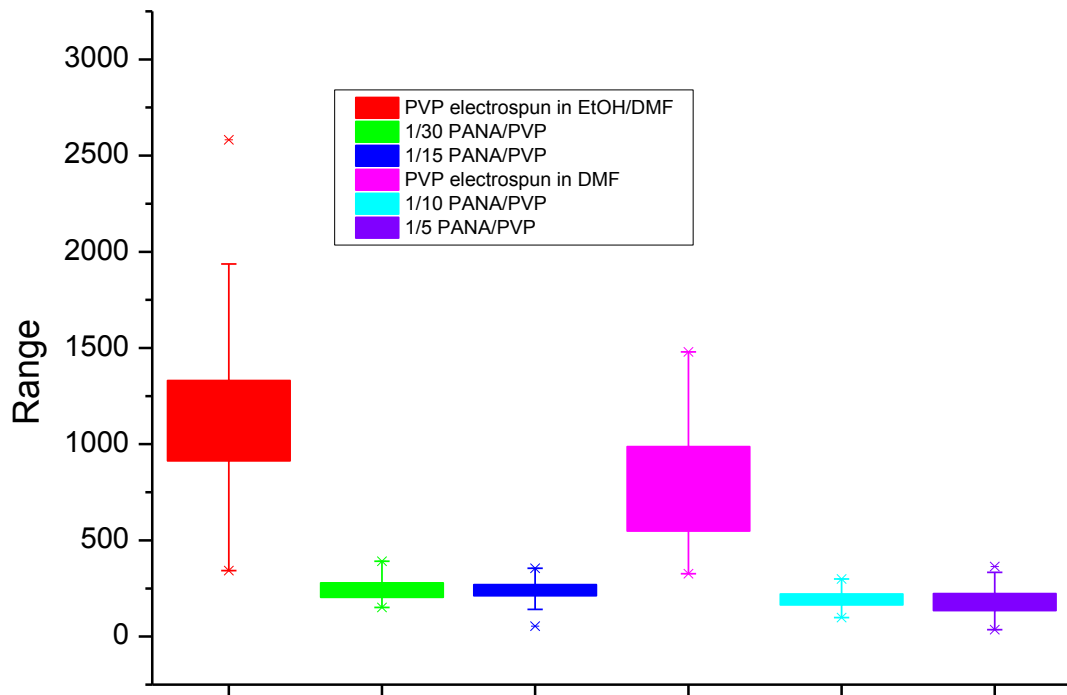


Figure 4.15 : Distribution of the PANA/PVP nanofibers with their diameters.

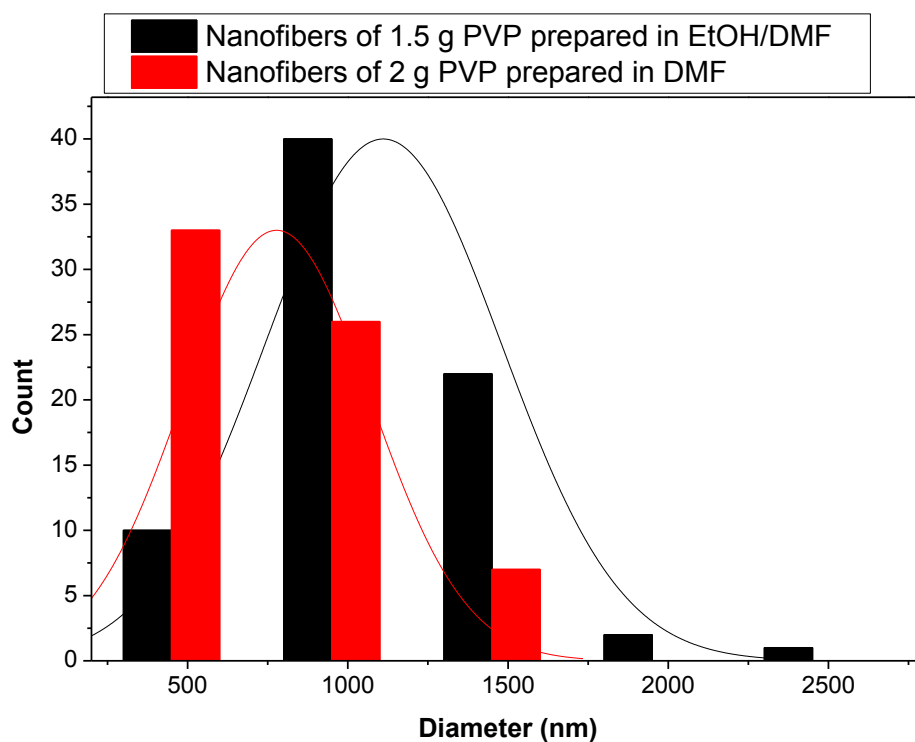


Figure 4.16 : Distribution of the diameters of nanofibers of PVP.

As the PANA content in electrospun nanofibers increased it was found that the average diameter was decreased as observed in Figure 4.17 and Figure 4.18. The details of electrospun nanofibers' diameter are presented in Table 4.1.

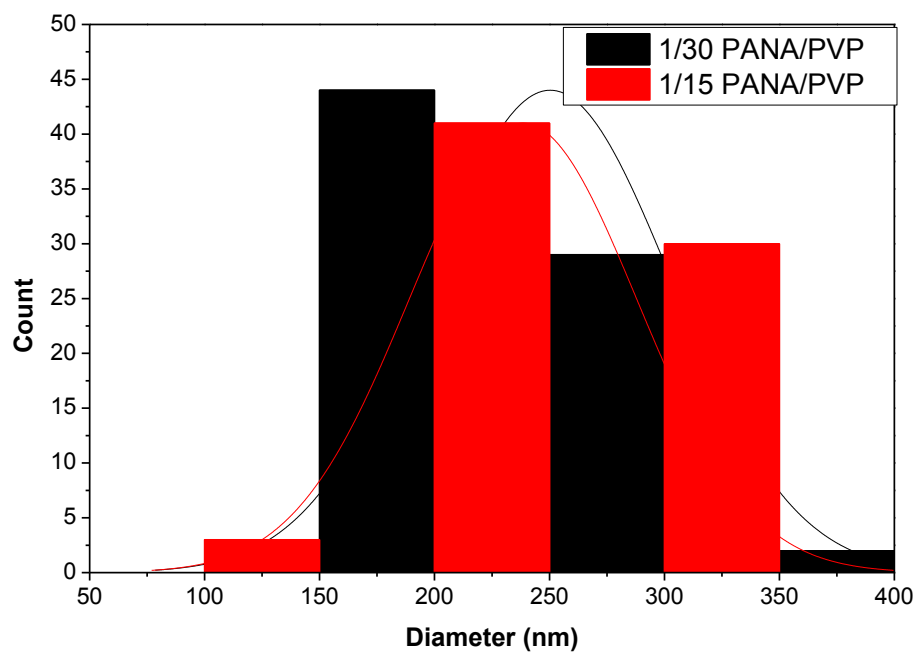


Figure 4.17 : Distribution of the diameters of nanofibers of PANA/PVP prepared in EtOH/DMF solution.

The decrease in the average diameter with the increase amount of PANA can be explained by the conductivity nature of PANA. As in some studies, conducting polymer containing nanofibers have smaller diameters [74].

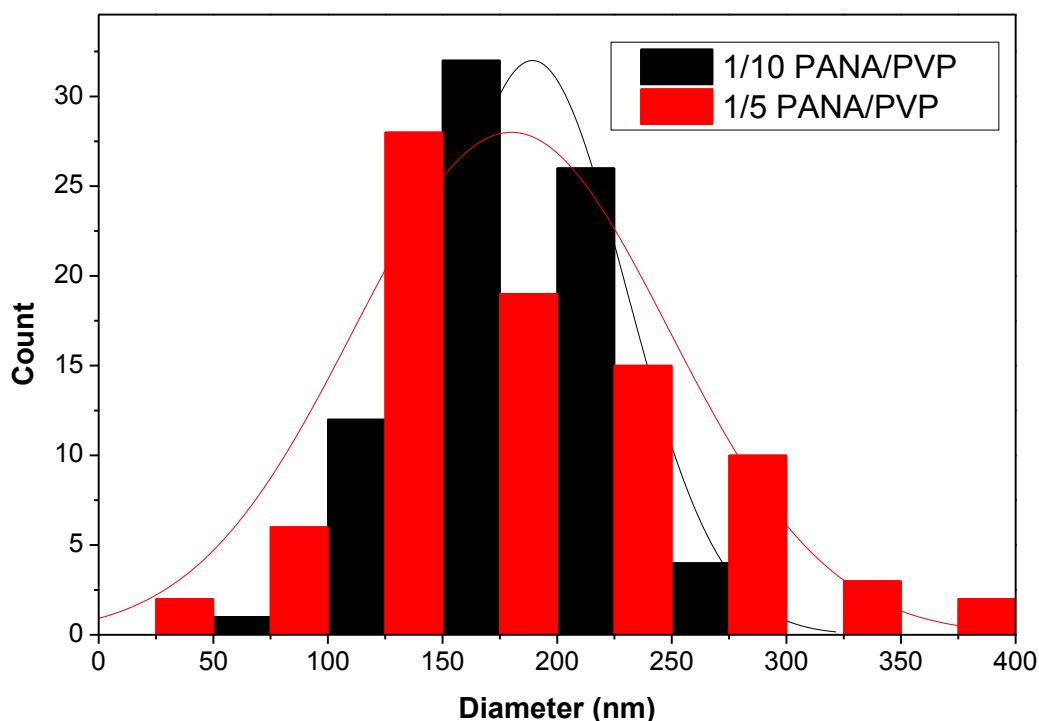


Figure 4.18 : Distribution of the diameters of nanofibers of PANA/PVP prepared in DMF solution.

Table 4.1: The summary of electrospun nanofibers with electrospinning conditions and diameters of nanofibers.

PANA (wt%)	Solvent	Flow rate (ml/h)	Distance (cm)	Applying Voltage (kV)	Diameters of Nanofibers (nm)
-	EtOH/DMF	0.5	20	15	1110±500
3.3	EtOH/DMF	0.5	20	15	250±90
6.7	EtOH/DMF	0.5	20	15	238±56
-	DMF	0.5	20	15	777±465
10	DMF	0.5	20	15	190±50
20	DMF	0.5	20	15	180±87

4.1.4 Electrochemical impedance results of EtOH/DMF and DMF solutions

For electrochemical impedance results, nyquist, bode phase, bode magnitude data were obtained. Nyquist results of electrospinning solutions that were prepared with EtOH/DMF solution is presented in Figure 4.19.

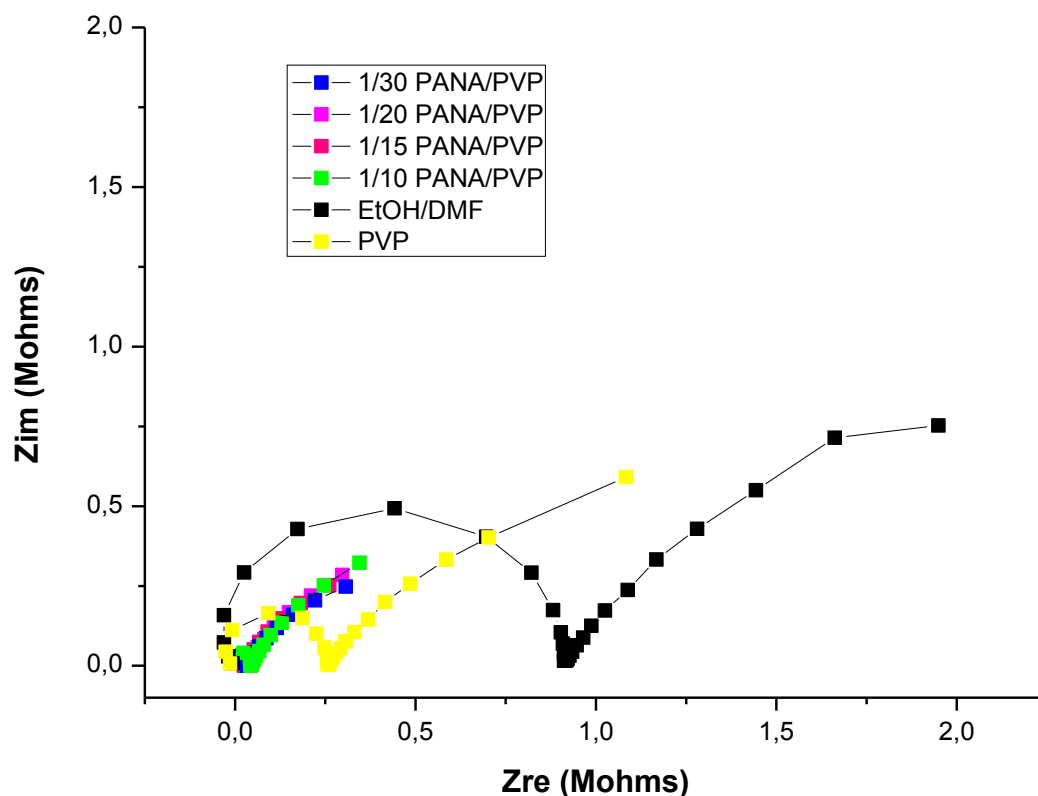


Figure 4.19: Nyquist diagram of electrospinning solutions prepared in EtOH/DMF.

The Zim and Zre values of the Figure 4.18 were read to have a comparison in the conductivity of the electrospinning solutions. The Zre and Zim values that are read from the graph are shown in Table 4.2.

Table 4.2: The impedance data of electrospinnig soluntions prepared in EtOH/DMF.

Solvent Content	Zim (Mohms)	Zre (Mohms)
EtOH/DMF solution	0.54395	0.91664
PVP	0.16677	0.2613
3.3 % PANA	0.02593	0.03398
5 % PANA	0.00255	0.0333
6.7 % PANA	0.02479	0.02639
10 % PANA	0.00335	0.04405

Moreover, the EtOH/DMF solution has the highest Zim and Zre data that can be explained by the lowest conductivity. Also, when PVP including electrospinning solution was measured the Zre and Zim value was decreased that can be explained by PVP properties which makes it suitable for electrochemical measurements [75]. When the EIS of solutions with PANA containing is investigated, 8 times higher

conductivity is observed as compared with electrospinning solutions. Moreover, EtOH conductivity was reported as 1.4×10^{-9} S/cm and DMF conductivity was reported as 6×10^{-8} S/cm [76].

As it is presented in Figure 4.20, bode phase angle at 0.1Hz is highest for PANA containing solutions by the time bode phase angle is the lowest for no polymer containing solvent system. While PANA containing solutions has phase angle of 42-50°, the angle was lower in EtOH/DMF system like 22° and PVP containing system 39°.

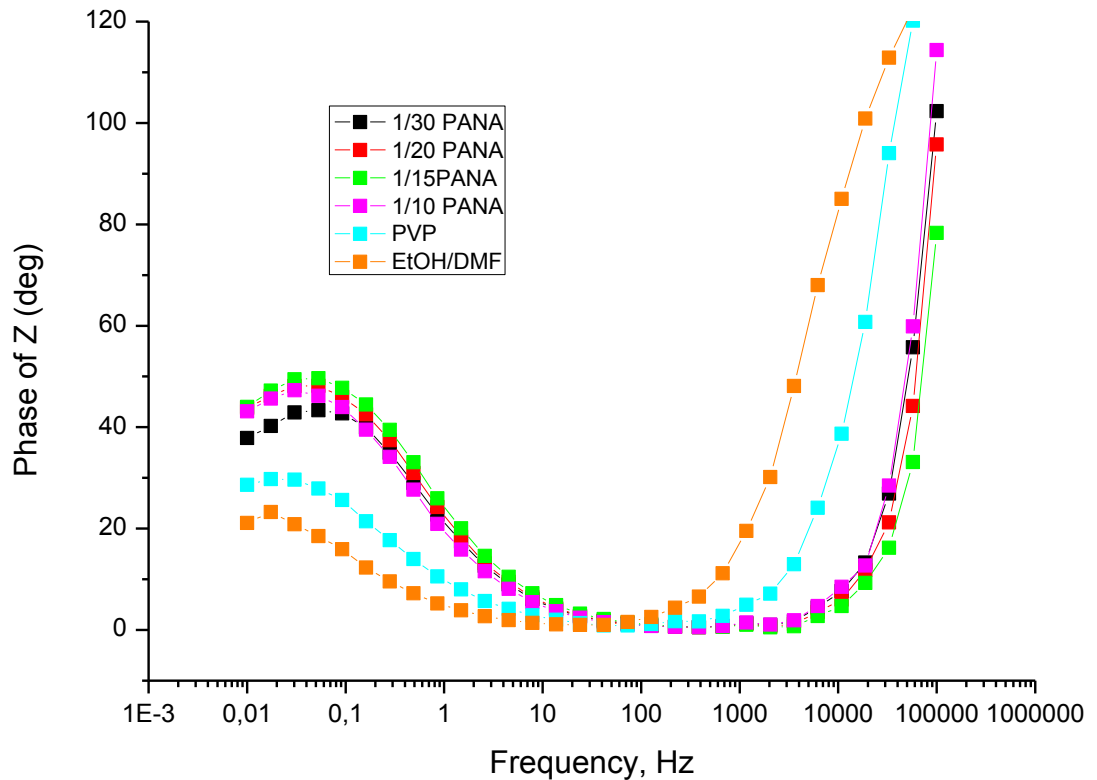


Figure 4.20: Bode phase of electrospinning solutions prepared in EtOH/DMF.

From magnitude graph at Figure 4.21 at frequency 1 Hz, $|Z|$ was read 9.47 M Ω for EtOH/DMF solution, 2.85 M Ω for PVP containing solvents and is nearly same for PANA containing solvents like 0.36 M Ω .

Double layer capacitance which is indicated as Cdl can also be calculated with the following equation (4.2). And, the results are shown in Table 4.3.

$$C_{dl} = 1/|Z| \quad (4.2)$$

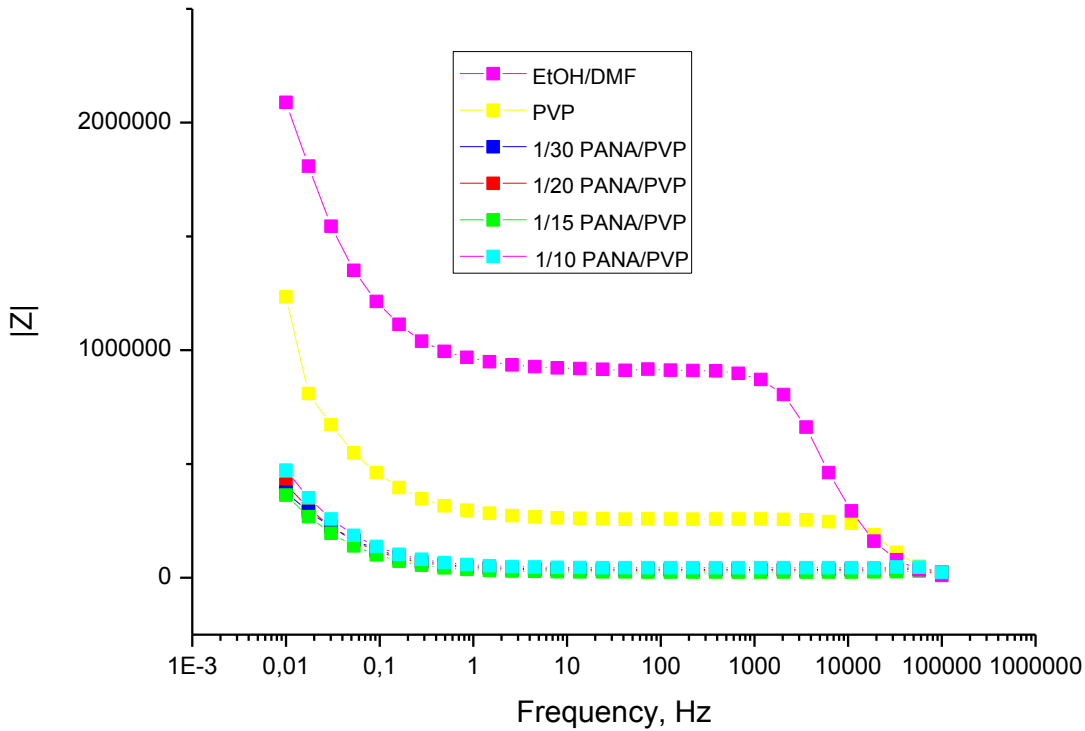


Figure 4.21: Bode magnitude of electrospinning solutions of PANA/PVP dissolved in EtOH/DMF.

Table 4.3: The double layer capacitance of electrospinning solutions prepared in EtOH/DMF.

Solvent Content	Cdl (mF)
EtOH/DMF solution	0.001
PVP	0.004
3.3 % PANA	0.024
5 % PANA	0.029
6.7 % PANA	0.033
10 % PANA	0.021

Nyquist results of electrospinning solutions that were prepared with DMF solution is seen in Figure 4.22. The Zim and Zre values of the Figure 4.22 were read to have a comparison in the conductivity of the electrospinning solutions. The Zre and Zim values that are read from the graph are shown in Table 4.4.

As a result, the DMF solution has the highest Zim and Zre data that can be explained by the lowest conductivity. Moreover, when PVP including electrospinning solution was measured the Zre and Zim value was decreased. When the EIS of solutions that PANA containing is investigated it is observed that there is about 4 to 10 times higher conductivity in electrospinning solutions.

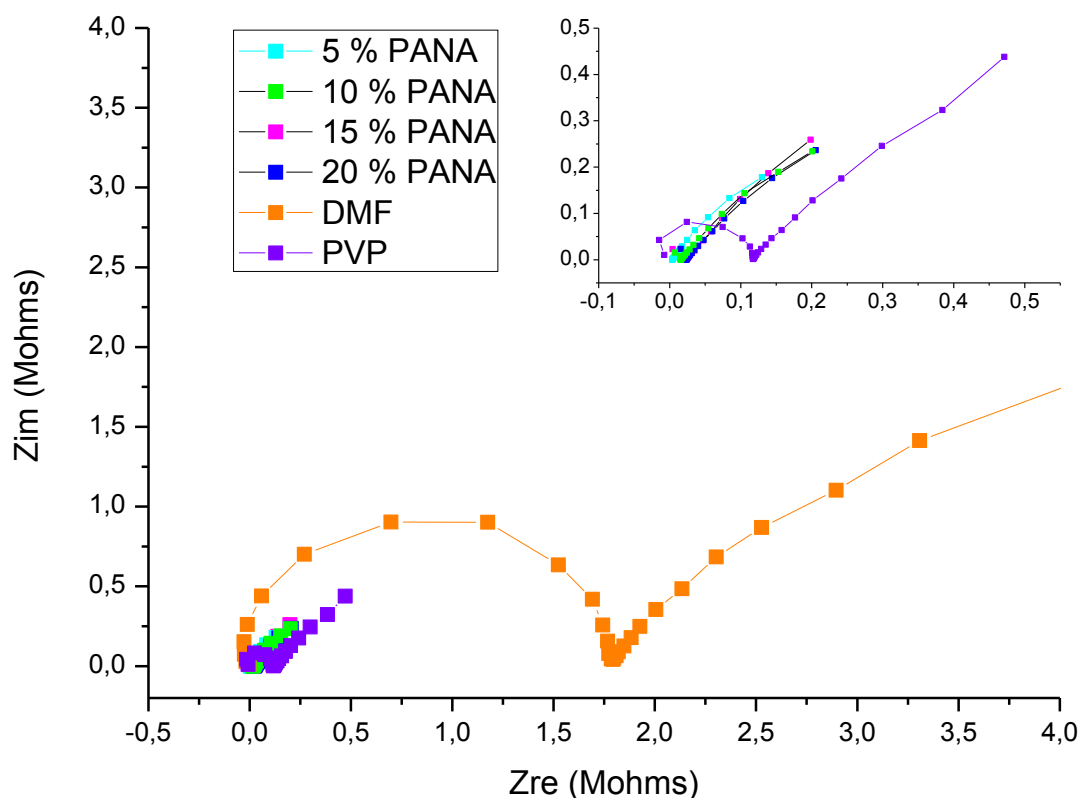


Figure 4.22: Nyquist diagram of electrospun prepared in DMF.

Table 4.4: The impedance data of electrospinnig solutions prepared in DMF.

Solvent Content	Zim (Mohms)	Zre (Mohms)
DMF solution	0.88	1.800
PVP	0.08	0.120
5 % PANA	0.0002	0.000
10 % PANA	0.0018	0.016
15 % PANA	0.0021	0.022
20% PANA	0.0022	0.025

As it is presented in Figure 4.23, bode phase angle at 0.1Hz is highest for 5% PANA containing solutions while is the lowest for no polymer containing solvent system. While 5 %PANA containing solutions has the highest phase angle of 59.59°, the angle was lower in EtOH/DMF system like 16.54.° and PVP containing system 31.87°.

From magnitude graph at Figure 4.24 at frequency 1 Hz, $|Z|$ is read and used for double layer capacitance calculation. Double layer capacitance was calculated and is shown in Table 4.5.

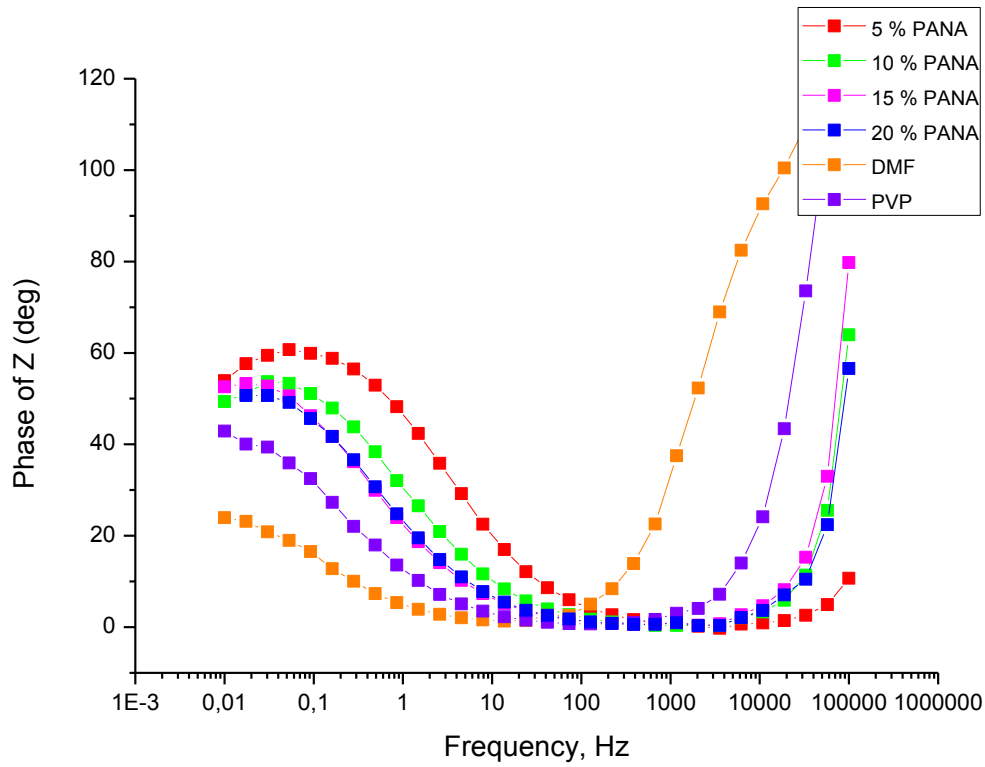


Figure 4.23: Bode phase of electrospinning solutions prepared in DMF.

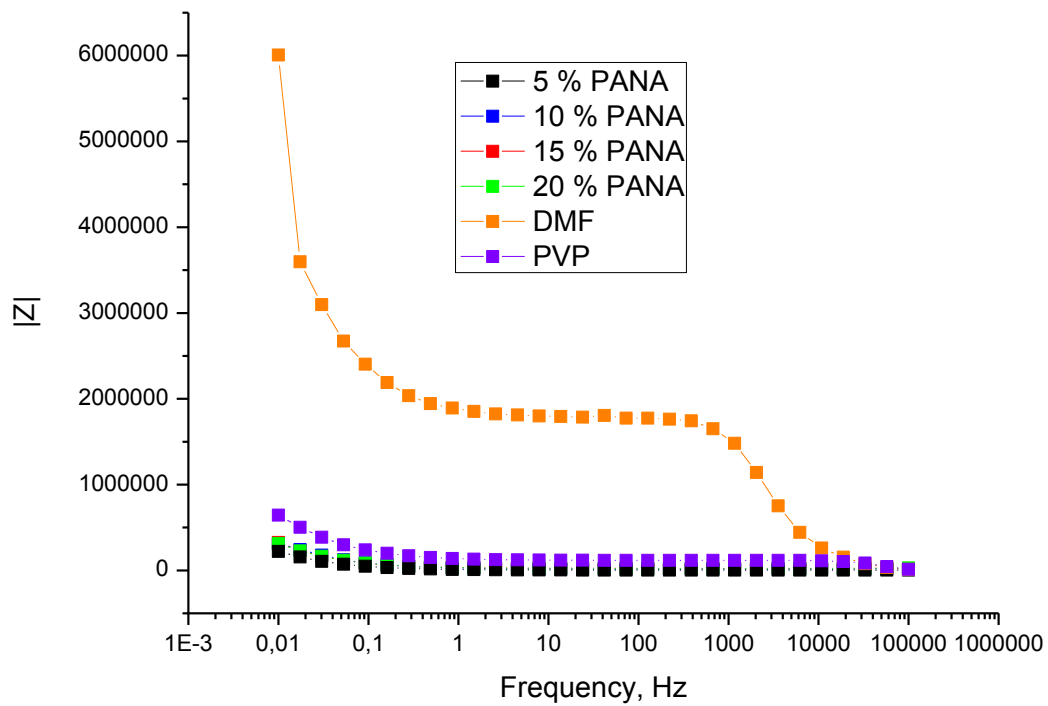


Figure 4.24: Bode magnitude of electrospinning solutions prepared in DMF.

Table 4.5: The double layer capacitance of electrospinning solutions prepared in DMF.

Solvent Content	Cdl (mF)
DMF solution	0.001
PVP	0.008
5 % PANA	0.140
10% PANA	0.030
15 % PANA	0.030
20 % PANA	0.030

4.2 Characterization of PANA/PCL Blends

4.2.1 UV-Vis spectrophotometric results of PANA/PCL blends

The UV-vis spectra of the PANA/PCL nanofibers dissolved in THF solution are presented in Figure 4.25. The absorption peaks at 361 nm and 500nm are observed. The absorption peak at 361 nm can be attributed to π - π^* transition in benzoid rings of PANA and the peak at 500nm can be attributed to exciton like transition from benzoid to quionoid.

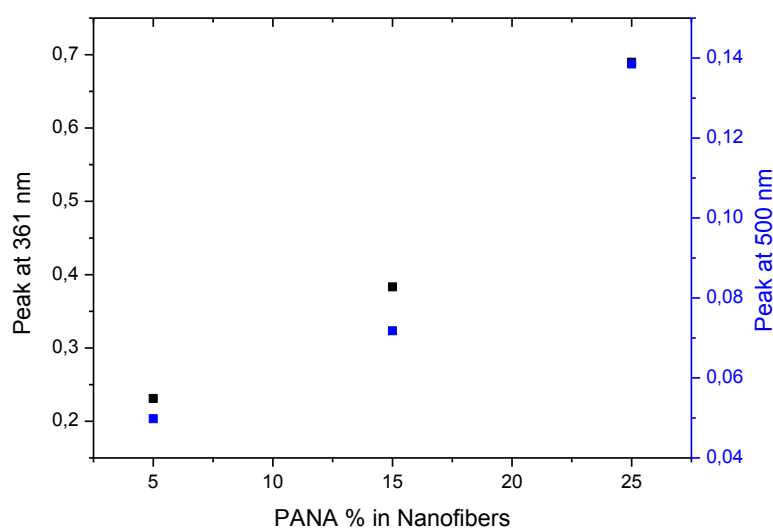


Figure 4.25: UV-Vis results of nanofibers of PANA/PCL blend dissolved in THF.

4.2.2 FTIR-ATR spectrophotometric analysis of PANA/PCL blends

The FTIR-ATR spectrum of nanofibers of PANA/PCL is seen in Figure 4.26. Characteristic peaks of PCL 1733–1725 cm^{-1} is attributed to C-O stretching, the peak at 1160 cm^{-1} can be assigned C-O stretching, 1397 cm^{-1} is attributed to C-H bending and peaks at 2856 cm^{-1} is attributed to C-H stretching [40]. As the PANA/PCL

blends FTIR-ATR spectrophotometry result is investigated, there is an additional peak at 1507 and 1567 cm^{-1} which can be defined as PANA specific peak due to the C=C stretching in PANA. In Figure 4.27, it is presented that peaks are increasing with the addition of PANA.

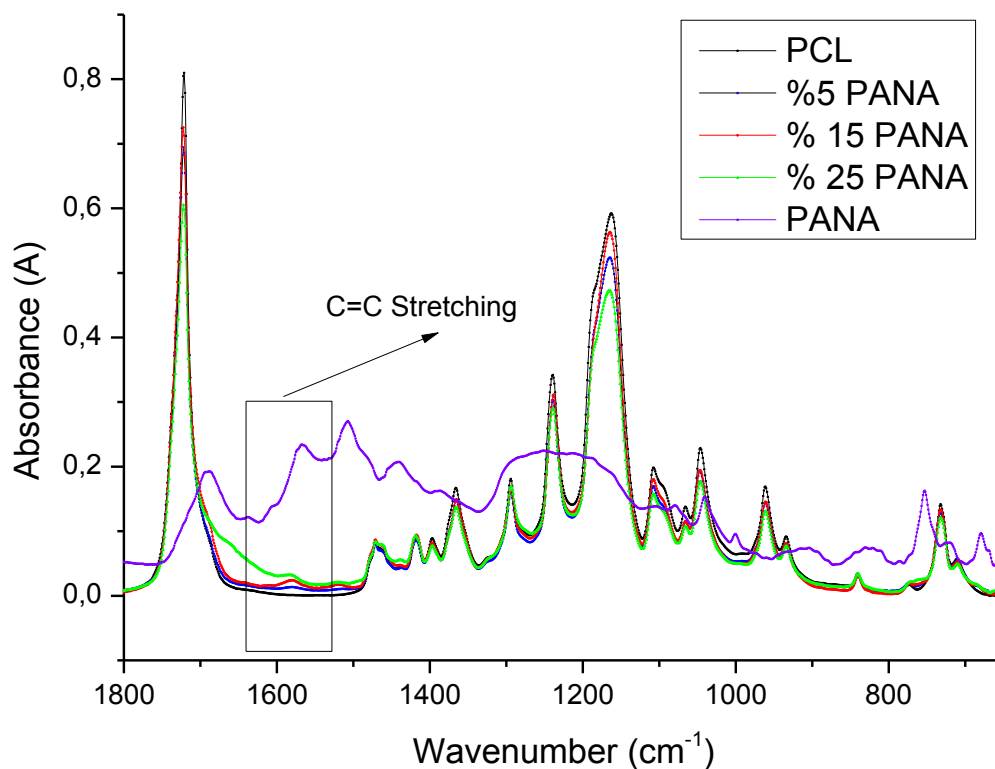


Figure 4.26 : FTIR-ATR spectrums of PANA/PCL nanofibers.

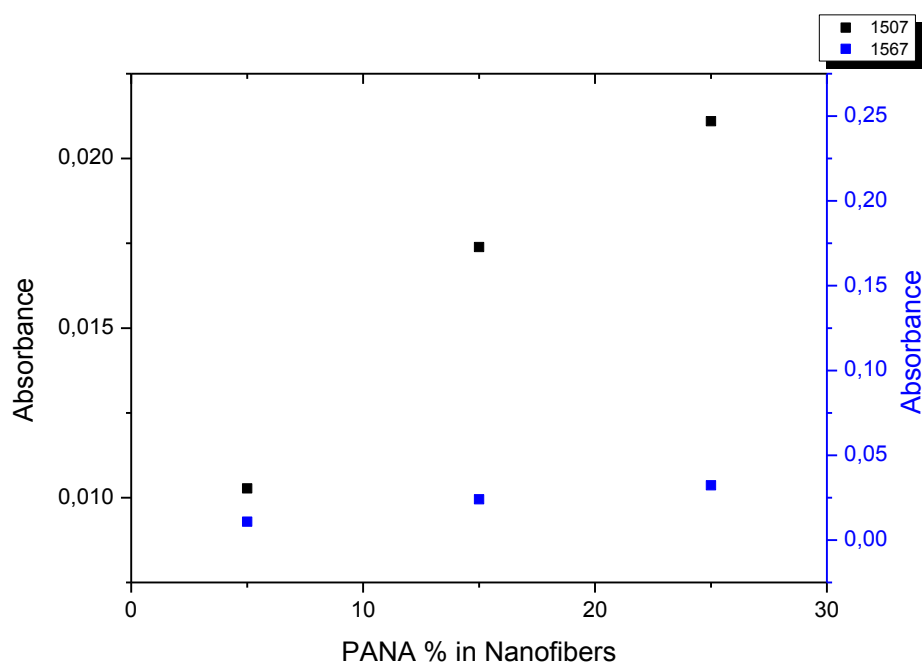


Figure 4.27: Specific peaks of PANA in PANA/PCL blended nanofibers.

4.2.3 SEM results of PANA/PCL blends

SEM result of PCL is presented in Figure 4.28. The average fiber diameter is 1160 nm. The average fiber diameter is decreased to 1060nm when PCL is blended with PANA as seen in Figure 4.29.

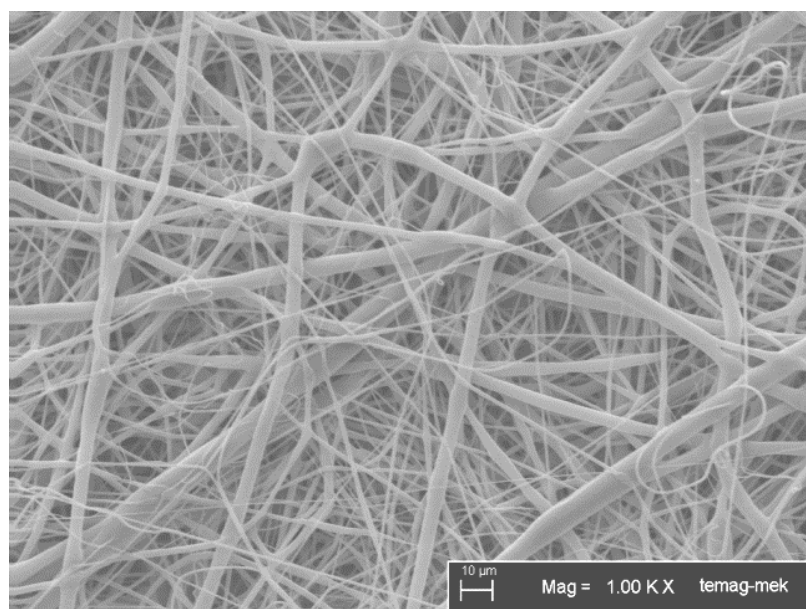


Figure 4.28 : SEM result of nanofibers of PCL prepared in THF.

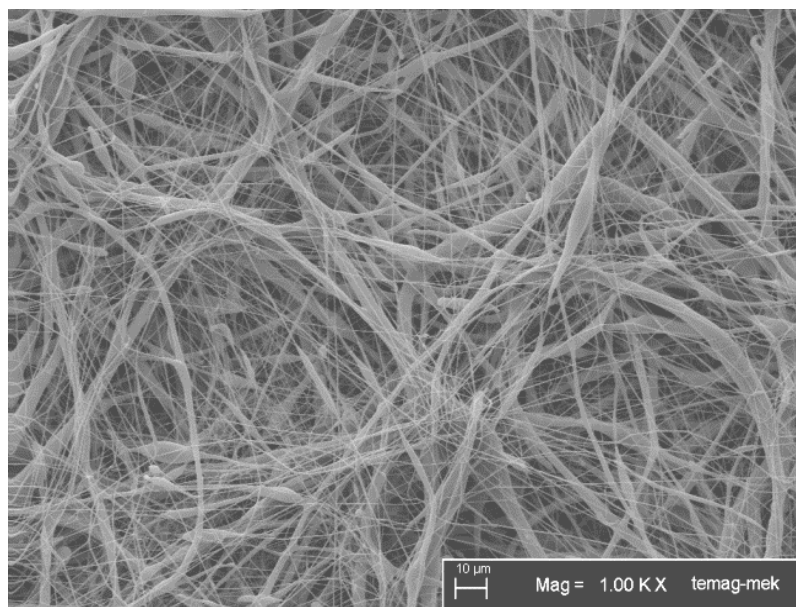


Figure 4.29 : SEM result of nanofibers that contain 5% of PANA.

For calculation of average nanofibers diameter, 220 to 274 numbers of nanofibers were counted using the software named Image J. After that, OriginPro 8.5.1 programme was used to plot their distribution.

In Figure 4.30 and 4.31, it is seen that the average diameter was 890 nm and 654 nm. As the SEM results is investigated, there is a non-homogenous fiber formation that are varying from micron to nanometer size.

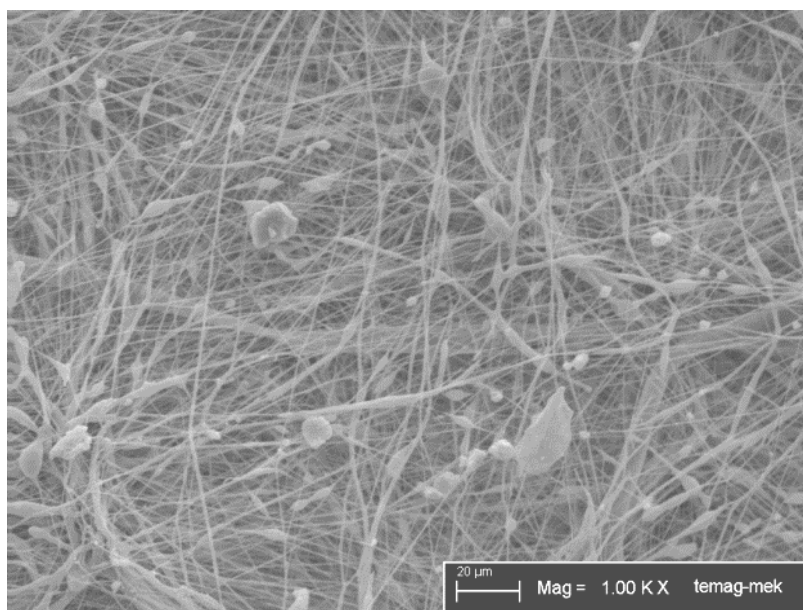


Figure 4.30: SEM result of nanofibers that contain 15% of PANA.

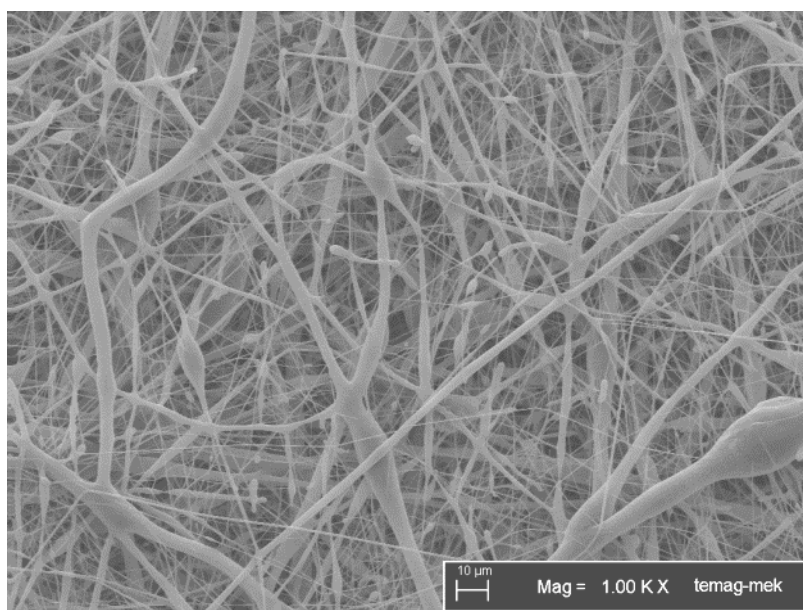


Figure 4.31: SEM result of nanofibers that contain 25% of PANA.

The non-homogenous and higher fiber diameter that can be explained by the electrospinning solution named THF which has low dielectric constant as 7.6 [76]. As it is found in previous study that higher dielectric property makes decrease in fiber diameter.

Figure 4.32 can be important to identify the average fiber diameter. As it is expected, the fiber diameter was decreased with the increase of PANA. Their average diameter was labelled in Table 4.6.

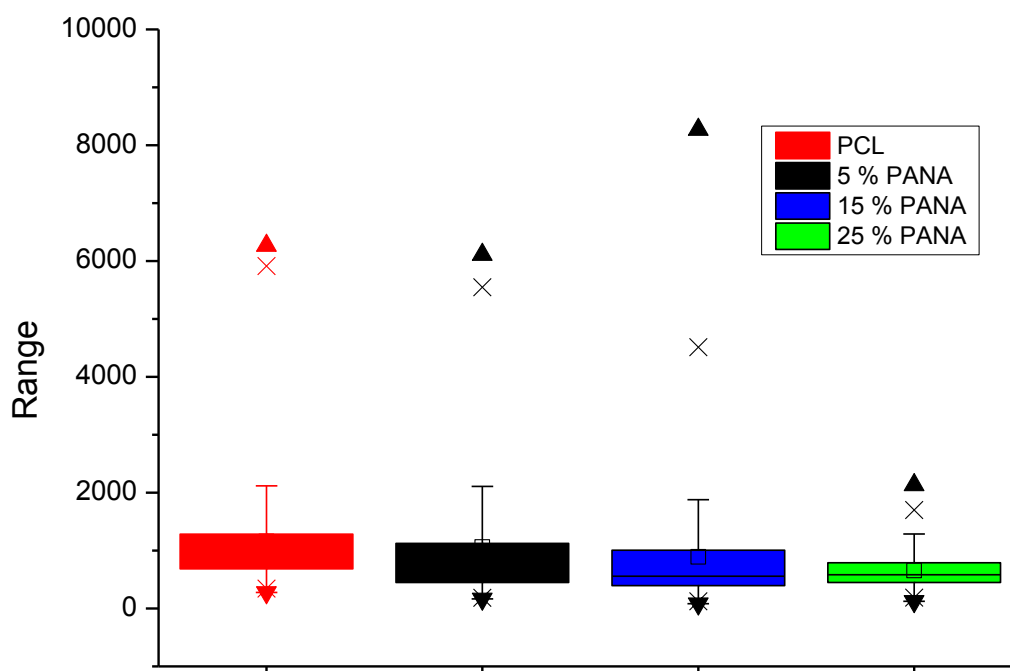


Figure 4.32 : Distribution of the PANA/PCL blend nanofibers diameters.

As it seen from the results, the PCL fiber that has the most homogenous nanofibers diameter as compared to others and its fiber average distribution is presented in Figure 4.33.

Table 4.6: The summary of electrospun nanofibers of PANA/PCLwith electrospinning conditions and diameters of nanofibers.

PANA (wt%)	Solvent	Flow rate (ml/h)	Distance (cm)	Applying Voltage (kV)	Diameters of Nanofibers (nm)
-	THF	1	20	15	1160 (277 nm to 6266nm)
5	THF	1	20	15	1060 (166 nm to 6111nm)
15	THF	1	20	15	890 (83 nm 8272 nm)
25	THF	1	20	15	655 (125 nm to 2135 nm)

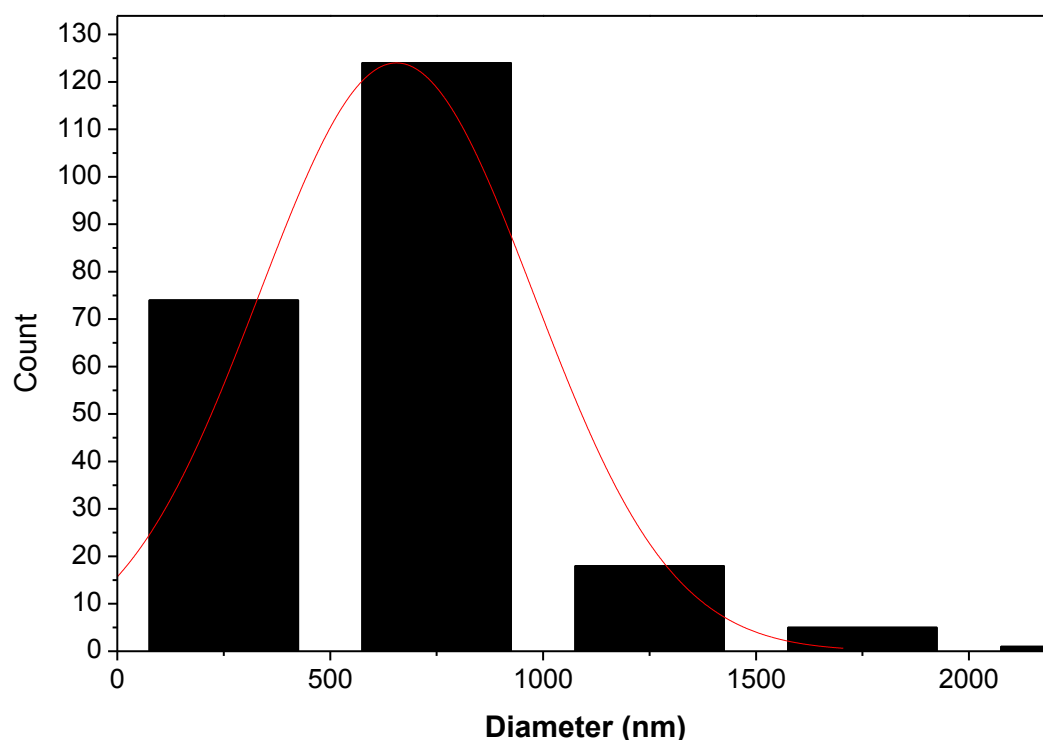


Figure 4.33 : Distribution of the diameters of nanofibers of PCL containing 25 % of PANA.

4.2.4 Electrochemical impedance results of THF solutions

For electrochemical impedance measurements, results are obtained as nyquist, bode phase, bode magnitude data. Nyquist results of electrospinning solutions that were prepared with THF solution is presented in Figure 4.34.

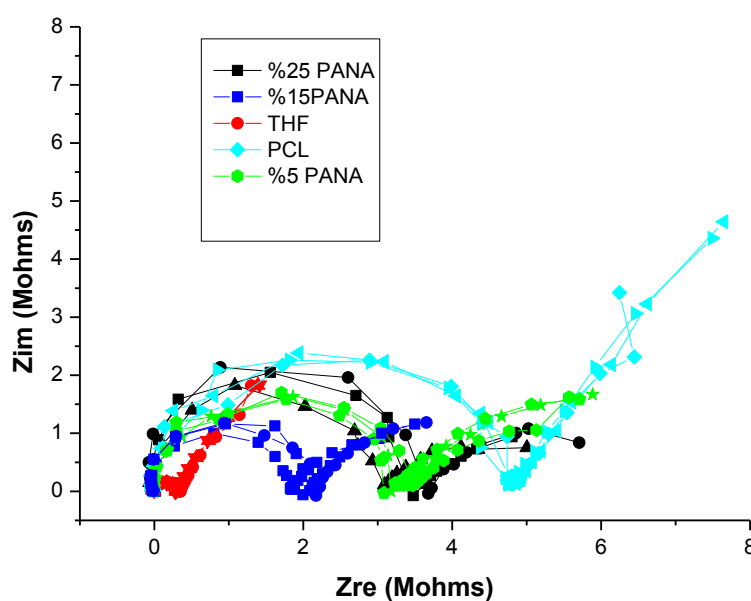


Figure 4.34: Nyquist diagram of electrospinning solutions of PANA/PCL prepared in THF.

The Zim and Zre values of the Figure 4.34 were read to have a comparison in the conductivity of the electrospinning solutions. The Zre and Zim values that are read from the graph were presented in Table 4.7.

Table 4.7: The impedance data of electrospinning solutions prepared in THF.

Solvent Content	Zim (Mohms)	Zre (Mohms)
THF solution	0.090	0.313
PCL	2.317	3.525
5 % PANA	1.688	3.125
15 % PANA	0.952	2.007
25 % PANA	1.559	4.819

As it is seen with the data, the THF solution has the lowest Zim and Zre data that can be explained by the highest conductivity as it is known 2×10^{-5} S/cm [75]. Moreover, when PCL added inside this solution the conductivity was decreased about 30 times. The PANA containing PCL solutions has lower resistance that may be explained as higher conductivity. As it seen in Figure 4.35, bode phase angle at 0.1Hz is highest for THF as it has 37.15° and nearly same for the PCL and PANA/PCL blends as 9.70° .

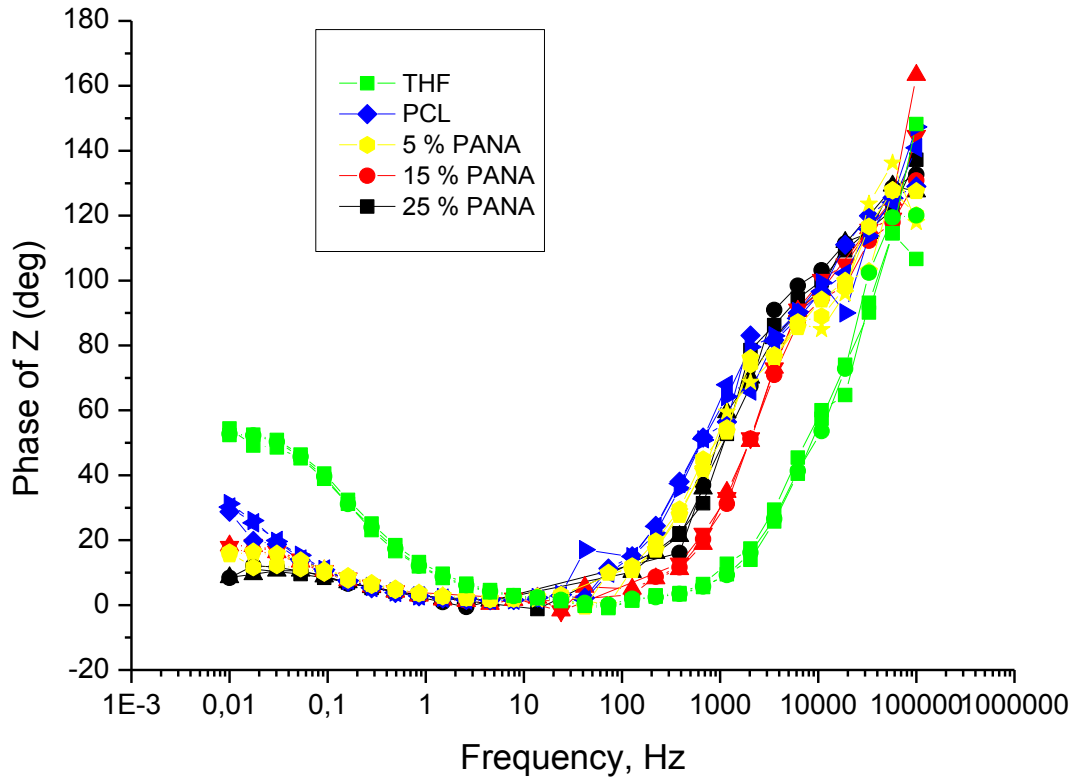


Figure 4.35: Bode phase of electrospinning solutions prepared in THF.

From magnitude graph at Figure 4.36 at frequency 1 Hz, $|Z|$ is read 0.32 M Ω for THF solution, 4.86 M Ω PCL containing solvents and 3.38 M Ω , 1.82 M Ω and 0.30 M Ω for 5%, 15% and 25% PANA containing diluted electrospinning solutions. These values are used to calculate double layer capacitance as shown in Table 4.8.

Table 4.8: The double layer capacitance of electrospinning solutions prepared in THF.

Solvent Content	Cdl (mF)
THF solution	0,0032
PCL	0,0002
5 % PANA	0,0003
15 % PANA	0,0005
25 % PANA	0,0033

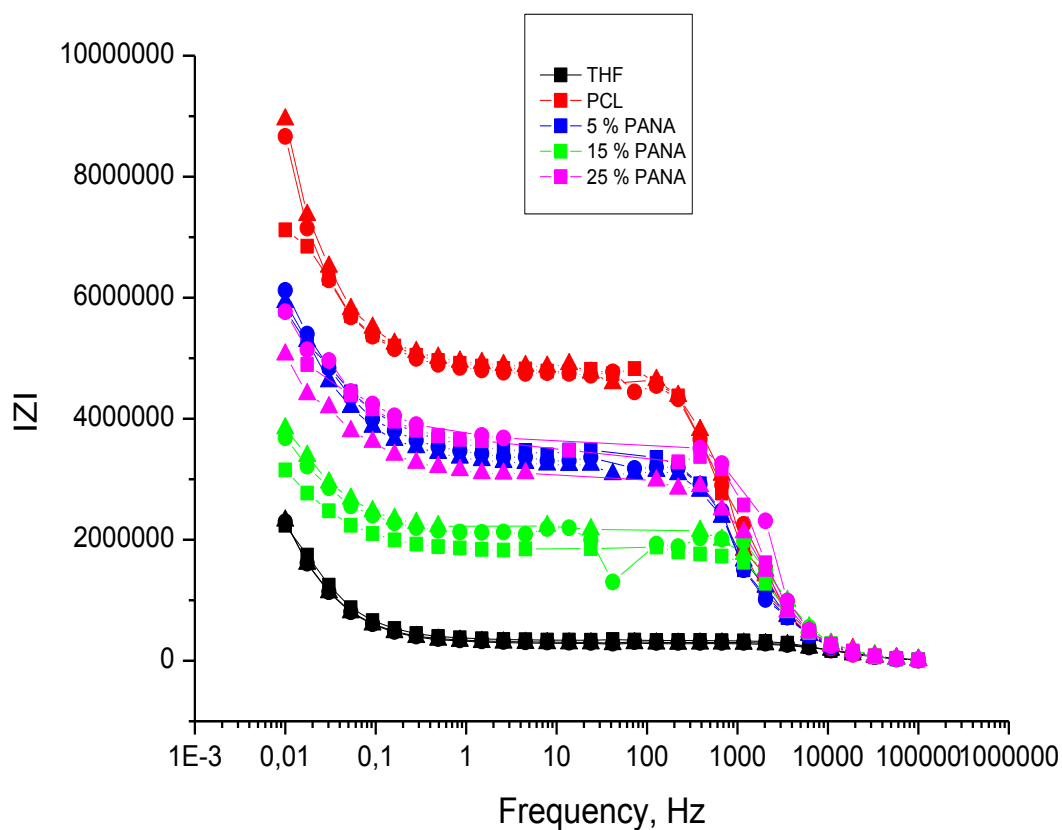


Figure 4.36: Bode magnitude of electrospinning solutions of PANA/PCL dissolved in THF.

4.3 Characterization of PANA/PCL/PVP Blends

4.3.1 UV-Vis spectrophotometric results of PANA/PCL/PVP blends

The UV-vis spectrum of the PANA/PCL/PVP nanofibers taken in THF/DMF solution is presented in Figure 4.37. The absorption peaks at 370 nm and 510nm can be attributed to π - π^* transition in benzoid rings of PANA and the peak at 500nm can be attributed to exciton like transition from benzoid to quionoid.

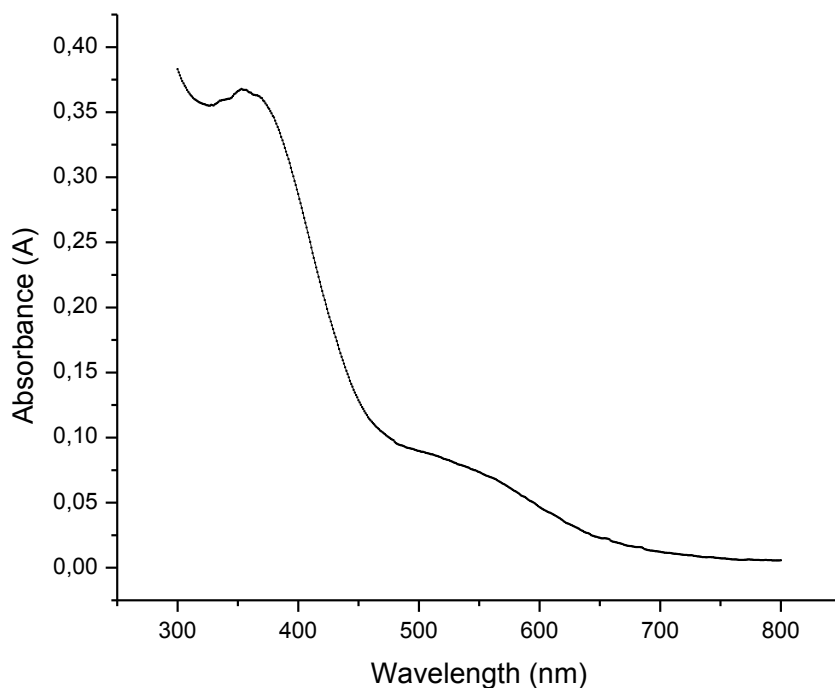


Figure 4.37: UV-Vis spectrum of PANA/PCL/PVP blend nanofibers dissolved in DMF/THF.

4.3.2 FTIR-ATR spectrophotometric analysis of PANA/PCL/PVP blends

FTIR-ATR results of PANA/PCL/PVP blends are presented in Figure 4.38. As obtained from the graph, the blend of PVP and PCL nanofibers has the specific peaks of PCL are observed as dominant and has also PVP peak around 1724 cm^{-1} which can be attributed to C=O stretching of PVP. Also, when it was blended with PANA, the absorbance of PVP specific peak was decreased and a new peak at 1576 cm^{-1} that is specific to PANA and named as C=C stretching can be obtained.

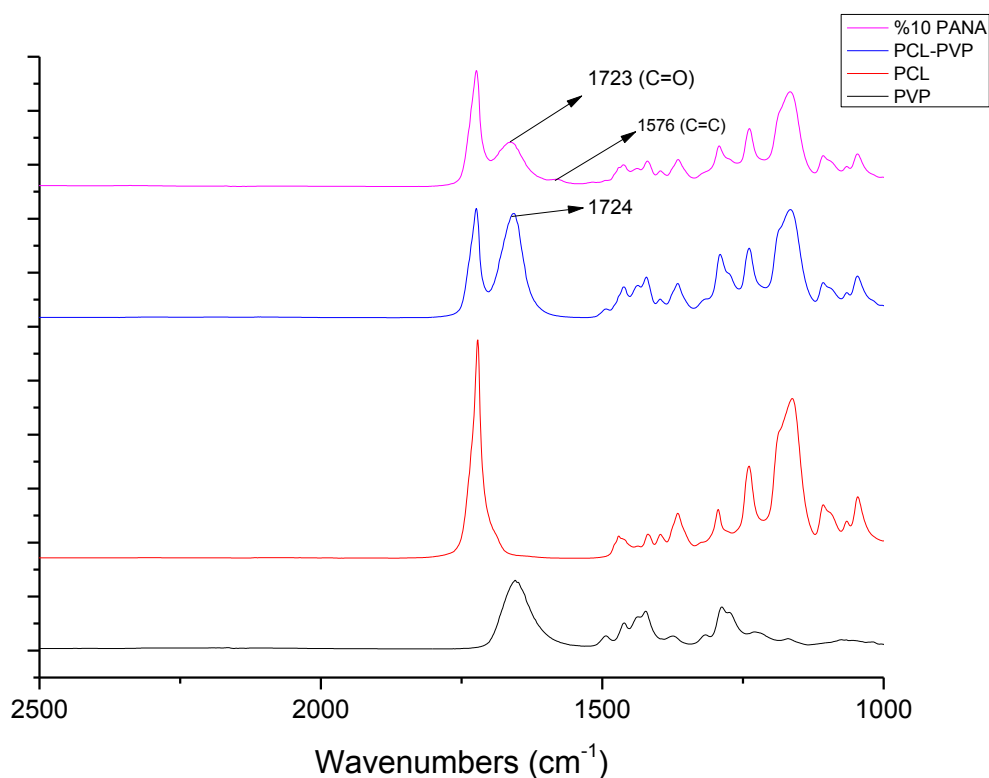


Figure 4.38 : FTIR-ATR spectra of PANA/PCL/PVP blended nanofibers.

4.3.3 SEM results of PANA/PCL/PVP blends

SEM result of PCL and PVP are presented in Figure 4.39. The average diameter of nanofibers is 1026 ± 900 nm. The distribution of those nanofibers are also shown in Figure 4.40.

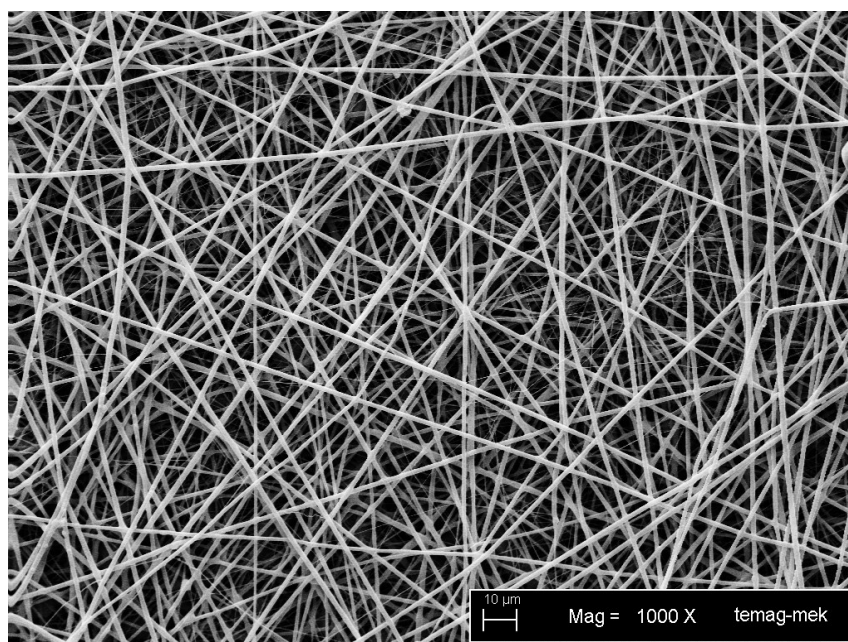


Figure 4.39 : SEM result of PCL/PVP blended nanofibers.

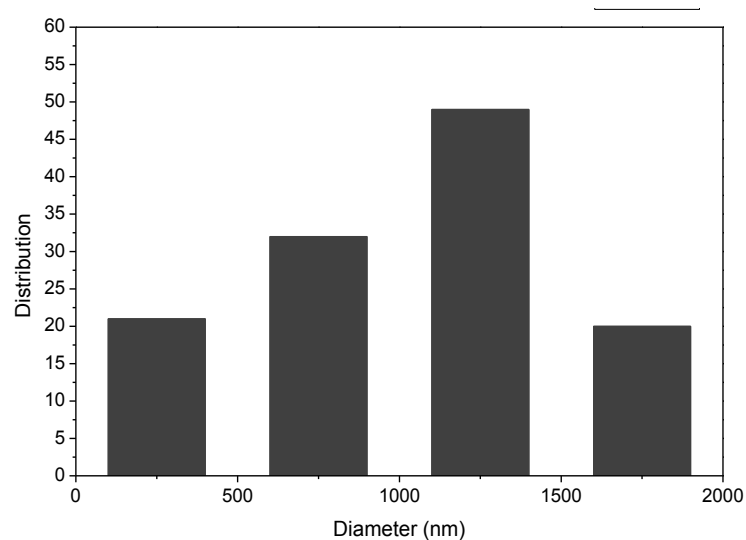


Figure 4.40: Diameter distribution of nanofibers of PCL/PVP.

The morphology of the nanofibers obtained with the blend of PANA/PCL/PVP is shown in Figure 4.41. The nanofiber diameter distribution diagram in Figure 4.42 showed that the average diameter was 652 nm for PANA/PCL/PVP blends.

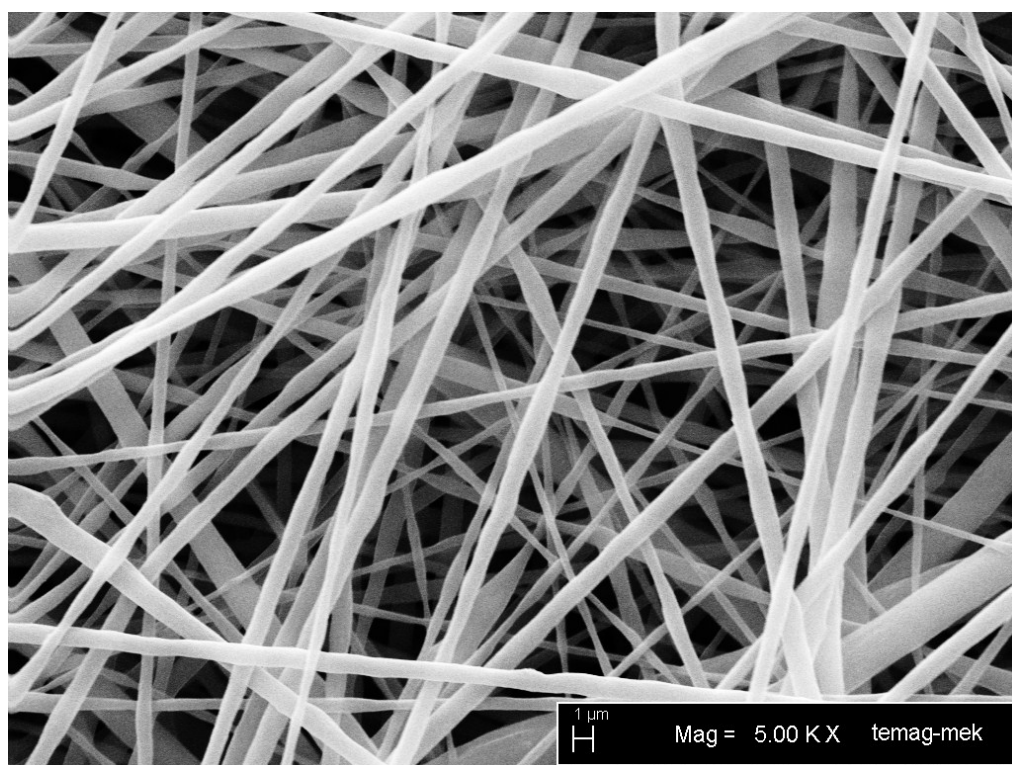


Figure 4.41: SEM results of PANA/PCL/PVP blended nanofibers.

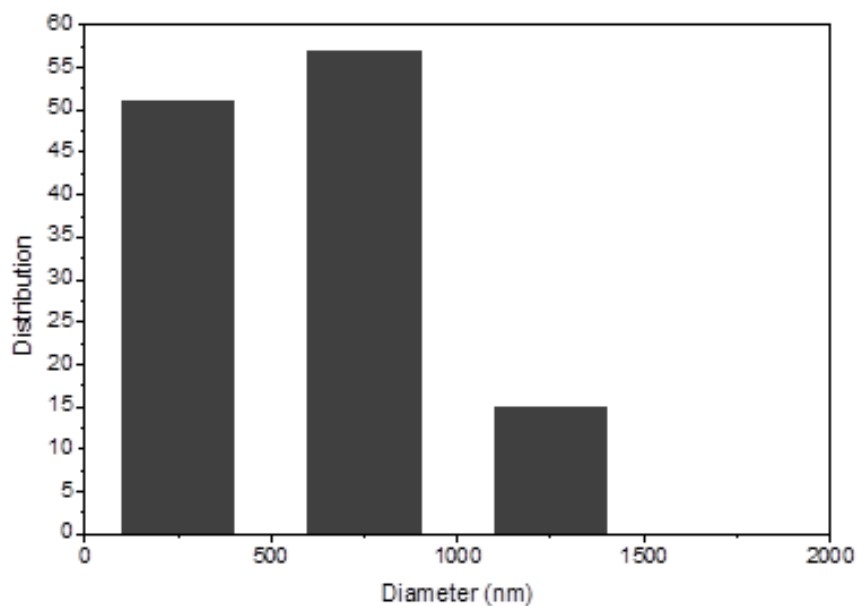


Figure 4.42: Diameter distribution of nanofibers of PANA/PCL/PVP blends.

The distribution nanafibers diameter is presented in Figure 4.43 and their detailed proroperties and their short summary is shown in Table 4.9

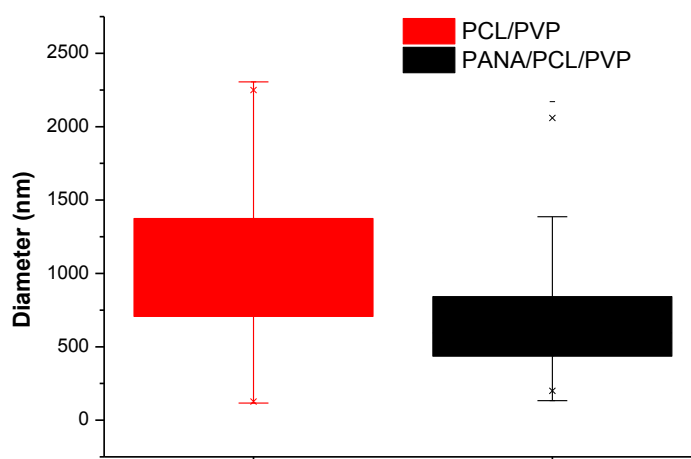


Figure 4.43: Distribution of nanofibers diameter of PANA/PCL/PVP blends.

Table 4.9: The summary of electrospun nanofibers of PANA/PCL/PVP with electrospinning conditions and diameters of nanofibers.

PANA (wt%)	Solvent	Flow rate (ml/h)	Distance (cm)	Applying Voltage (kV)	Diameters of Nanofibers (nm)
-	DMF/THF	0.5	20	15	1026 ±910
10	DMF/THF	0.5	20	15	652±519

4.3.4 Electrochemical impedance results of DMF/THF solutions

For electrochemical impedance measurement, the results of nyquist, bode phase, bode magnitude data were obtained. Nyquist results of electrospinning solutions that were prepared in DMF/THF solution are presented in Figure 4.44.

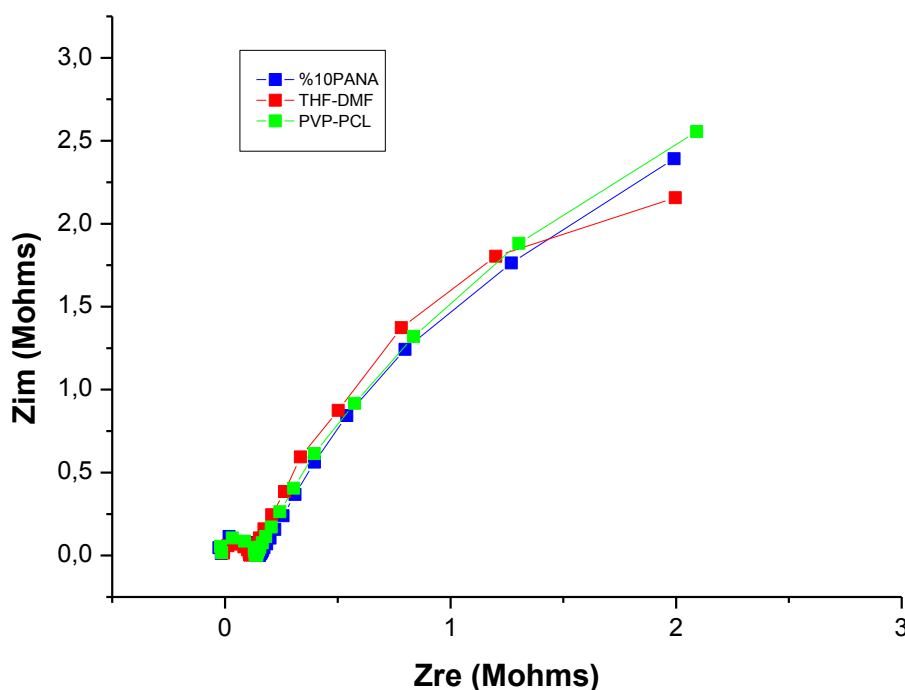


Figure 4.44: Nyquist diagram of electrospun solutions prepared in DMF/THF.

The Zim and Zre values of the Figure 4.44 were compared in the conductivity of the electrospinning solutions. The Zre and Zim values that are read from the graph were seen in Table 4.10.

Table 4.10: The impedance data of electrospinning solutions prepared in DMF/THF solutions.

Solvent Content	Zim (Mohms)	Zre (Mohms)
DMF/THF solution	0.071	0.114
PCL/PVP	0.099	0.126
10 % PANA	0.094	0.118

DMF/THF solution has the lowest Zim and Zre data that can be explained by the highest conductivity. Moreover, when PCL added inside this solution the conductivity was not too much. The PANA containing PCL/PVP solutions has lower resistance that may be explained as higher conductivity than PCL/PVP containing solutions.

As it is presented in Figure 4.45, bode phase angle at 0.1Hz is highest for DMF/THF as it has 60.80° and nearly same for the PCL/PVP as 57.12° and 10 % PANA containing blends as 54.86°.

From magnitude graph at Figure 4.46 at frequency 1 Hz, $|Z|$ is read 0.20 M Ω for DMFTHF solution, 0.18 M Ω for PCL containing solvents 0.15 M Ω for 10% of PANA containing diluted electrospinning solutions. These values are used to calculate double layer capacitance as seen in Table 4.11.

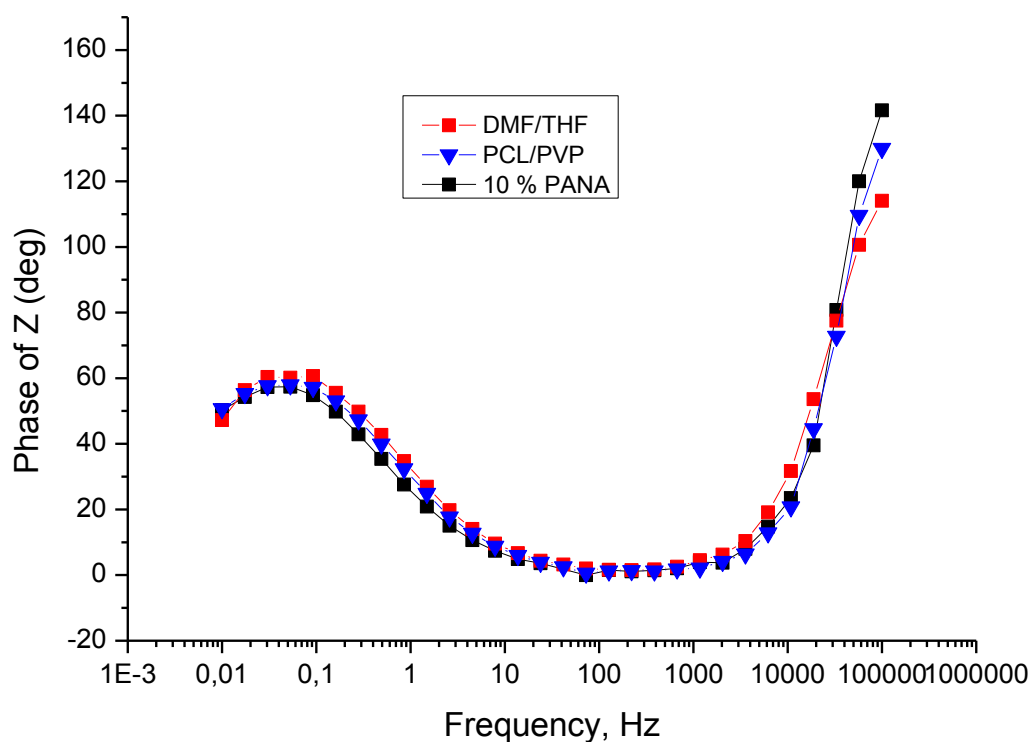


Figure 4.45: Bode phase of electrospinning solutions prepared in DMF/THF.

Table 4.11: The double layer capacitance of solutions prepared in DMF/THF solutions.

Solvent Content	Cdl (mF)
DMF/THF solution	0.0049
PCL/PVP	0.0055
10 % PANA	0.0066

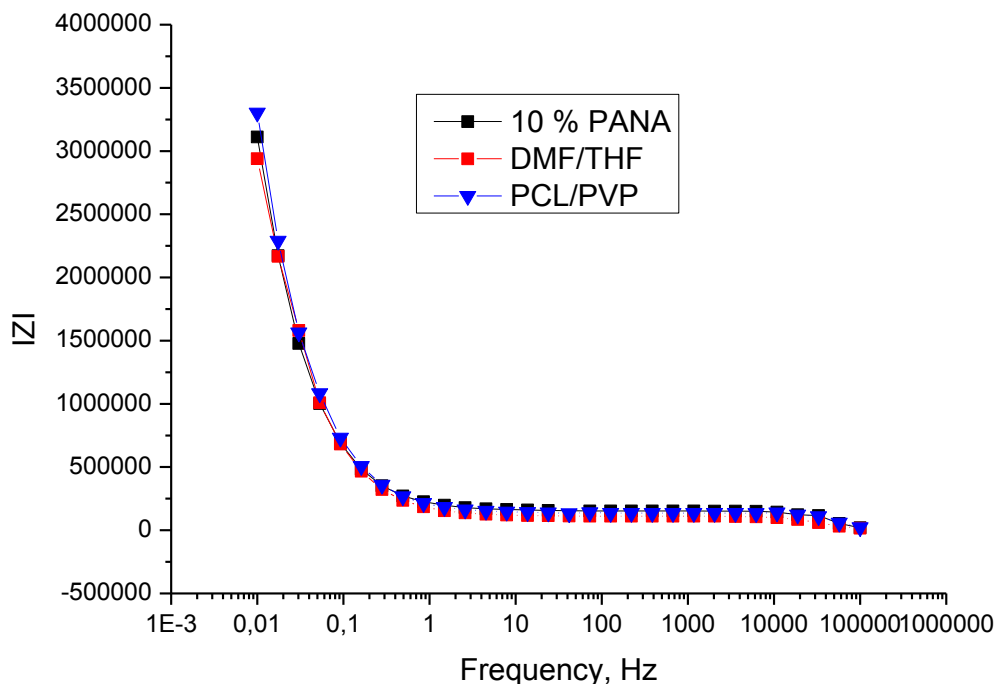


Figure 4.46: Bode magnitude of electrospinning solutions prepared in DMF/THF.

4.4 Electrochemical Impedance Spectroscopy (EIS) and Equivalent Circuit Modelling (ECM) for Electrospun Nanofibers

For electrochemical measurement PANA/PCL nanofibers were preferred due to their high hydrophobicity. The electrical properties of PANA/PCL were determined by electrochemical impedance measurements in monomer free solution of 0.1 M HCl, and dPBS. Due to the little amount of PANA solubility in dPBS, the modelling was not applied to obtained data. Nyquist data that was obtained in impedance measurement is shown in Figure 4.47.

The Bode- phase peaks of the nanofibers in the frequency range of 10Hz -10000 Hz appeared from 6° to 18° can be explained by the more capacitive property of PCL nanofibers containing 25% of PANA (Figure 4.48). From magnitude graph at Figure 4.49 at frequency 1 Hz, $|Z|$ is read 1651, 2071 and 1538 respectively. These values are used to calculate double layer capacitance as presented in Table 4.12.

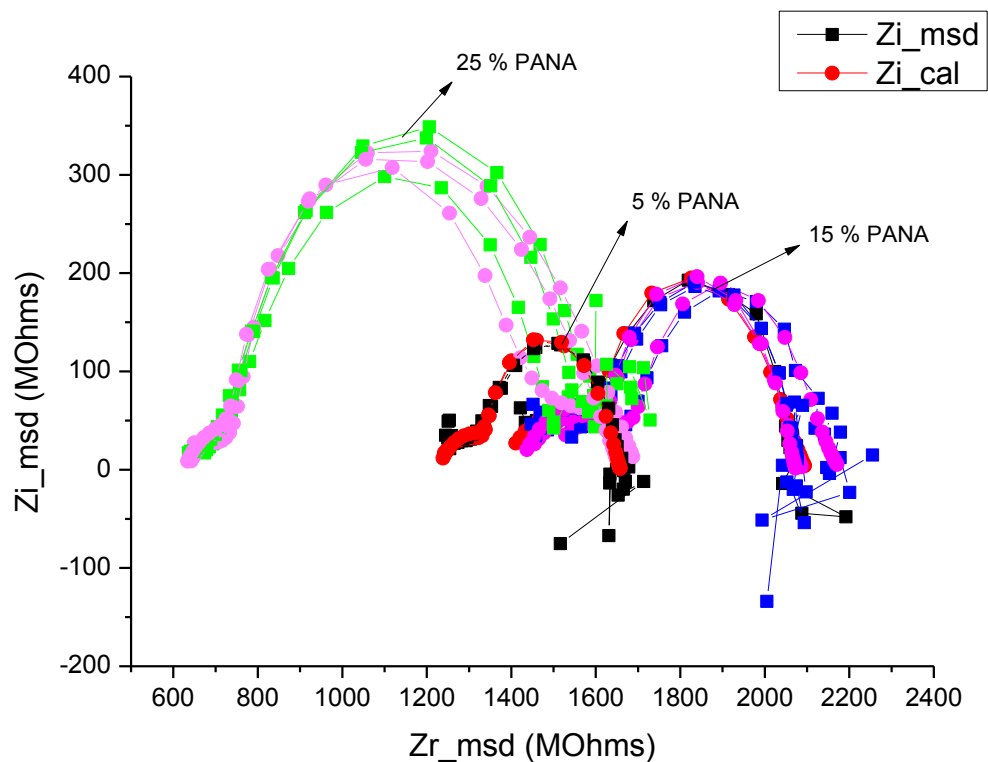


Figure 4.47: Nyquist plots of PANA/PCL blended nanofibers; correlated with the calculated data from the equivalent circuit model; $R(Q(R(CR)))$.

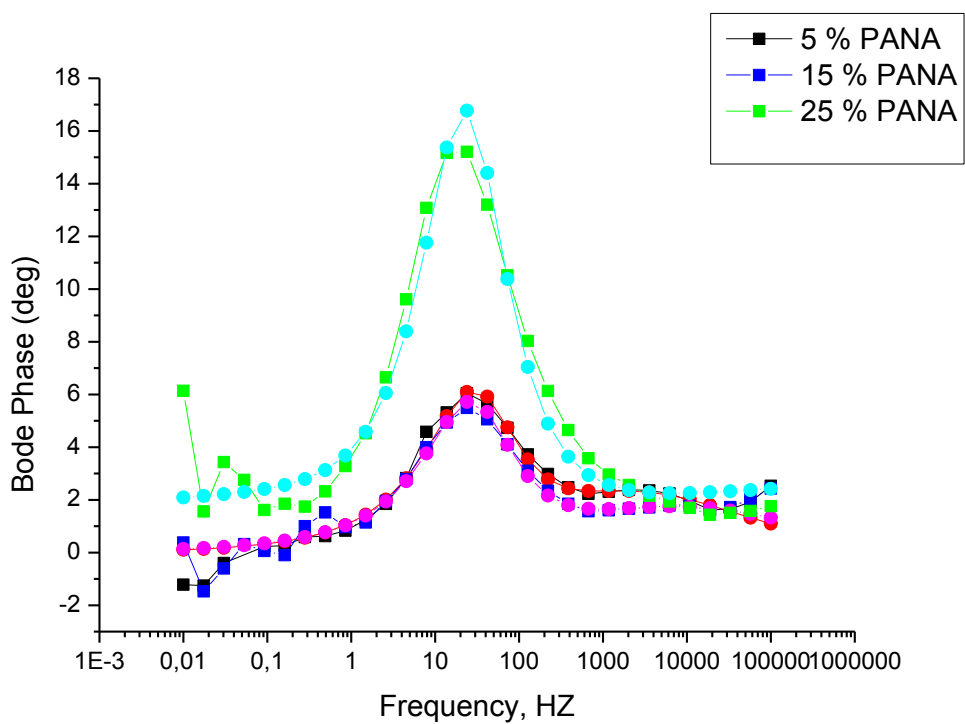


Figure 4.48: Bode Phase plots of PANA/PCL blended nanofibers; correlated with the calculated data from the equivalent circuit model; $R(Q(R(CR)))$.

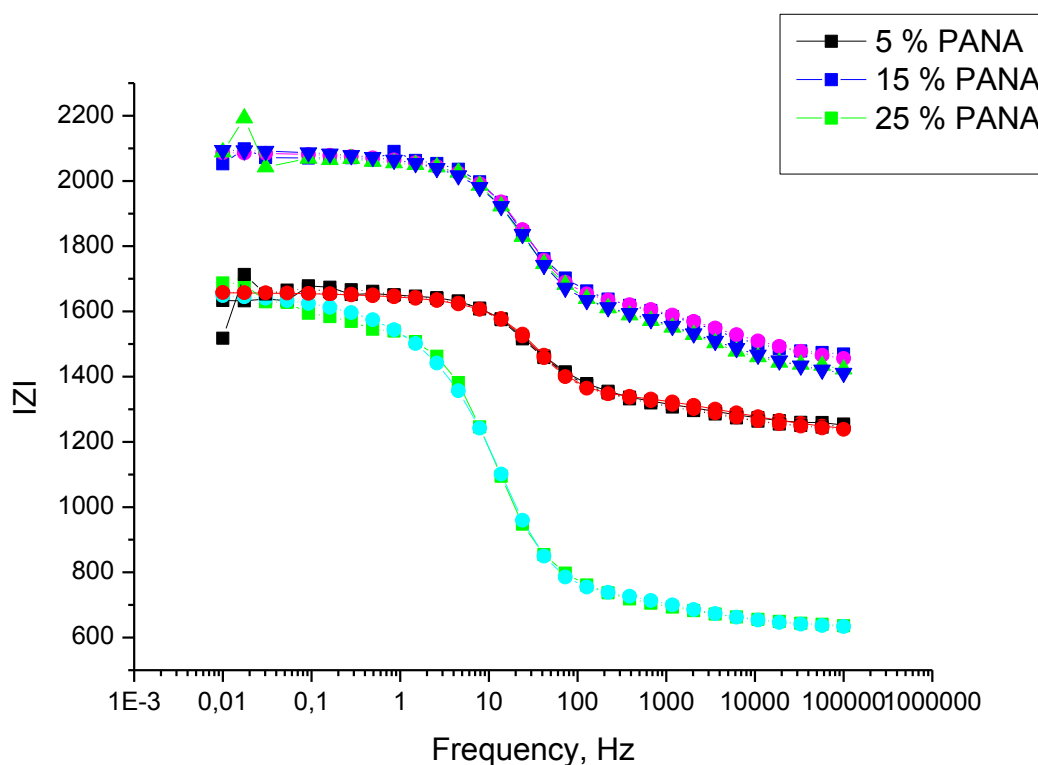


Figure 4.49: Bode Magnitude plots of PANA/PCL blended nanofibers; correlated with the calculated data from the equivalent circuit model; $R(Q(R(CR)))$.

Table 4.12: The double layer capacitance of the nanofibers.

PANA %	Z	Cdl (mF)
5	1651	0.6056
15	2071	0.4828
25	1538	0.6501

The EIS data were fitted with an equivalent electrical circuit in order to characterize the electrochemical properties of the nanofibers of PANA/PCL as one of their use as an electrode.

PANA/PCL blend nanofibers correlated with the calculated data from the equivalent circuit model that is defined as $R(Q(R(CR)))$. The model was shown in Figure 4.50. The model is composed of the electrolyte and pore resistance (R_s), C_a , R_a and charge-transfer resistance (R_{ct}), resistance and capacitance of the nanofibers (R_f and C_f).

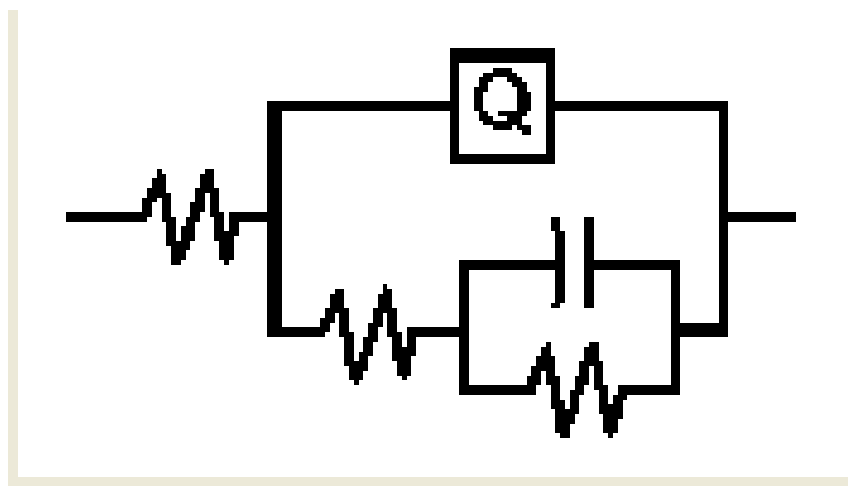


Figure 4.50: The equivalent circuit model of PANA/PCL blended nanofibers. (R_s =solution and pore resistance; R_{ct} = charge transfer resistance; CPE is used for modelling the double layer capacitance, C_{dl} ; R_f and C_f are resistance and capacitance of nanofibers).

The most widely used is the constant phase element (CPE) use to define capacitor and $n=0.8$ as shown in Table 4.13 can refer to capacitive behavior as it is known that $n=0$ is defined as resistor and $n=1$ is defined as ideal capacitor.

Table 4.13: Parameters calculated from the equivalent circuit model of $R(Q(R(CR)))$.

	5 % PANA	15 % PANA	25 % PANA
R_s/Ω	1473	1458	625.4
Q	3.92×10^{-10}	5.176×10^{-5}	0.00645
n	0.8	0.8	0.8
R_{ct}/Ω	320.5	305.5	182.4
C_f/mF	1.27×10^{-5}	1.418×10^{-5}	1.02×10^{-5}
R_f/Ω	404.4	404.4	851.5
$\text{Chi Squared}/\chi^2$	2.591×10^{-4}	4.796×10^{-4}	5.534×10^{-4}

4.5 Streptavidin Immobilization

FTIR-ATR spectrophotometry was used to determine the protein immobilization onto nanofibers. Streptavidin specific characteristic peaks are shown in Figure 4.51.

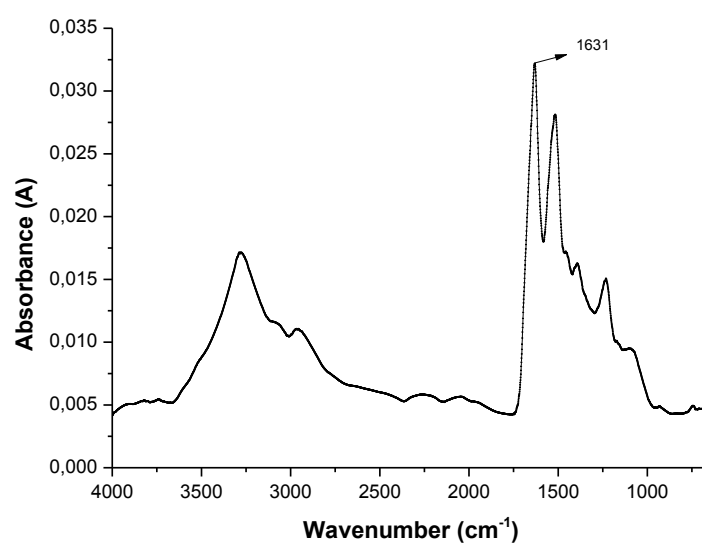


Figure 4.51: FTIR-ATR spectra of streptavidin.

As it is presented in Figure 4.51, Streptavidin specific peak at 1631 cm^{-1} was observed in nanofibers that are indicating for protein immobilization (Figure 4.52).

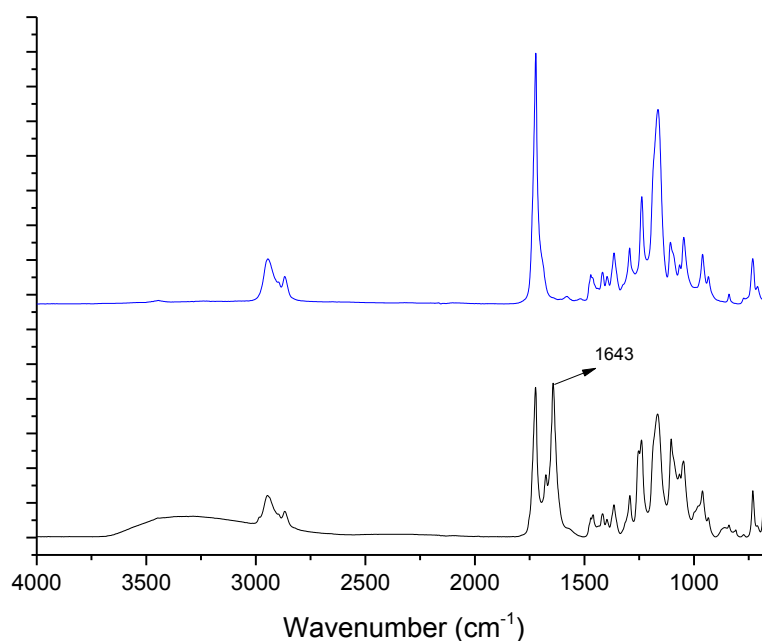


Figure 4.52 : FTIR-ATR spectra of nanofibers with and without streptavidin.

As control experiment, the EDC-NHS system without immobilization of streptavidin was also investigated. As it is presented in Figure 4.53, the immobilization was proved with the obtained FTIR-ATR data.

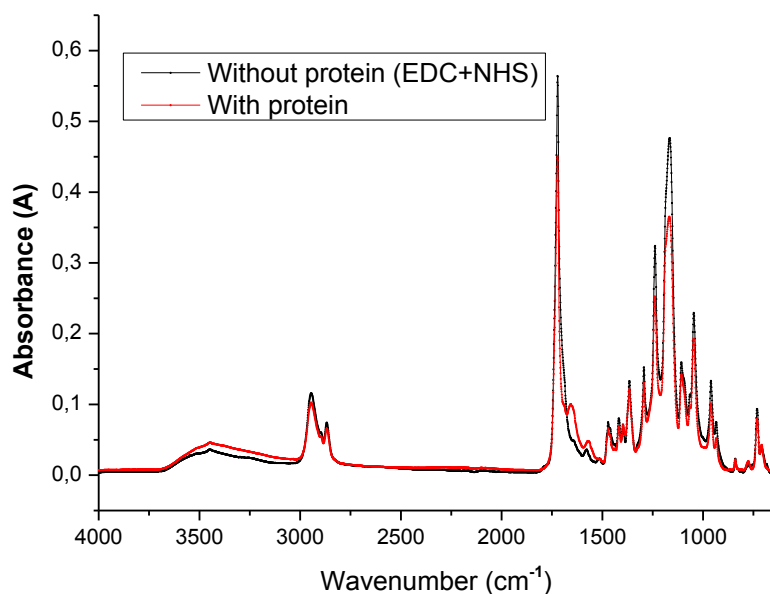


Figure 4.53 : FTIR-ATR spectra of nanofibers modified with EDC-NHS with and without streptavidin.

For control reaction, the adhesion of the dye and streptavidin was investigated as presented in Figure 4.54 and Figure 4.55. Moreover, the adhesion of only dye was also investigated as shown in Figure 4.56. As it is obtained from the results both chemical immobilization and adhesion of streptavidin on nanofibers were observed.

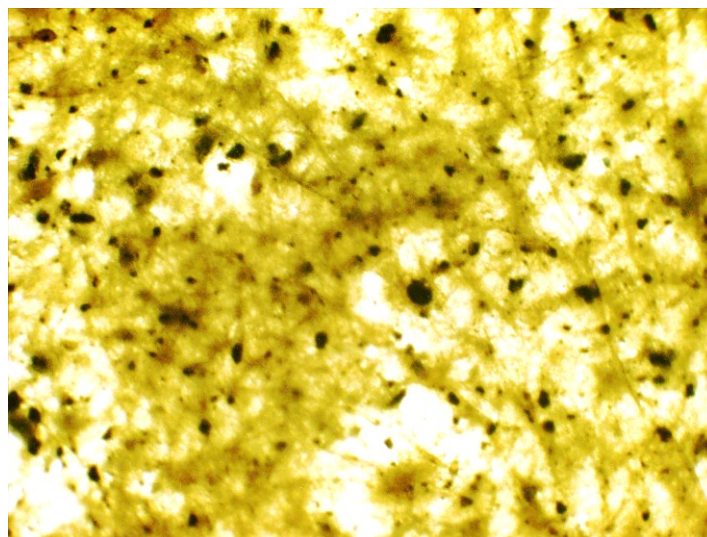


Figure 4.54 : Microscopic observation of nanofibers after streptavidin immobilization.

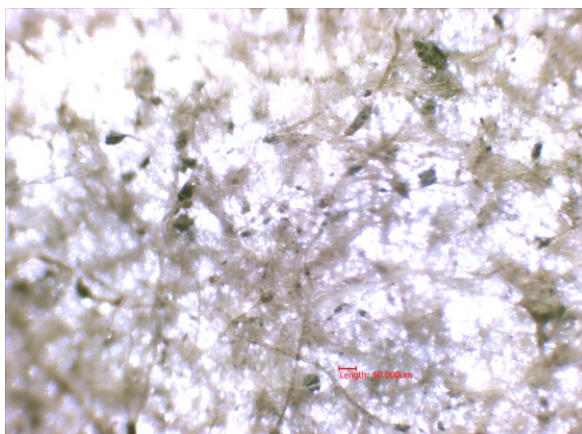


Figure 4.55 : Microscopic observation of nanofibers after streptavidin adhesion not immobilization without EDC and NHS.



Figure 4.56 : Microscopic observation of nanofibers after modification with dye.

5. CONCLUSIONS AND RECOMMENDATIONS

In this thesis, biocompatible polymers with the blend of poly (anthranilic acid) were obtained with electrospinning method. PANA and PCL blends were not successfully electrospun by using DMF due to gel formation of PCL. The electrospun fibers resulted in DMF solution makes fibers with smaller diameter as compared to THF with non-homogeneous distribution diameters that may differ from micron to nanometer sizes. FTIR-ATR spectroscopy was important method to ensure that the PANA even in small amount from 0.05 g to 0.5 g can be detected by PANA's specific peak (1570 cm^{-1}). UV-Vis spectroscopy was very efficient to determine the PANA content in PANA/PCL, PANA/PVP and PANA/PCL/PVP blends by using THF, EtOH/DMF. Streptavidin was immobilized efficiently with EDC/NHS method as its specific peak of -COOH (1631 cm^{-1}) was realized in immobilized fibers. For future investigations, some modifications or additional characterizations can be done. Hydrophilic property of PVP nanofibers can be overcome by using crosslinking modifications like UV treatment. PANA/PCL fibers have non-homogenous diameter that have wide range of from $8\text{ }\mu\text{m}$ to 200 nm . Using another solvent system can overcome the problem of having non-homogenous fiber formation and fibers that are named as more nano-sized and homogenous can be obtained. For protein immobilization studies, microscopes like confocal or fluorescence can be used to visualize the protein that may easily be defined as biosensor. The PANA/PCL nanofiber surfaces are important for adhesion. Cell proliferation can be applied to those produce nanofiber surfaces. PANA/PCL/PVP nanofibers have both hydrophilic and hydrophobic nature that may be used in drug release studies with high efficiency as also wound dressing applications and many other purposes.

REFERENCES

- [1]Green, R. A, Baek, S., Poole-Warren, L. A., & Martens, P. J. (2010). Conducting polymer-hydrogels for medical electrode applications. *Science and Technology of Advance Materials*, 11, 01107.
- [2]Rzepa, H. S. (2003). *Conducting Polymers*. Date retrieved: 04.05.2012, adress: <http://www.ch.ic.ac.uk/local/organic/tutorial/steinke/4yrPolyConduct2003.pdf>
- [3]Freund, M. S., and Deore B. A. (2007). *Self-Doped Conducting Polymers*. Date retrieved: 10.06.2012, adress: http://media.wiley.com/product_data/excerpt/92/04700296/0470029692.pdf
- [4]Hosseini, S. H., Khalkhali, R. A., and Noor, P. (2010). Study of polyaniline conducting/electroactive polymer as sensor for some agricultural phosphorus pesticides. *Monatshefte für Chemie*, 141, 1049–1053.
- [5]Gibbs, K. (2010). *Semiconductors*. Date retrieved: 12.05.2012, adress: http://www.schoolphysics.co.uk/age1619/Electronics/Semiconductors/text/Semiconductors_/index.html
- [6]Biewer, M. C. (2011). *Conjugated Systems*. Date retrieved: 12.05.2012, adress: <http://www.utdallas.edu/~biewerm/15total.pdf>
- [7]Han, D., Song, J., Ding, X., Xu, X., & Niu, L. (2007). Fabrication and characterization of self-doped poly (aniline-co-anthranilic acid) nanorods in bundles. *Materials Chemistry and Physics*, 105, 380-384.
- [8]Gomes, E C., and Oliveira, M. A. S. (2012). Chemical Polymerization of Aniline in Hydrochloric Acid (HCl) and Formic Acid (HCOOH) Media Differences Between the Two Synthesized Polyanilines. *American Journal of Polymer Science*, Vol. 2, no. 2, pp. 5-13.
- [9]Wu, M., Wen, T., and Gopalan, A. (2001). Electrochemical Copolymerization of Diphenylamine and Anthranilic Acid with Various Feed Ratios. *Journal of The Electrochemical Society*, 148, 65-73.
- [10]Dash, M. P., Tripathy, M., Sasmal, A., Mohanty, G. C., & Nayak, P. L. (2010). Poly (anthranilic acid)/multi-walled carbon nanotube composites: spectral, morphological, and electrical properties. *Journal of Materials Science*, 45, 3858–3865.
- [11]Gooch, J. W. (2010). *Biocompatible Polymeric Materials and Tourniquets for Wounds*. Springer, New York.
- [12]Shinyashiki, N., Sengwa, R. J., Tsubotani, S., Nakamura, H., Sudo, S., & Yagihara, S. (2006). Broadband Dielectric Study of Dynamics of

Poly(vinyl pyrrolidone)-Ethylene Glycol Oligomer Blends. *Journal of Physical Chemistry*, 110, 4953-4957.

- [13]Cerveny, S., Alegría, A., and Colmenero, J. (2006). Broadband dielectric investigation on poly(vinyl pyrrolidone) and its water mixtures. *Journal of Chemical Physics*, 128, 044901.
- [14]Srivastava, Y., Marquez, M., and Thorsen, T. (2007). Multijet Electrospinning of Conducting Nanofibers from Microfluidic Manifolds. *Journal of Applied Polymer Science*, 106, 3171-3178.
- [15] Higa, O. Z., Rogero, S. O., Machado, L. D. B, Mathor, M. B., Lugaño, A. B. (1999). Biocompatibility study for PVP wound dressing obtained in different conditions, *Radiation Physics and Chemistry*, 55, 705-707.
- [16] Chen, X. J., Zhang, J., Ma, D. F., Hui, S. C., Liu, Y. L., & Yao, W. (2011). Preparation of Gold-Poly(vinyl pyrrolidone) Core-Shell Nanocomposites and Their Humidity-Sensing Properties. *Polymer*, 121, 1685-1690.
- [17] Moran, C. H., Rycenga, M., Zhang, Q. and Xia, Y. (2011). Replacement of Poly(vinyl pyrrolidone) by Thiols: A Systematic Study of Ag Nanocube Functionalization by Surface-Enhanced Raman Scattering, *Journal of Physical Chemistry C*, 115, 21852–21857.
- [18]Lu, J., Nguyen, Q., Zhou, J., and Ping, Z., (2003). Poly(vinyl alcohol)/Poly(vinyl pyrrolidone) Interpenetrating Polymer Network: Synthesis and Pervaporation Properties. *Journal of Applied Polymer Science*, 89, 2808–2814.
- [19]Jiao, Y., Liu, Z., Ding, S., Li, L., and Zhou, C. (2006). Preparation of Biodegradable Crosslinking Agents and Application in PVP Hydrogel. *Journal of Applied Polymer Science*, 101, 1515-1521.
- [20]Ignatova, M., Manolova, N., and Rashkov, I. (2007). Novel antibacterial fibers of quaternized chitosan and poly (vinyl pyrrolidone) prepared by electrospinning, *European Polymer Journal*, 43, 1112–1122.
- [21]Xin, Y., Huang, Z. H., Yan, E.Y., Zhang, W., and Zhao, Q. (2006). Controlling polyp-phenylene vinylene/poly vinyl pyrrolidone composite nanofibers in different morphologies by electrospinning. *Applied Physics Letters*, 89, 053101.
- [22]Lopergolo, L. C, Lugao, A. B., and Catalani, L. H., (2003). Direct UV photocrosslinking of poly(N-vinyl-2-pyrrolidone) (PVP) to produce hydrogels, *Polymer*, 44, 6217-6222.
- [23]Jovanović, Z., Krkljės, A., Stojkovska, J., Tomić, S., Obradović, B., Misković-Stanković, V., and Kaćarević-Popovic, Z. (2011). Synthesis and characterization of silver/poly(N-vinyl-2-pyrrolidone) hydrogel nanocomposites obtained by in situ radiolytic method, *Radiation. Physics and Chemistry*, 80, 1208–1215.
- [24]Rutkowska, M., Krasowska, K., Heimowska, A., Steinka, H., Haponiuk, J., Karlsson, S. (2002). Biodegradation of Modified Poly(ϵ -caprolactone) in Different Environments. *Polish Journal of Environmental Studies*, Vol. 11, no. 14, pp. 413-420.

- [25]Edwards, M. D., Mitchell, G. R., Mohan, S. D., and Olley, R. H. (2010). Development of orientation during electrospinning of fibres of poly(ϵ -caprolactone). *European Polymer Journal*, 46, 1175–1183.
- [26]Chen, F., Lee, C. N., and Teoh, S. H. (2007). Nanofibrous modification on ultra-thin poly(ϵ -caprolactone) membrane via electrospinning. *Materials Science and Engineering C*, 27, 325–332.
- [27]Wang, Y., Rodriguez-Perez, M. A., Reis, R. L., and Mano, J. F. (2005). Thermal and Thermomechanical Behaviour of Polycaprolactone and Starch/Polycaprolactone Blends for Biomedical Applications. *Macromolecular Materials Engineering*, 290, 792–801.
- [28]Krouit, M., Bras, J., and Belgacem, M. N. (2008). Cellulose surface grafting with polycaprolactone by heterogeneous click-chemistry. *European Polymer Journal*, Vol. 44, no. 12, pp. 4074-4081.
- [29]Chronakis, I. S., Grapenson, S., and Jakob, A. (2006). Conductive polypyrrole nanofibers via electrospinning: Electrical and morphological properties. *Polymer*, 47, 1597–1603.
- [30]Zhang, X., (2009). Processing-Structure Relationships of Electrospun Nanofibers. In W. N. Chang (Ed.), *Nanofibers: Fabrication, Performance, and Applications* (pp. 239-270). Nova Science Publishers.
- [31]Pham, Q. P., Sharma, U., and Mikos, A., (2006). Electrospinning of Polymeric Nanofibers for Tissue Engineering Applications: A Review. *Tissue Engineering*, Vol. 12, no. 5, pp. 1197-1211.
- [32]George, J. H., Shaffer, M. M., and Stevens, M. M. (2006). *5th Conference and Post Graduate day UK Society of Biomaterials*, Manchester, June 28-29. Date retrieved: 07.06.2012, adress: <http://www.centropede.com/UKSB2006/ePoster/background.html>
- [33]Ramakrishna, S., Fujihara, K., Teo, W. E., Lim, T. C., & Ma, Z., (2005). *An Introduction to Electrospinning and Nanofibers*. World Scientific Publishing, Singapore.
- [34]Wannatong, L., Sirivat, A., and Supaphol, P., (2004). Effects of solvents on electrospun polymeric fibers: preliminary study on polystyrene. *Polymer International*, 53, 1851–1859.
- [35]Dalton, L. R. (2011). Date retrieved: 07.06.2010, adress: http://depts.washington.edu/eoopic/linkfiles/dielectric_chart%5B1%5D.pdf
- [36]Fong, H., Chun, I., and Reneker, D. H. (1999). Beaded nanofibers formed during electrospinning. *Polymer*, 40, 4585–4592.
- [37]Lin, T., Wang, H., Wang, H., and Wang, X. (2004). Charge effect of cationic surfactants on the elimination of fibre beads in the electrospinning of polystyrene. *Nanotechnology*, 15, 1375-1381.
- [38]Arinstein, A., and Zussman, E., (2007). Postprocesses in tubular electrospun nanofibers. *Physical Review*, 76, 056303.

- [39]Casper, C. L., Stephens, J. S, Tassi, N. G., Chase, D. B. and Rabolt, J. F. (2004). Controlling Surface Morphology of Electrospun Polystyrene Fibers: Effect of Humidity and Molecular Weight in the Electrospinning Process. *Macromolecules*, 37, 573-578.
- [40]Bölgen, N., Menceloğlu, Y. Z., Acatay, K., Vargel, I., and Pişkin, E., (2005). In vitro and in vivo degradation of non-woven materials made of poly(ϵ -caprolactone) nanofibers prepared by electrospinning under different conditions. *Journal of Biomaterials Science Polymer Edition*, Vol. 16, no. 12, pp. 1537–1555.
- [41]Jalili, R., Hosseini, S. A., and Morshed, M. (2005). The Effects of Operating Parameters on the Morphology of Electrospun Polyacrylonitrile Nanofibres. *Iranian Polymer Journal*, Vol. 14, no. 12, pp. 1074-1081.
- [42]Vrieze S., VanCamo, E. T., Nelvig, E. A., Hagstrom, E. B., Westbroek, P., and DeClerck, K. (2009). The effect of temperature and humidity on electrospinning. *Journal of Material Science*, 44, 1357-1362.
- [43]Laforgue, A. (2011). All-textile flexible supercapacitors using electrospun poly(3,4-ethylenedioxythiophene) nanofibers. *Journal of Power Sources*, 196, 559–564.
- [44]Lee, S., and Obendorf, S. K. (2007). Use of Electrospun Nanofiber Web for Protective Textile Materials as Barriers to Liquid Penetration. *Textile Research Journal*, Vol. 77, no. 9, pp. 696-702.
- [45]Liu, L., Liu, Z., Bai, H., and Delai Sun, D. D. (2012). Concurrent filtration and solar photocatalytic disinfection/ degradation using high-performance Ag/TiO₂ nanofiber membrane. *Water Research*, 46, 97–102.
- [46]Wang, M., Vail, S. A., Keirstead, A. E., Marquez, M., Gust, D., and Gracia, A. A. (2009). Preparation of photochromic poly(vinylidene fluoride-co-hexafluoropropylene) fibers by electrospinning. *Polymer*, Vol. 50, no. 16, pp. 3974-3980.
- [47]Chronakis, I. S., Grapenson, S., and Jakob, A., (2006). Conductive polypyrrole nanofibers via electrospinning: Electrical and morphological properties. *Polymer*, 47, 1597–1603.
- [48]Singh, S., Wu, B. M., and Dunn, J. C. Y. (2012). Delivery of VEGF using collagen-coated polycaprolactone scaffolds stimulates angiogenesis. *Journal of Biomedical Materials Research A*, Vol. 100, no. 3, pp. 721-727.
- [49]Zahedi, P., Rezaeia, I., Ranaei-Siadat, S. O., Jafaria, S. H., and Supaphol, P. (2010). A review on wound dressings with an emphasis on electrospun nanofibrous polymeric bandages. *Polymer Advance Technology*, 21, 77-95.
- [50]Yu, D. G., Branford-White, C., Li, L., Wu, X. M., and Zhu, L. M. (2009). The Compatibility of Acyclovir with Polyacrylonitrile in the Electrospun Drug-Loaded Nanofibers. *Journal of Applied Polymer Science*, 117, 1509-1515.
- [51]Meng, Z. X., Xu, X. X., Zheng, W., Zhou, H. M., Li, L., Zheng, Y. F., and Lou, X. (2011). Preparation and characterization of electrospun

PLGA/gelatin nanofibers as a potential drug delivery system. *Colloids and Surfaces B: Biointerfaces*, 84, 1101-1112.

- [52]Ramalingam, M., Young, M. F., Thomas, V., Sun, L., Chow, L. C., Tison, C. K., Chatterjee, K., Miles, W. C., and Simon, C. G. (2012). Nanofiber scaffold gradients for interfacial tissue engineering. *Journal of Biomaterials Applications*, 0, 1–11 doi: 10.1177/0885328211423783.
- [53]Xiang, P., Li, M., Zhang, C, Chen, D., and Zhou, Z. (2011). Cytocompatibility of electrospun nanofiber tubular scaffolds for small diameter tissue engineering blood vessels. *International Journal of Biological Macromolecules*, 49, 281-288.
- [54]Jang, J. H., Castano, O., Kim, H. W. (2009). Electrospun materials as potential platforms for bone tissue engineering. *Advanced Drug Delivery Reviews*, 61, 1065–1083.
- [55]Agarwal, S., Wendorff, J. H., and Greiner, A. (2010). Chemistry on Electrospun Polymeric Nanofibers: Merely Routine Chemistry or a Real Challenge?. *Macromolecular Rapid Communications*, 31, 1317-1331.
- [56]Yoo, H. S., Kim, T. G., and Park, T. G. (2009). Surface-functionalized electrospun nanofibers for tissue engineering and drug delivery. *Advanced Drug Delivery Reviews*, 61, 1033-1042.
- [57]UV spectroscopy. (n.d.). In *King Fahd University of Petroleum & Minerals*. Date retrieved: 07.06.2010, address: [http://opencourseware.kfupm.edu.sa/colleges/cs/chem/chem303/files %5C3-Lecture_Notes_CHEM-303_UV_Spectroscopy.pdf](http://opencourseware.kfupm.edu.sa/colleges/cs/chem/chem303/files/%5C3-Lecture_Notes_CHEM-303_UV_Spectroscopy.pdf)
- [58]Kumar, S. (2006). *Organic Chemistry Spectroscopy of Organic Compounds*. Date retrieved: 01.06.2010, address: <http://nsdl.niscair.res.in/bitstream/123456789/793/1/spectroscopy+of+organic+compounds.pdf>
- [59]Basic UV-Vis Theory. (n.d.). *Concepts and Applications Introduction Thermo Spectronic*. Date retrieved: 27.05.2010, address: [http://www.plant.uoguelph.ca/research/homepages/raizada/Equipment /RaizadaWeb%20Equipment%20PDFs/5B.%20UV%20VIS%20theory%20ThermoSpectric.pdf](http://www.plant.uoguelph.ca/research/homepages/raizada/Equipment/RaizadaWeb%20Equipment%20PDFs/5B.%20UV%20VIS%20theory%20ThermoSpectric.pdf)
- [60]What is ATR. (n.d.). In *Keck Interdisciplinary Surface Science Center*. Date retrieved: 05.06.2010, address: <http://www.nuance.northwestern.edu/KeckII/Instruments/FT-IR/keck-ii%20pages1.html>
- [61]Gauglitz, G., and Vo-Dinh, T. (2003). *Handbook of Spectroscopy*. Wiley-VCH, New York.
- [62]Microscopes. (n.d). In *A Review of the Universe - Structures, Evolutions, Observations, and Theories*. Date retrieved: 20.06.2010, address: <http://universe-review.ca/R11-13-microscopes.htm>
- [63]Lasia, A. (1999). Electrochemical Impedance Spectroscopy and Its Applications. In B. E. Conway, J. Bockris, and R. E. White (Eds.), *Modern Aspects*

of *Electrochemistry* (pp. 143-248). Kluwer Academic/Plenum Publishers, New York.

- [64]Aaron, D. S. (2010). Transport in fuel cells: electrochemical impedance spectroscopy and neutron imaging studies, *PhD Thesis*, Georgia Institute of Technology.
- [65]Ragoisha, G. (2008). *Potentiodynamic Electrochemical Impedance Spectroscopy*. Date retrieved: 30.06.2012, adress: <http://www.abc.chemistry.bsu.by/vi/>
- [66]Maeda, Y., Yoshino, T., Takahashi, M., Ginya, H., Asahina, J., Tajima, H., and Matsunaga, T. (2008). Noncovalent Immobilization of Streptavidin on In Vitro- and In Vivo-Biotinylated Bacterial Magnetic Particles, *Applied and Environmental Microbiology*, Vol. 74, no. 16, pp. 5139-5145.
- [67]Matsumoto, T., Tanaka, T. and Kondo, A. (2012). Sortase A-Catalyzed Site-Specific Coimmobilization on Microparticles via Streptavidin. *American Chemical Society Langmuir*, 28, 3553-3557.
- [68]Kim, M., Wang, C., Benedetti, F., Rabbi, M., Bennett, V., and Marszalek, P.E. (2011). Nanomechanics of Streptavidin Hubs for Molecular Materials. *Advance Materials*, 23, 5684–5688.
- [69]Daguer, J., Ciobanu, M., Barluenga, S., and Winssinger, N. (2012). Discovery of an entropically-driven small molecule streptavidin binder from nucleic acid-encoded libraries. *Organic and Biomolecular Chemistry*, 10, 1502-1505.
- [70]Han, D., Song, J., Ding, X., Xu, X., and Niu, L. (2007). Fabrication and characterization of self-doped poly (aniline-co-anthranilic acid) nanorods in bundles. *Materials Chemistry and Physics*, 105, 380–384.
- [71]Lu, J., Nguyen, Q., Zhou, J., and Ping, Z. H. (2003). Poly(vinyl alcohol)/Poly(vinyl pyrrolidone)Interpenetrating Polymer Network: Synthesis and Pervaporation Properties. *Journal of Applied Polymer Science*, 89, 2808–2814.
- [72]Sophia, I. A., Gopu, G., and Vedhi, C. (2012). Synthesis and Characterization of Poly Anthranilic Acid Metal Nanocomposites. *Open Journal of Synthesis Theory and Applications*, 1, 1-8.
- [73]Avci, M. Z. (2012). Electrospun nanofibers of methyl methacrylate and butyl acrylate copolymers, *Master Thesis*, ITU.
- [74]Khan, S. N. (2007). *Conducting polymer nanofibers - electrical and optical characterization* (Doctoral dissertation). Retrieved from http://etd.ohiolink.edu/view.cgi?acc_num=ohiou1200600595
- [75]Hatta, F. F., Kudin, T. I. T., Subban, R. H. Y., Ali, A. M. M., Harun, M. K. and Yahya, M. Z. A. (2009). Plasticized PVA/PVP-KOH Alkaline Solid Polymer Blend Electrolyte For Electrochemical Cells. *Functional Materials Letters*, Vol. 2, no. 3, pp. 121-125.

[76] **Smallwood, I. M.** (1996). *Handbook of Organic Solvent Properties*. Arnold, New York.

CURRICULUM VITAE



Name Surname: Ece POLAT

Place and Date of Birth: Kartal-11.06.1988

Address: Cavusoglu M. Oncu Sk. Dogan A. No:6/16 Kartal
34873 Istanbul

E-Mail: ecepolat@yahoo.com, polatec@itu.edu.tr

B.Sc.: Istanbul Technical University Double Major
Programme in Environmental Engineering and
Molecular Biology & Genetics

M.Sc.: Istanbul Technical University Institute of Science,
Engineering and Technology NanoScience &
NanoEngineering

PUBLICATIONS/PRESENTATIONS ON THE THESIS

- **Polat, E.,** Timuçin, B. and Saraç, A.S., 2012: Fabrication and Characterization of Poly(anthranilic acid)/ Poly(vinyl pyrrolidone) Electrospun Nanofibers. *International Conference – NANO-Structures Self Assembly* June 25-29, 2012 Sardinia, Italy.

